NAC INTERNATIONAL

Atlanta Corporate Headquarters
3930 East Jones Bridge Road, Suite 200
Norcross, GA 30092
Phone 770-447-1144
Fax 770-447-1797
www.nacintl.com

November 3, 2009

U.S. Nuclear Regulatory Commission
11555 Rockville Pike
Rockville, MD 20852-2738

Attn: Document Control Desk

Subject: Request for Authorization for the Model NAC-LWT Cask with Impact Limiters Containing an Alternate Attachment Gusset Tab Configuration.

Docket No. 71-9225

Reference:
1. Safety Analysis Report (SAR) for the NAC Legal Weight Truck Cask, Revision 39, NAC International, October 2008
2. Model No. NAC-LWT Package, U.S. Nuclear Regulatory Commission (NRC) Certificate of Compliance (CoC) No. 9225, Revision 51, September 24, 2009
3. 10 CFR 71.95 Report for Instances Where the Conditions of Approval in the Certificate of Compliance Were Not Observed During a Shipment, NAC International, September 9, 2009

NAC International (NAC) herewith requests authorization to use the model NAC-LWT cask with impact limiters containing an alternate attachment gusset tab configuration. This request for authorization has been developed as a followup to the Reference 3 submittal. Authorization is being requested for a period not to exceed one year, during which time the authorized alternate gusset tab configuration will be incorporated into the next amendment request to Reference 2.

Reference 3 described a condition of the impact limiter gusset tab (the part of the gusset that connects the impact limiter to the cask) that is currently not an authorized configuration per Reference 2. NAC has developed this request for authorization submittal in order to obtain authorization to complete the necessary repair of the affected gusset tab(s) and to bring all NAC-LWT packaging into full compliance with the approved license documentation.

As discussed with the NRC Staff in an October 28, 2009 public meeting, the alternate repaired gusset tab configuration consists of a gusset made of two pieces that are joined by a full penetration weld. Authorization of the use of the alternate gusset tab configuration will enable NAC to repair the affected impact limiter tab and return the LWT unit to service.

This submittal includes eight copies of this transmittal letter and Revision LWT-09E changed pages to the Reference 1 SAR. The changed pages incorporate the requested changes and the applicable evaluations performed to justify the addition of the proposed

NMSS01
NMSS

alternate repaired gusset tab configuration. Attachment 1 contains a detailed summary of the changes to the SAR for the amendment.

Once authorized, NAC will incorporate the changed pages into the next scheduled NAC-LWT amendment request. Revision bars identify the SAR text changes on the Revision LWT-09E pages. This submittal also includes two revised license drawings. Attachment 2 to this transmittal letter lists all drawing changes in detail. The included List of Effective Pages identifies the current revision level of all pages in the Reference 1 SAR plus subsequent amendments as approved by the NRC.

In order to better facilitate the review process, NAC is providing the Revision LWT-09E change pages as complete sections of the NAC-LWT SAR. Consequently, most of Revision LWT-09E pages included contain no revision bars.

In Revision LWT-09E, the proposed changes to the impact limiter attachment tabs are described in Chapters 1, 2, 8 and 9. Chapter 1 contains the revised impact limiter drawings, Chapter 2 was revised to add the necessary analyses performed to justify the repair of the gusset tab, Chapter 8 contains a detailed description of the repair procedure for the impact limiter gusset tabs and Chapter 9 has been updated with the codes called out in Chapter 8. All other chapters of Reference 1 are unaffected.

This request for authorization is submitted in support of upcoming domestic commercial and research reactor fuel shipments (including the General Atomics' TRIGA fuel shipment), as well as Foreign Research Reactor (FRR) fuel shipments within the U.S. Department of Energy National Nuclear Security Administration FRR fuel acceptance program. NRC authorization is being requested by November 30, 2009 in order to allow timely completion of the necessary repair of the affected gusset tab.

If you have any comments or questions, please contact me on my direct line at 678-328-1274.

Sincerely,

Anthony L Patko

Anthony L. Patko
Director, Licensing
Engineering

Attachment 1 – List of Changes – NAC-LWT SAR
Attachment 2 – List of Drawing Changes – NAC-LWT SAR

Enclosures

Attachment 1

List of Changes

NAC-LWT SAR, Revision LWT-09E

Impact Limiter Gusset Weld Amendment

List of Changes, NAC-LWT SAR, Revision LWT-09E

Note: The List of Effective Pages and the Chapter Tables of Contents, including the List of Figures and the List of Tables, were revised as needed to incorporate the following changes.

Chapter 1

- Page 1-iii – revised License Drawings 315-40-05 (Rev. 10) and 315-40-06 (Rev. 10), and these drawings are included in this amendment request.

Chapter 2

- Page 2.6.7-11, Section 2.6.7.4.7, subsection titled "Impact Limiter Attachment During Normal Handling and Transport", 2nd sentence – revised to address the "10-g axial loading associated with rail transport [10 CFR 71.45 (b)]." Old 2nd sentence is now the 3rd sentence and is revised by adding "This bounds the …." The calculation presented in this paragraph is revised accordingly.
- Page 2.6.7-12, 1st line – changed "6061-T6 aluminum" to "6061-T651 aluminum"; subsections titled "Tension Across the Net Section" and "40-Degree Shearout" – revised throughout to reflect gusset plate impact limiter attachment tab issue.
- Pages 2.6.7-18 & 2.6.7.-19, subsection titled "Response of Secondary Impact Limiter During Initial Impact of Packages," 3rd sentence to the end of subsection – revised to reduce the acceleration to 30 g's and to address the welded gusset.
- Pages 2.6.7-20 & 2.6.7-21, subsection titled "Analysis of Impact Limiter Lug," – 1st paragraph, 2nd sentence – changed "Table 2.3.1-5" to "Table 2.3.1-4"; subsections titled "Tension Across the Net Section" and "40-Degree Shearout" – revised throughout to reflect gusset plate impact limiter attachment tab issue and to reference Section 8.2.1.1.
- Page 2.6.7-76, Figure 2.6.7-15 – changed "6061-T6 Aluminum" to "6061-T651 Aluminum."

Chapter 8

- Page 8.2-2 – added new Section 8.2.1, "Authorized Repairs," and new subsection 8.2.1.1, "Impact Limiter Attachment Lug Repairs" to address inspection of impact limiter lugs and repair procedure/documentation.

Chapter 9

- Pages 9-10 & 9-11 – added new references required by new Section 8.2.1 and subsection 8.2.1.1.

Attachment 2

List of Drawing Changes

NAC-LWT SAR, Revision LWT-09E

Impact Limiter Gusset Weld Amendment

Drawing 315-40-05, NAC-LWT Transport Cask, Upper Impact Limiter, Revision 10

- Updated drawing with current Border, Title Block and BOM. Changed 1/8 scale in the scale box to N.T.S.
- Added Sheet 2.
- Sheet 1, Zone D5, Added detail view call-out B-B in gusset tab area.
- Sheet 1, Zone B4-6, Moved assembly 98 "HANDLE" drawing to Sheet 2 in Zone C2-C4, and delete note "SCALE: FULL" from view label.
- Sheet 1, Zone F4, Changed weld symbol to "Seal Weld, All Around, TYP 4 Places"; was "3/32 Bevel Weld, 3 Sides, 4 Places."
- Sheet 1, Zone A6, Added note 14 as follows: "GUSSET ITEM 10, MAY BE TWO PIECES JOINED AS SHOWN, OR MAY BE PARTIAL WELD REPAIRED."
- Sheet 2, Zone C6, 7, Added detail view B-B showing item 10 "GUSSET" constructed of two pieces, joined by full penetration bevel weld and labeled as follows: " DETAIL B-B, ALTERNATE REPAIRED GUSSET CONFIGURATION, TYP UP TO 4 PLACES."

Drawing 315-40-06, NAC-LWT Transport Cask, Lower Impact Limiter, Revision 10

- Updated drawing with current Border, Title Block and BOM. Changed 1/8 scale in the scale box to N.T.S.
- Zone D5, Added detail view call-out B-B in gusset tab area.
- Zone F4, Changed weld symbol to "Seal Weld, All Around, TYP, 4 Places"; was "3/32 Bevel Weld, 3 Sides, 4 Places."
- Zone A6, Added note 14 as follows: "GUSSET ITEM 5, MAY BE TWO PIECES JOINED AS SHOWN, OR MAY BE PARTIAL WELD REPAIRED."
- Zone B5, Added detail view B-B showing item 5 gusset constructed of two pieces, joined by full penetration bevel weld and labeled as follows: "DETAIL B-B, ALTERNATE REPAIRED GUSSET CONFIGURATION, TYP UP TO 4 PLACES."

October 2009

Revision LWT-09E

NAC-LWT

Legal Weight Truck Cask System

SAFETY ANALYSIS REPORT

Volume 1 of 2

Docket No. 71-9225

NAC INTERNATIONAL

Atlanta Corporate Headquarters: 3930 East Jones Bridge Road, Norcross, Georgia 30092 USA
Phone 770-447-1144, Fax 770-447-1797, www.nacintl.com

List of Effective Pages

LIST OF EFFECTIVE PAGES

LIST OF EFFECTIVE PAGES

LIST OF EFFECTIVE PAGES (Continued)

Chapter 1

Table of Contents

List of Figures

List of Tables

List of Drawings

* Packaging Unit Nos. 1, 2, 3, 4 and 5 are constructed in accordance with this revision of drawing.

List of Drawings (continued)

315-40-100	Sheets 1 - 3	Rev 4	Lids, PWR/BWR Transport Canister
315-40-101		Rev 0	4 × 4 Insert, PWR/BWR Transport Canister
315-40-102		Rev 1	5 × 5 Insert, PWR/BWR Transport Canister
315-40-103		Rev 0	Pin Spacer, PWR/BWR Transport Canister
315-40-104	Sheets 1 - 2	Rev 5	Legal Weight Truck Transport Cask Assy, PWR/BWR Transport Canister
315-40-105	Sheets 1 - 2	Rev 3	PWR Insert PWR/BWR Transport Canister
315-40-106	Sheets 1 - 3	Rev 1	MTR Plate Canister, LWT Cask
315-40-108	Sheets 1 - 3	Rev 1	Weldment, 7 Cell Basket, Top Module, DIDO Fuel
315-40-109	Sheets 1 - 3	Rev 1	Weldment, 7 Cell Basket, Intermediate Module, DIDO Fuel
315-40-110	Sheets 1 - 3	Rev 1	Weldment, 7 Cell Basket, Base Module, DIDO Fuel
315-40-111		Rev 2	Legal Weight Truck, Transport Cask Assy, DIDO Fuel
315-40-113		Rev 0	Spacers, Top Module, DIDO Fuel
315-40-120	Sheets 1 - 3	Rev 2	Top Module, General Atomics IFM, LWT Cask
315-40-123	Sheets 1 - 2	Rev 1	Spacer, General Atomics IFM, LWT Cask
315-40-124		Rev 1	Transport Cask Assembly, General Atomics IFM, LWT Cask
315-40-125	Sheets 1 - 3	Rev 3	Transport Cask Assembly, Framatome/EPRI, LWT Cask
315-40-126	Sheets 1 - 2	Rev 2	Weldments, Framatome/EPRI, LWT Cask
315-40-127	Sheets 1 - 2	Rev 2	Spacer Assembly, TPBAR Shipment, LWT Cask
315-40-128	Sheets 1 - 2	Rev 3	Legal Weight Truck, Transport Cask Assy, TPBAR Shipment
032230		Rev A	RERTR Secondary Enclosure, General Atomics
032231		Rev A	HTGR Secondary Enclosure, General Atomics
032236		Rev B	RERTR Primary Enclosure, General Atomics
032237		Rev B	HTGR Primary Enclosure, General Atomics
315-40-129		Rev 1	Canister Body Assembly, Failed Fuel Can, PULSTAR
315-40-130		Rev 1	Assembly, Failed Fuel Can, PULSTAR
315-40-133	Sheets 1 - 2	Rev 1	Transport Cask Assembly, PULSTAR Shipment, LWT Cask
315-40-134		Rev 1	Body Weldment, Screened Fuel Can, PULSTAR Fuel
315-40-135		Rev 1	Assembly, Screened Fuel Can, PULSTAR Fuel
315-40-139		Rev 1	Legal Weight Truck Transport Cask Assy, ANSTO Fuel
315-40-140	Sheets 1 - 2	Rev 1	Weldment, 7 Cell Basket, Top Module, ANSTO Fuel
315-40-141	Sheets 1 - 2	Rev 1	Weldment, 7 Cell Basket, Intermediate Module, ANSTO Fuel
315-40-142	Sheets 1 - 2	Rev 1	Weldment, 7 Cell Basket, Base Module, ANSTO Fuel
315-40-145		Rev 0	Irradiated Hardware Lid Spacer Assembly, LWT Cask
315-40-148		Rev 0	Legal Weight Truck Transport Cask Assembly, ANSTO-DIDO Combination Basket

Figure Withheld Under 10 CFR 2.390

NAC INTERNATIONAL

LEGAL WEIGHT TRUCK TRANSPORT CASK UPPER IMPACT LIMITER SAFETY ANALYSIS REPORT

PROJECT 315-40	DRAWING 05	REV 10
SCALE N.T.S.	EST.WT. 1535 LBS.	SH 1 OF 2 · 9:57AM 10-22-2009

Figure Withheld Under 10 CFR 2.390

NAC INTERNATIONAL

LEGAL WEIGHT TRUCK TRANSPORT CASK UPPER IMPACT LIMITER SAFETY ANALYSIS REPORT

PROJECT 315-40		DRAWING 05	REV 10
SCALE N. T. S.	WEIGHT AS NOTED	SH 2 OF 2	9:57AM 10-22-2009

Figure Withheld Under 10 CFR 2.390

NAC INTERNATIONAL

LEGAL WEIGHT TRUCK TRANSPORT CASK LOWER IMPACT LIMITER SAFETY ANALYSIS REPORT

PROJECT 315-40		DRAWING 06	REV 10
SCALE N.T.S.	EST.WT.1320 LBS	SH 1 OF 1	10:08AM 10-27-2009

Chapter 2

Table of Contents

Table of Contents (continued)

Table of Contents (continued)

Table of Contents (continued)

Table of Contents (continued)

Table of Contents (continued)

List of Figures

List of Figures (continued)

List of Figures (continued)

List of Figures (continued)

List of Figures (continued)

List of Figures (continued)

List of Tables

List of Tables (continued)

List of Tables (continued)

List of Tables (continued)

List of Tables (continued)

List of Tables (continued)

List of Tables (continued)

List of Tables (continued)

List of Tables (continued)

List of Tables (continued)

List of Tables (continued)

List of Tables (continued)

2.6.7 Free Drop (1 Foot)

The free drop scenario outlined by Subpart F of 10 CFR 71 requires the NAC-LWT cask to be structurally adequate for a 1-foot drop (normal transport conditions) onto a flat, essentially unyielding, horizontal surface in the orientation that inflicts the maximum damage to the cask. The following sub-sections evaluate the cask body; the impact limiters; the closure lid and bolts; the neutron shield shell; the expansion tank shell; and the upper ring components; for the end, side, and corner drop orientations.

2.6.7.1 End Drop (1 Foot)

2.6.7.1.1 Discussion

The NAC-LWT cask is analyzed for the effects of a normal operations end drop impact condition. The event scenario is that the NAC-LWT cask, equipped with an impact limiter, drops 1 foot onto a flat, unyielding, horizontal surface. The cask strikes the surface in a vertical position on either its bottom or its top end.

The 1-foot end drop analysis can be carried out in an identical fashion as was used in the 30-foot accident end drop analysis, Section 2.7.1.1. The general comments, analysis descriptions and the analysis method described in Section 2.7.1.1 also apply to this section.

The only difference between the 30-foot end drop analysis (Section 2.7.1.1) and this 1-foot end drop analysis is the magnitude of the impact force, i.e., impact load, which is expressed in terms of a g factor. The magnitude of the impact force varies with the different drop heights. As calculated in Section 2.6.7-4, the g loads for the 1-foot end drop condition and for the 30-foot end drop condition are 15.8 g and 60 g, respectively. These g loads are conservatively based on a maximum crush strength of 3850 psi for the aluminum honeycomb impact limiters, although the design maximum crush strength is 3675 psi. Also, these analyses conservatively use a 1.12-inch thick outer shell, although the actual outer shell thickness is 1.20 inches. Using the analysis results obtained in Section 2.7.1.1 to represent the structural response of the NAC-LWT cask for the 1-foot end drop condition is conservative and acceptable. Therefore, Tables 2.7-1 through 2.7-15 were used to compose Table 2.6.7-1 through Table 2.6.7-16, for the 1-foot drop analyses. The most critical sections for each component during a particular loading condition are shown in Figure 2.6.7-1 through Figure 2.6.7-5. The critical P_m, $P_m + P_b$, and total stresses for each component are documented in Table 2.6.7-1 through Table 2.6.7-16. The allowable stresses are those defined in Section 2.1.2 for the normal operations conditions based on 300°F. Note that the maximum cask component temperatures are below 300°F for all of the conditions that are considered. Additionally, the stresses at representative sections throughout the cask are presented in the tables in Section 2.10.7. These tables document the maximum stress locations tabulated for each component.

The secondary stresses (thermal) are conservatively included in the primary stress categories and margin of safety calculations; therefore, the 3 S_m limit on the S_n stress intensity range is satisfied. This is because it is enveloped by the 1.5 S_m limit on $P_m + P_b$ stress intensity.

2.6.7.1.2 Results and Conclusions

Since the margins of safety are positive for all of the cask components, the NAC-LWT cask maintains its containment capability and satisfies the 10 CFR 71 requirements for the 1-foot normal operations end drop condition.

2.6.7.2 Side Drop (1 Foot)

2.6.7.2.1 Discussion

This section presents the evaluation of the structural adequacy of the NAC-LWT cask for the 1-foot side drop impact condition. In this event, the NAC-LWT cask with impact limiters attached over each end experiences a free drop through a distance of 1 foot onto a flat, unyielding surface, and strikes the surface in a horizontal position.

The 1-foot side drop analysis is performed in the same manner as was done for the 30-foot side drop analysis in Section 2.7.1.2. The general comments, analysis descriptions, and the analysis methods described in Section 2.7.1.2 also apply to this section.

The difference between the 30-foot side drop analysis and the 1-foot side drop analysis is the magnitude of the impact force, which varies because of the different drop heights. As determined in Section 2.6.7.4, the g loads for the 1-foot side drop condition and for the 30-foot side drop accident condition are 24.3 g and 49.7 g, respectively.

Analysis of the NAC-LWT cask for the normal operations conditions side drop follows the same methodology as used for the accident side drop analysis. Because all calculations for the accident side drop analysis are performed on a basis of linear elastic behavior, the stress components for the 1-foot side drop condition are calculated by multiplying the 30-foot side drop stress components (resulting from the effects of inertial and impact loads) by the ratio of the 1-foot side drop g load to the 30-foot side drop g load. These stress components are then combined with those induced by the thermal effects, internal pressure, and bolt preload.

2.6.7.2.2 Results and Conclusions

Since the material properties of the cask structure are temperature-dependent, varying environmental temperatures will produce changes in the calculated stresses in the cask for the thermal load cases. Environmental temperatures will not change the calculated stresses in the cask produced by other types of loads. This is verified by comparing the finite element results for the NAC-LWT cask subjected to a gravity load for different temperature conditions. Also, the stress levels produced by the following thermal loading conditions were evaluated: (1) 100°F ambient temperature with maximum decay heat load, (2) -40°F ambient temperature with maximum decay heat load, and (3) -40°F ambient temperature with no decay heat load. The combination effect of the thermal loads with other load types (e.g., inertial body load) has also been studied. It is determined that the side drop event with 100°F ambient temperature represents the worst case for the normal operations 1-foot side drop condition. Therefore, only the stress results produced by a 1-foot side drop with 100°F ambient temperature are reported.

Stress components and stress intensities are calculated throughout the finite element model for the combined loads due to internal pressure, bolt preload, thermal, inertia, and impact. Table 2.6.7-16 through Table 2.6.7-19 report the P_m stress intensities, the $P_m + P_b$ stress intensities, the S_n stress intensities, and the total stress intensities for each cask component, which are obtained from the finite element side drop analysis. Additionally, the stresses at representative sections throughout the cask are presented in the tables in Section 2.10.7. These tables document the maximum stress locations tabulated for each component.

As mentioned previously, the finite element cask model conservatively ignores the effect of the neutron shield shell on the overall bending of the cask structure.

The margins of safety reported in Table 2.6.7-16 through Table 2.6.7-18 are positive for all cask components. It has been demonstrated that all margins of safety are positive for the normal operations 1-foot side drop condition.

The NAC-LWT cask maintains its containment capability and satisfies the 10 CFR 71 requirements for the normal operations 1-foot side drop condition.

2.6.7.3 Corner Drop (1 Foot)

2.6.7.3.1 Discussion

The analysis of the NAC-LWT cask for a 1-foot corner drop condition uses the same methods as those used for the hypothetical accident oblique drop analyses. The general comments, analysis descriptions, and analysis methods discussed in Section 2.7.1.3 also apply to this section. The difference between the hypothetical accident analysis and the normal operations conditions analysis in this section is the drop height. Refer to Section 2.6.7.4 for the calculation of the g loads induced by a normal operations conditions 1-foot corner drop and by an accident condition 30-foot corner drop. These g loads are conservatively based on a maximum crush strength of 3850 psi for the aluminum honeycomb impact limiters, although the design maximum crush strength is 3675 psi. The stress components for the 1-foot corner drop are calculated by multiplying the accident condition stress components (resulting from the effects of inertial and impact loads) by the ratio of the 1-foot corner drop g load to the 30-foot corner drop g load. These stress components, then, are combined with those resulting from internal pressure, bolt preload, and thermal effects. These analyses conservatively use a 1.12-inch thick outer shell, although the actual outer shell thickness is 1.20 inches.

2.6.7.3.2 Results and Conclusions

The most critical sections for each component during a particular loading condition are shown in Figure 2.6.7-7 through Figure 2.6.7-9. Table 2.6.7-20 through Table 2.6.7-23 report the maximum P_m stress intensities, the maximum $P_m + P_b$ stress intensities, the maximum S_n stress intensities, and the maximum total stress intensities for each component resulting from the 1-foot top corner drop condition with a 130°F ambient temperature and maximum decay heat load. Similarly, Table 2.6.7-24 through Table 2.6.7-27 report those stress intensities resulting from the 1-foot bottom corner drop condition with a 130°F ambient temperature and maximum decay heat load. Also, Table 2.6.7-28 through Table 2.6.7-31 report the stress intensities for each component resulting from the 1-foot top corner drop condition with a -40°F ambient temperature. Additionally, the stresses at representative sections throughout the cask are presented in the tables in Section 2.10.7. These tables document the maximum stress locations for each component.

It has been demonstrated that all margins of safety are positive for the normal operations 1-foot corner drop condition. The NAC-LWT cask maintains its containment capability and satisfies the 10 CFR 71 requirements for the normal operations 1-foot corner drop condition.

2.6.7.4 Impact Limiters

2.6.7.4.1 Introduction

Removable impact limiters are supplied with the NAC-LWT cask to ensure that the design impact loads on the cask are not exceeded for any of the defined impact conditions. These defined conditions are:

1. The cask falls 1 foot and lands on: (a) its side, impacting both limiters simultaneously; (b) flat on one limiter at either end; or (c) oblique on either corner (the center of gravity is directly above the corner of the impact limiter).
2. The cask, having experienced a normal operating conditions 1-foot drop, is dropped through a distance of 30 feet and lands on its end, its side, or at any oblique angle. The impact limiter analysis considers a 31-foot drop (1 foot + 30 feet). This provides conservative impact loads, which are used in the cask analyses.

2.6.7.4.2 Assumptions

The following assumptions form the basis for the impact limiter analysis:

1. The cask impacts on an unyielding surface.
2. The impact limiter remains in position on the cask during all impact events. (The qualification of the impact limiter attachment is presented in Section 2.6.7.4.7.)

2.6.7.4.3 Load Conditions

The impact limiters described and analyzed in the following paragraphs decelerate the cask by applying a force in the direction opposite the motion of the cask. The deceleration force is generated by crushing the aluminum honeycomb material of the limiter between the cask and the unyielding surface. The energy absorbed during crushing is the net force, the vector sum of the cask weight (downward) and the deceleration force (upward), multiplied by the distance crushed. The amount of energy an impact limiter can absorb is calculated for various cask impact orientations, from vertical (0°) to horizontal (90°).

The specific loading conditions for the impact limiters are defined by 10 CFR 71.71(c)(7), 10 CFR 71.73(c)(1) and Regulatory Guide 7.8, as follows:

1. A 1-foot fall of the cask on one limiter, impacted at any angle from vertical (flat end) to corner (cask center of gravity is directly above the point of impact).
2. A 1-foot fall of the cask horizontally, so that the side surfaces of both limiters impact the unyielding surface simultaneously.
3. Any of the 1-foot falls can be followed by a 30-foot fall at an end, a side, or an oblique orientation.

Based on these loading conditions, the NAC-LWT cask impact limiters are designed for a 31-foot fall. Either of the first two conditions plus the third condition is equivalent to a single drop at the combined heights, as explained in Section 2.6.7.4.5. The maximum impact force and the maximum crush depth for the 1-foot falls are obtained from the computer output for the 31-foot fall analyses at the value of the energy dissipated in a 1-foot fall. This method is explained in Section 2.6.7.4.5.

2.6.7.4.4 Descriptions - Impact Limiters

Figure 2.6.7-10 shows the location on the cask and the primary dimensions of the impact limiters. A different impact limiter is used on the bottom of the cask to reduce weight. The top impact limiter diameter is larger because it is required to clear the cask lifting trunnions and to be of sufficient depth over the trunnions to prevent the limiter from behaving as a solid in the event of a side impact. The larger diameter provides greater distance from the point of impact to the cask body; however, the effective depth of the limiter is maintained at the trunnions and the same corner impact absorption capability is retained. Figure 2.6.7-11 shows a cross-section of the top impact limiter.

The bottom impact limiter does not have the cut-outs for the trunnions. It has a smaller outside diameter and larger bottom depth than the top impact limiter.

Each impact limiter consists of two different layers of aluminum honeycomb, which are enclosed in a thin outer aluminum shell. The layers of aluminum honeycomb are separated by a thin aluminum sheet. The honeycomb material absorbs the impact energy as it is crushed. A typical load versus deflection curve for aluminum honeycomb is presented in Figure 2.6.7-12. The force deflection curves and test data for the NAC-LWT cask impact limiters at the various drop angles are provided in Appendix 2.10.12. The nominal crush strength of the bottom layer of aluminum honeycomb is 250 psi axially, and is negligible radially. The nominal crush strength of the second layer is 3500 psi in both the axial and the radial directions. The tolerance on the crush strength is +5, -10 percent. The bottom, 250-psi crush strength, single-directional layer of honeycomb material absorbs the majority of the energy in a 1-foot flat impact on the end, and limits the impact force to a value acceptable for normal operations. The lower crush strength is necessary because the impact area is considerably greater in a flat bottom impact than in any other orientation. The second, 3500-psi crush strength, multi-directional layer of honeycomb material absorbs the majority of the energy in an impact on the corner of the impact limiter, and all of the energy in an impact on the side of the impact limiter. Both crushable aluminum honeycomb materials behave as a solid when compressed to 30 percent of their original depth.

The outside diameters of the impact limiters are 65.25 inches and 60.25 inches for the top and bottom impact limiters, respectively. The depth of the bottom aluminum honeycomb layer is 1.5 inches on each limiter. The second aluminum honeycomb layer is 14.0 inches deep for the top impact limiter and 14.5 inches for the bottom impact limiter. The top impact limiter has four recesses to provide clearance around the trunnions. This clearance is closed during the impact for a 30-foot side drop. Therefore, the trunnion provides a rigid foundation for the impact limiter in the region near the trunnion.

The impact limiter shells are positioned against the cask lid and bottom surfaces; the impact limiters overlap the cask cylinder by a length of 12 inches. The shells are mechanically attached to the cask as described in Section 2.6.7.4.7.

For each of the impact load conditions considered in this analysis, the impact limiters remain in position on the cask and absorb the energy of the impact; thus, they limit the impact load to the values calculated in this section.

2.6.7.4.5 Method of Analysis

The primary areas of analytical evaluation that are required in an impact limiter analysis are: (1) crush depth; (2) maximum crush force; and (3) attachment to the cask. The crush depth and maximum crush force are dependent on the crush strength of the crushable material, the area engaged in crushing, the geometry of the impact limiter, and the energy to be dissipated.

Deceleration forces for constant crush strength aluminum honeycomb impact limiters are directly related to the area crushing. The area engaged in crushing can be best explained by examining the experimental results of a top end drop impact test. Figure 2.6.7-13 shows a quarter-scale model impact limiter just before crushing begins. The cask and the unyielding surface are rigid and undeformable compared to the honeycomb material. The 3.9 inches of honeycomb material are trapped in place between the cask and the impacted surface.

The 250-psi crush strength honeycomb is designed to absorb the potential energy of the cask in a 1-foot drop. The area of the 250-psi honeycomb covering the entire bottom of the impact limiter is 208.7 square inches. The higher crush strength honeycomb structurally supports or "backs" the lower crush strength honeycomb, even if just the cask backs the higher crush strength honeycomb. The force necessary to begin crushing the 250 psi crush strength material is 52,168 pounds. The quarter-scale model weighs approximately 800 pounds; therefore, the 52,168 pounds of force is equivalent to 65 g for the model (The normal operation g-load for the full-size cask is calculated to be 16.3 g).

The 3500-psi crush strength honeycomb absorbs the kinetic energy of the cask in a 30-foot drop. The area of the bottom of the scale model cask is 40.7 square inches. The force necessary to crush the 3500-psi crush strength honeycomb trapped between the model cask and the impacted surface is 142,500 pounds, or 178 g, based on the model weight of 800 pounds.

A force imbalance is immediately established between the lower and higher strength honeycombs at the onset of crushing. It requires 52,168 pounds to crush the lower strength honeycomb, which is 2.7 times smaller than the force required to crush the higher strength honeycomb. The lower strength honeycomb of constant crush strength will crush until lock-up occurs. When lock-up occurs, the crush strength of the lower strength honeycomb increases and exceeds that of the higher strength honeycomb. Crushing now begins beneath the cask because the force to crush the 16.3-inch diameter of the locked-up, lower strength honeycomb exceeds the 142,500 pounds necessary to crush the backed-up higher strength honeycomb.

The cask has kinetic energy gained while falling prior to the impact limiter contacting the unyielding surface. (Section 2.10.12 gives a more complete description of the kinetic energy gain.) Some kinetic energy was dissipated in crushing the lower strength honeycomb. The remaining energy will be absorbed by crushing the higher strength honeycomb between the cask and the impacted surface. The cask "backs" the higher crush strength honeycomb; therefore, the maximum force is easily compared with the average maximum force from the quasi-static test as adjusted to reflect the dynamic crush strength of the honeycomb (For an explanation of the term "dynamic" as applied to quasi-static tests, refer to Appendix 2.10.12).

Figure 2.6.7-14 is a photograph of a section of an end impact tested quarter-scale limiter. The average maximum force from the end drop quasi-static crush test is 158,400 pounds. If the backed and unbacked area were to crush, the required force would be 3500 psi x $\pi/4$ $(16.3)^2$ = 730,400 pounds of force. This is a factor of 4.6 times more than the actual measured force and shows that the unbacked area did not contribute to the limiter force. The calculated maximum force using the backed-up area of the limiter is approximately 11 percent lower than the test results. The scale model limiter crush test, therefore, demonstrates that the unbacked area did not crush and generate a force. One reason for the difference is the shearing of the high crush strength honeycomb, which is clearly visible in Figure 2.6.7-14. Shearing acts in a plane, surrounding the shear area. In an end impact crush, the plane is a thin ring with a diameter equal to the diameter of the cask. Since the crush force is proportional to the backed area, which depends on the square of the cask diameter, for the full-scale impact limiters, shearing becomes a much less significant part of the maximum force.

Figure 2.6.7-14 shows the sequence of crushing and the backed area as described above. The lower crush strength honeycomb is crushed to stack height completely to the outer edge of the cask. Higher crush strength honeycomb beneath the cask is crushed, while material on the "other side" of the shear plane is uncrushed.

The combination of the accurate prediction of measured impact limiter crush forces and the visual evidence in the sectioned limiter after the test shows that only the backed-up area crushes for aluminum honeycomb with a 3500-psi, multi-directional, dynamic crush strength.

The cask orientation for a corner impact is defined by the angle from vertical of the cask's longitudinal axis when the cask center of gravity is vertically aligned with the impact point on the limiter. This angle is 15.74 degrees for the top limiter and 14.52 degrees for the bottom limiter.

A proprietary computer program, RBCUBED, is used to analyze an impact limiter for an impact event, to determine the dynamics of the event, to determine the forces generated during that event, and to determine the depth of crush (Section 2.10.1.2).

The computer program, RBCUBED, is run for many combinations of crushable material strength until satisfactory results are obtained. Two runs are made for each impact orientation. One run is made using the maximum value of the aluminum honeycomb crush strength, 105 percent of the nominal crush strength, to determine the maximum force on the cask. A second run, using the minimum value for the aluminum honeycomb crush strength, 90 percent of the nominal crush strength, is also made to find the maximum crush depth of the crushable material.

A single RBCUBED run is necessary to determine the reaction force for a 1-foot fall and a subsequent 30-foot fall. The 1-foot fall crushes the limiter a distance (δ_1), and absorbs

12 inches × 52,000 lbs = 0.624 × 10^6 inch-pounds of energy. Then, the impact limiter must absorb the additional energy of 360 inches × 52,000 lbs = 18.72 × 10^6 inch-pounds by crushing an additional distance (δ_2) from a 30-foot drop. The total displacement is $\delta_1 + \delta_2$ and the total energy is (18.72 + 0.624) × 10^6 = 19.344 × 10^6 inch-pounds. Dividing this energy by the cask weight gives 372 inches (31 feet), which demonstrates that a 1-foot fall followed by a 30-foot fall can be evaluated from data for a 31-foot fall. The maximum impact force and the maximum crush depth for the 1-foot fall can be obtained from the RBCUBED output for the 31-foot fall analysis at the value of the energy dissipated in a 1-foot fall.

2.6.7.4.6 Results

The data in Table 2.6.7-32 and Table 2.6.7-33 give the results of the impact limiter design analyses for a 1-foot fall and a subsequent 30-foot fall, respectively. The calculated g loads for the 30-foot fall side impact are based on the 3675-psi design maximum crush strength of the multidirectional aluminum honeycomb. The calculated g loads for all of the other 1-foot and 30-foot fall impacts are conservatively based on an aluminum honeycomb maximum crush strength of 3850 psi. A design cask weight of 52,000 lbs is used.

The calculated (RBCUBED) and measured (quasi-static, adjusted for dynamic crush strength) force-deflection curves for the NAC-LWT cask impact limiters for all drop orientations are presented in Appendix 2.10.12. To verify the results, the area under the curves is calculated by the trapezoidal method. This area represents the energy dissipated for each of the cases, i.e., E_{max} = 19.344 × 10^6 inch-pounds for the top limiter at maximum strength, and E_{min} = 19.206 × 10^6 inch-pounds for the bottom limiter at minimum strength. The potential energy to be dissipated consists of the cask weight (52,000 lbs) multiplied by the distance the cask falls (372 inches), i.e., E_p = 372 × 52,000 = 19.344 × 10^6 inch-pounds. The calculated and actual values compare within 0.71 percent, which indicates that the proper amount of potential energy is dissipated in the RBCUBED analysis. Another check is to multiply the total crush area (the maximum area backed by the cask) by the crush strength of the impact limiters to determine the reacting force. This hand-calculated value of the reaction force for maximum impact limiter crush strength compares within 0.38 percent of the RBCUBED calculated value for the bottom impact limiter and within 1.88 percent for the top impact limiter. The hand-calculated value of the reaction force for minimum impact limiter crush strength compares within 0.46 percent of the RBCUBED calculated value for the bottom impact limiter and within 1.83 percent for the top impact limiter. These results verify both the energy absorption and the reaction force calculations of RBCUBED for the impact limiters.

A study of a side drop shows that the cask will come to rest at an angle of 0.76 degrees with the horizontal because the radius of the top limiter is 2.5 inches larger than that of the bottom limiter.

The RBCUBED analysis, analyzing the side drop as horizontal, is not affected by this small angle because the horizontal component of the forces is negligible.

With both impact limiters at their minimum allowable crush strength (maximum crush depth case), clearance is maintained between the neutron shield/expansion tank and the unyielding surface for the 1-foot side impact.

An evaluation of the displacements obtained from the RBCUBED runs is as follows:

1. The RBCUBED run for the 31-foot side drop assumes the cask is a rigid element and does not include the trunnions; therefore, the displacement from the 31-foot drop must be analyzed, by referring to Figure 2.6.7-11, as follows:

   The free distance of crushable material between the impact limiter and the trunnion equals 14.995 inches. The aluminum honeycomb compresses to 70 percent of its free height before exhibiting behavior as a solid (10.497 inches). The RBCUBED run for the 31-foot side drop with the crushable material at minimum strength calculates a crush depth of 10.00 inches; thus, 0.497 inch of crushable material remains before solid height occurs. Therefore, an impact directly on a trunnion does not change the energy absorbing characteristics of the impact limiter for this condition.

   The impact from a 31-foot side drop on the bottom impact limiter with the crushable material at minimum strength exhibits solid behavior at a displacement of 10.73 inches, which leaves 0.43 inch displacement before solid height occurs (crush depth = 10.30 inches).

2. The impact from a 31-foot flat end drop onto the top impact limiter with the crushable material at minimum strength exhibits solid behavior at a displacement of 10.85 inches, which leaves 0.61 inch displacement before solid height occurs. Similarly, for the bottom impact limiter, solid behavior occurs at 11.20 inches, which leaves 0.90 inch displacement before solid height occurs.

3. For a 31-foot corner drop on the top impact limiter with the crushable material at minimum crush strength, the crush distance of 12.72 inches is much less than the solid height displacement of 16.86 inches. Similarly, for the bottom impact limiter, the 12.70-inch crush distance is much less than the 15.83-inch solid height displacement.

The cask analysis for these impact conditions is based on the maximum deceleration (g) derived from the RBCUBED results. The critical condition for maximum lateral deceleration from both a 1-foot and a 31-foot drop is the side drop with the crushable material at its maximum strength. The critical condition for maximum longitudinal deceleration from a 1-foot drop is the flat bottom drop with the crushable material at its maximum strength, and from a 31-foot drop is the corner drop. The longitudinal component of the deceleration from the 31-foot corner drop was used as the longitudinal criteria; that is, 60.4 cos 15.74 degrees equals 58.1 g. Nevertheless, a 60.0 g (deceleration) is conservatively used as the maximum longitudinal deceleration. The design g load factors (deceleration values) for the NAC-LWT cask analyses are summarized in Table 2.6.7-34. The design g load for the 31-foot side drop is based on the 3675-psi design maximum crush strength of the aluminum honeycomb impact limiters. The design g loads for all of the other 1-foot and 31-foot drops are conservatively based on an aluminum honeycomb maximum crush strength of 3850 psi.

2.6.7.4.7 Impact Limiter Attachment Analysis

A three-part design criteria applies to the method of attachment of the impact limiters to the cask body. These three criteria are as follows:

1. The impact limiters must remain attached to the cask body during normal handling and transport. Satisfaction of this criterion ensures that the limiters will be in a proper position to perform their impact limiting function in the event of a free drop (normal or accident).
2. In a free drop (normal or accident), the limiter(s) making initial contact with the unyielding surface must remain in position on the end(s) of the cask for the full duration of the initial impact. Satisfaction of this criterion ensures that the limiter(s) will be able to properly perform their impact limiting function.
3. In a free drop (normal or accident) involving an initial impact on a single impact limiter, the limiter on the opposite end of the cask must remain attached to the cask during the initial impact. Satisfaction of this criterion ensures that the limiter will be in a proper position to perform its impact limiting function in a subsequent secondary impact following the initial impact.

Section 2.6.7.4.7 demonstrates that each of the above criterion are satisfied.

Impact Limiter Attachment During Normal Handling and Transport

Attachment of the impact limiters to the cask body during normal handling and transport is ensured by demonstrating that the attachment hardware (pins, lugs and associated welds) does not yield under normal handling and transport conditions. The worst case loading associated with normal handling and transport is taken to be a 10-g axial loading associated with rail transport [10 CFR 71.45 (b)]. This bounds the 2.0-g load corresponding to the peak shock loading expected as the result of truck transport (per ANSI N14.23 for air ride suspensions). For this normal condition evaluation, it will be assumed that only two of the four attachment points for each limiter are effective. The load, P, per attachment point therefore becomes:

$$P = 10.0(1535)/2$$
$$= 7,675 \text{ lbs}$$

where 1,535 lbs is the weight of the heaviest (top) impact limiter.

Analysis of Impact Limiter Lug

The geometry of the impact limiter lug is as shown in Figure 2.6.7-15. As shown, the lug has an outer width of 2.0 inches, a hole diameter of 0.53 inch and an edge distance of 1.7 inches. The lug is made of 6061-T651 aluminum and is 0.5-inch thick. According to Table 2.3.1-4, the yield strength of the aluminum at 150°F is 32,700 psi. Potential failure modes of tension across the net section and 40-degree shearout are considered as follows:

Tension Across the Net Section

$P = 7{,}675$ lbs

$A = 0.5(2.0 - 0.53)$

$= 0.735\ in^2$

$S_t = 7{,}675/0.735 = 10{,}442$ psi ($S_y = 32{,}700$ psi)

$MS = 32{,}700/10{,}442 - 1$

$= +\underline{2.13}$

40-Degree Shearout

$P = 7{,}675$ lbs

$e = 1.7 - (0.53/2) \cos 40°$

$= 1.497$ inches

$A_s = 2(0.5)(e)$

$= 1.497\ in^2$

$S_s = 7{,}675/1.497$

$= 5{,}127$ psi ($0.6\ S_y = 19{,}620$ psi)

$MS = 19{,}620/5{,}127 - 1$

$= +\underline{2.83}$

An optional impact limiter lug configuration permits the gusset plate impact limiter attachment tab to be an assembly of the tab and gusset plate using a full-penetration weld. The structural strength of the weld using a mock-up test confirms that the minimum weld yield strength is equal to or greater than 10 ksi. The only stress applicable to the weld is the tension across the entire section of the weld. Using the bounding load of 7,675 pounds, the margin of safety for the weld region is:

$MS = 10{,}000/7{,}675 - 1$

$= \underline{+0.30}$

Both the 6061-T651 continuous tab gusset configuration and the optional full-penetration weld assembly configuration are confirmed to maintain the attachment of the impact limiters to the cask body for truck or rail transport.

Analysis of Cask Lug

The geometry of the cask lug is a shown in Figure 2.6.7-16. As shown, the lug actually consists of two, 0.5-inch thick lugs, which are integral to a common base plate (the lugs and base plate are machined from one piece). Each of these two lugs is 2.0 inches wide, has a hole diameter of 0.53 inch and has a minimum edge distance of 0.72 inch. The base plate is 1.6 inches wide and 2.0 inches long. The material used is Type 304 stainless steel, which exhibits a yield strength at 150°F of 27,500 psi. Potential failure modes of 40-degree shearout and failure of the weld (3/8-inch bevel plus 3/8-inch fillet), which attaches the base plate to the cask body, are considered as follows:

40-Degree Shearout

$F = P/2 = 1535/2$

$= 768$ lbs

$e = 0.72 - (0.53/2) \cos 40°$

$= 0.517$ in

$A_s = 2(0.5)(e)$

$= 0.517\ in^2$

$S_s = 768/0.517$

$= 1485$ psi ($0.6\ S_y = 16{,}500$ psi)

MS = 16,500/1485 - 1 = +Large

Weld Stresses

The analysis of the weld will conservatively ignore the 3/8-inch bevel weld and only consider the 3/8-inch fillet weld around the perimeter of the base plate. Stresses in this weld resulting from the imposed bending moment and the imposed direct shear load will both be treated as shear stresses, combined using a square root sum of squares approach and compared against a shear allowable limit. The stress in the weld due to the applied moment is as follows:

$s_1 = 4.24M/(h[b^2 + 3L(b + h)])$

$= 2006$ psi

where:

M = 1.78(P) = 2732 in-lb

P = 1,535 lbs

h = 3/8 = 0.375 in

b = 2.0 inches

$L = 1.6$ inches

The stress in the weld due to the applied shear load is:

$s_2 = P/A_s$

$= 804$ psi

where:

$P = 1{,}535$ lbs

$A_s = 2(1.6 + 2.0)(0.707)(0.375)$

$= 1.909 \text{ in}^2$

The combined stress is therefore:

$s = (s_1^2 + s_2^2)^{0.5}$

$= 2161$ psi ($0.6\ S_y = 16{,}500$ psi)

$MS = 16{,}500/2161 - 1$

$= +$Large

Analysis of Ball-Lock Pin

The 1/2-inch, AVIBANK 57459-1 ball-lock pins have a 36,800-pound capacity in double shear. With an applied load of 1,535 lbs, the margin of safety is very large.

Response of Impact Limiter(s) During Initial Impact of Package with Ground

The second criterion applicable to the impact limiters requires that the limiter(s) making initial contact with the unyielding surface must remain in position on the end(s) of the cask for the full duration of the initial impact. To satisfy this criterion, attachment hardware (pins, lugs and/or associated welds) may fail during an impact event as long as the limiter(s) being crushed remains in position on the end of the cask and does not separate from the cask. The ability of the limiter to remain in position during an impact is demonstrated with reference to a series of dynamic, free drop tests (end, center of gravity over corner, side and oblique), during which some attachment hardware failure occurred, and to several static crush tests, during which the only attachment mechanism was a strip of duct tape. All of the tests were performed using quarter-scale models of the limiters. Analytic evaluations are also presented to further justify that the limiters will remain in position during the impact.

Dynamic Free Drop Test Results

As presented in Appendix 2.10.8, a series of 30-foot free drop tests were performed on a quarter-scale model of the NAC-LWT cask. Drop orientations included an end drop, a center of gravity over struck corner drop, a side drop and an oblique drop with a subsequent secondary impact. A study of the drop test photographs presented in Appendix 2.10.8 indicates that although attachment hardware failed in some of the dynamic free drop tests, the limiters did not physically separate from the cask body and did completely perform their intended impact limiting function. In fact, the limiters wedged themselves even more securely onto the cask body.

At all times during the testing, the limiters remained in position on the ends of the cask. Notably, rebound from the drop pad due to the whipping action of the restraint cables, did not result in the limiters separating from the cask even though some attachment hardware failure had occurred. This observation demonstrates a tendency for the limiters to become wedged onto the cask body as the result of an impact.

Based on the above test observations, the conclusion reached is that the limiters will remain in position on the cask body during the full duration of the free drop impact event.

Static Crush Test Results

A series of quasi-static crush tests have been performed on quarter-scale models of the bottom impact limiter for the NAC-LWT cask. The limiter orientations tested were end (axial), side and center of gravity over corner (15.7 degrees from axial). The purpose of the quasi-static crush tests was to document the force-deflection and energy absorption characteristics of the honeycomb material used in the impact limiter. Additionally, the tests demonstrated that the limiters need not be mechanically attached to the cask body in order to remain in position to absorb the energy of crushing. No attachment between the model limiter and the test fixture was used for the end (axial) test. A strip of duct tape was adequate to retain the model limiters in position on the side (90-degree) and center of gravity over corner (15.7-degree) fixtures. Once crushing of the limiter is initiated, its cup-shaped geometry causes it to maintain its position on the fixture, which is identical to a quarter-scale model cask body. Thus, attachment of the impact limiter to the cask body is not necessary for maintaining proper position and energy absorption capability.

Analytic Evaluations

Although the results from the above discussed test programs are considered to be the primary proof that the limiters will remain in position during the impact event and properly perform their impact limiting function, analytic studies can also be used to confirm the test observations. Analytic assessments presented in this evaluation indicate that failure of the attachment hardware can be expected to occur for some drop orientations, but subsequent to such failure, the cask tends to wedge into the limiter and separation of the limiter from the cask does not occur. As shown, a significant resistance to the applied separation moment exists due to a combination of crushing of the limiter at the cask interface and due to frictional resistance that exists there. This total resistance is shown to be greater than the applied separation moment and is approximately 7.9 times greater than that provided by the attachment hardware alone.

Additionally, it is noted that the maximum applied separation moment occurs early in the impact when crush depths are small. As crush depths increase, the moment arm and the separation moment decrease to zero. The maximum separation moments occur early in the impact event when the package still possesses a significant downward velocity (87 percent of the initial impact velocity). Additionally, the duration of the impact is very short (approximately 0.04 to 0.06 seconds) and minimal rotation (approximately 1 degree) of the package occurs during the impact. Thus, the cask "drives" into the limiter and physically "traps" the limiter between the cask body and the ground.

The remainder of this section presents a detailed analytic study of the center of gravity over top corner impact event. This near vertical orientation, coupled with the fact that little energy will be converted into rotational energy of the entire package (that is, the center of gravity is over the impacted corner), makes this particular orientation a representative worst case regarding the development of significant separation moments. The available impact limiter analysis program results associated with the corner drop are summarized in Figure 2.6.7-17. The crush depths, crush forces and package velocities presented in the summary figure are directly available from the impact limiter analysis program, RBCUBED, and the separation moment is calculated based on the geometry (that is, the crush footprint) existing at the particular position of interest. Of note, the velocity of the package is still 466.2 inches/second (87 percent of the initial impact velocity) when the maximum separation moment of 7.67×10^6 inch-pounds has developed.

Capability of Attachment Hardware

Figure 2.6.7-18 presents a free body diagram for the top impact limiter during a top down center of gravity over corner impact. With point "A" being the pivot point of the impact limiter on the cask, taking moments about point "A" yields the following:

$$F_i x_i = 14.45\ F_2 + (14.45 + 16.1)\ F_1$$
$$= 14.45\ F_1 + 30.55\ F_1$$
$$= 45.0\ F_1 = \text{separation moment}$$

where:

F_1 = maximum force on a lug

$F_2 = 2(F_1/2) = F_1$

F_3 = 0.0 (approximately)

F_i = impact force at limiter to ground interface

x_i = moment arm for force F_i

According to the section titled "Response of Secondary Impact Limiter During Initial Impact of Package," the failure mode for the attachment hardware is tension on the net section of the impact limiter lug. Failure will occur at a load of 28,445 pounds, which corresponds to a stress equal to the ultimate strength of the aluminum lug. Substitution into the above separation moment equation indicates that a moment of 1.28×10^6 inch-pounds can be expected to fail the attachment hardware. As seen from Figure 2.6.7-17, this moment is exceeded prior to 2 inches of crush occurring for the limiter. Attachments may, therefore, fail in the center of gravity over top corner drop.

Resistance to Separation Following Attachment Hardware Failure

If attachments do fail, the cask tends to wedge itself into the limiter as shown in the free body diagram presented as Figure 2.6.7-19. From that figure:

f_{max} = force required to crush limiter honeycomb

= 28.9 S_c (projected area x crush strength) = 28.9(3850)

= 111,265 lb/in

where:

S_c = crush strength of honeycomb used in limiter

= 3850 psi (conservative upper bound crush strength, which was the case selected for Figure 2.6.7-17; the design upper bound crush strength is 3675 psi)

From moment equilibrium:

$F_i x_i = (6\ f_{max}) = 36\ f_{max}$

$= 4.006 \times 10^6$ in-lb

A significant frictional resistance to separation of the limiter also exists. Selecting a coefficient of friction of approximately 0.5 for aluminum on steel (Baumeister, pages 3-26), the frictional resistance to the separation moment is:

$M_f = F_f\, d$

$= 6.145 \times 10^6$ in-lb

where:

F_f = friction force

$0.5(6\ f_{max}) = 3\ f_{max} = 333{,}795$ lbs

and with the centroid of a 180-degree arc (that is, the arc over which f_{max} acts) being located at 63.7 percent of its radius:

d = 0.637(28.9)

= 18.41 inches

The total resistance to separation, therefore, becomes:

$$M_t = 4.006 \times 10^6 + 6.145 \times 10^6$$
$$= 10.151 \times 10^6 \text{ in-lb}$$

This total resistance to separation exceeds the maximum applied separation moment of 7.67×10^6 inch-pounds (Figure 2.6.7-17). Separation of the limiter from the cask body will not occur. As discussed in the section titled "Dynamic Free Drop Test Results," this particular center of gravity over corner case was tested. Test results are consistent with the preceding analysis in that attachment hardware did fail, that the cask did tend to wedge itself into the impact limiter, and that physical separation did not occur (Appendix 2.10.8, Figures 2.10.8-15 and 2.10.8-16).

Response of Secondary Impact Limiter During Initial Impact of Package

The final criterion to be satisfied is for a free drop (normal or accident) involving an initial impact on a single impact limiter, that the limiter on the opposite end of the cask (secondary limiter) must remain attached to the cask during the initial impact. This ensures that the secondary limiter will be in position to absorb the secondary impact and, as discussed in the section titled "Response of Impact Limiter(s) During Initial Impact of Package with Ground," it remains in position for the full duration of the secondary impact and performs its impact limiting function. Attachment is ensured by demonstrating that the attachment hardware (pins, lugs and associated welds) does not fail during the initial impact while the far end of the transport cask is rotating about the end that is in contact with the ground. For this evaluation, the worst case loading on the secondary impact limiter to separate it from the cask is bounded by the condition that all of the kinetic energy at the time of impact is converted to angular rotation. The angular rotation speed (ω) results in a radial angular acceleration (A_r) of the far end of the cask (a radius of r) that is computed by $r\omega^2$. The angular speed is determined by using conservation of energy,

$$\omega = \sqrt{\frac{2WH}{I}}$$

where:

The moment of inertia of the cask (I) about the point of rotation is computed for a 199.8-in long, 39.23-in diameter, right circular cylinder about the edge in conjunction with the impact limiter (M_L) (see page 34 of "Formulas for Natural Frequency and Mode Shape," Robert D. Blevins, Ph.D, Krieger Publishing Co., Inc., 1984):

$$I = (M)\times\left[\frac{1}{12}\left(3\times(R)^2 + (L)^2\right) + (R)^2\right] + M_L \times L^2$$

$$= \left(118.2\ \text{lb}\cdot\text{sec}^2/\text{in}\right)\times\left[\frac{1}{12}\left(3\times\left(\frac{39.23\ \text{in}}{2}\right)^2 + (199.8\ \text{in})^2\right) + \left(\frac{39.23\ \text{in}}{2}\right)^2\right] + 3.97\times 199.8^2$$

$$= 6.09\times 10^5\ \text{lb}\cdot\text{sec}^2\cdot\text{in}$$

where,

M = mass of the empty cask, less the weight of one impact limiter = $\frac{45{,}673\ \text{lbs}}{386.4\ \text{in}/\text{sec}^2} = 118.2\ \text{lb}\cdot\text{sec}^2/\text{in}$

M_L = mass of the impact limiter = $\frac{1{,}535\ \text{lbs}}{386.4\ \text{in}/\text{sec}^2} = 3.97\ \text{lb}\cdot\text{sec}^2/\text{in}$

The bounding angular velocity is therefore:

$$\varpi = \sqrt{\frac{2\times W\times H}{I}} = \sqrt{\frac{2\times 47{,}208\ \text{lbs}\times 360\ \text{in}}{6.09\times 10^5\ \text{lb}\cdot\text{sec}^2\cdot\text{in}}} = 7.47\ \text{rad}/\text{sec}$$

The radial acceleration (A_r) (g) using a radius of 200 inches from the bottom to the top end of the cask is:

$$A_r(g) = \frac{200\ \text{in}\times\left(7.47\ \text{rad}/\text{sec}\right)^2}{386.4} = 28.9\ \text{g's}$$

The calculations for the stress conservatively use the maximum acceleration of 30 g's. With four attachment points, the load, P, per attachment point therefore becomes:

P = 30 × 1,535/4

= 11,513 lbs

where 1,535 pounds is the weight of the heaviest (top) impact limiter.

Analysis of Impact Limiter Lug

The impact limiter lug is evaluated using the same approach as was used in the section titled "Analysis of Impact Limiter Lug," but the allowable limit is based on ultimate strength rather than yield strength. As shown in Table 2.3.1-4, the ultimate strength of 6061-T651 aluminum at 150°F is 38,700 psi. Potential failure modes of tension across the net section and 40-degree shearout are considered as follows:

Tension Across the Net Section

$P = 11{,}513$ lbs

$A = 0.5(2.0 - 0.53)$

$= 0.735$ in^2

$S_t = 11{,}513/0.735$

$= 15{,}664$ psi ($S_u = 38{,}700$ psi)

$MS = 38{,}700/15{,}664 - 1$

$= +1.47$

40-Degree Shearout

$P = 11{,}513$ lbs

$e = 1.7 - (0.53/2) \cos 40°$

$= 1.497$ inches

$A_s = 2(0.5)(e)$

$= 1.497$ in^2

$S_s = 11{,}513/1.497$

$= 7{,}691$ psi ($0.6\ S_u = 23{,}220$ psi)

$MS = 23{,}220/7{,}691 - 1$

$= +2.02$

An optional impact limiter lug configuration permits the gusset plate impact limiter attachment tab to be an assembly of the tab and gusset plate using a full-penetration weld, as described in Section 8.2.1.1, Impact Limiter Attachment Lug Repairs. Structural strength of the weld using a mock-up test confirms that the minimum weld tensile strength is equal to or greater than 20 ksi. The only stress applicable to the weld is the tension across the entire section of the weld. Using the bounding load of 11,513 pounds, the tensile stress is 11,513 (2×1/2) or 11,513 psi and the margin of safety for the weld region is:

$MS = 20{,}000/11{,}513 - 1$

$= \underline{+0.74}$

Both the 6061-T651 continuous tab gusset configuration and the optional full-penetration weld assembly configuration are confirmed to maintain the attachment of the impact limiters during the bounding condition of the accident side drop condition.

Analysis of Cask Lug

The cask lug is evaluated using the same approach as was used in the section titled "Analysis of Impact Limiter Lug," but the allowable limit is based on ultimate strength rather than yield strength. The ultimate strength of Type 304 stainless steel at 150°F is 73,000 psi. Potential failure modes of 40-degree shearout and failure of the weld (3/8-inch bevel plus 3/8-inch fillet), which attaches the base plate to the cask body, are considered as follows:

40-Degree Shearout

$F = P/2 = 23{,}179/2$

$= 11{,}590$ lbs

$e = 0.72 - (0.53/2) \cos 40°$

$= 0.517$ in

$A_s = 2(0.5)(e)$

$= 0.517 \text{ in}^2$

$S_s = 11{,}590/0.517$

$= 22{,}418$ psi ($0.6\ S_u = 43{,}800$ psi)

$MS = 43{,}800/22{,}418 - 1$

$= +0.95$

Weld Stresses

The analysis will again conservatively ignore the 3/8-inch bevel weld and only consider the 3/8-inch fillet weld around the perimeter of the base plate.

The stress in the weld due to the applied moment is:

$s_1 = 4.24\ M/(h[b^2 + 3\ L(b + h)])$

$= 30{,}292$ psi

where:

$M = 1.78(P) = 41{,}259$ in-lb

$P = 23{,}179$ lbs

$h = 3/8 = 0.375$ in

$b = 2.0$ in

$L = 1.6$ in

The stress in the weld due to the applied shear load is:

$s_2 = P/A_s$

$= 12{,}142$ psi

where:

$P = 23{,}179$ lbs

$A_s = 2(1.6 + 2.0)(0.707)(0.375)$

$= 1.909 \text{ in}^2$

The combined stress is therefore:

$s = (s_1^2 + s_2^2)^{0.5}$

$= 32{,}635$ psi ($0.6\ S_u = 43{,}800$ psi)

MS = 43,800/32,635 - 1

= +0.34

Analysis of Ball-Lock Pin

The 1/2-inch, AVIBANK 57459-1 ball-lock pins have a 36,800-pound capacity in double shear. With an applied load of 23,179 pounds, the margin of safety becomes:

MS = 36,800/23,179 - 1

= +0.59

2.6.7.5 Closure Lid

2.6.7.5.1 Discussion

The NAC-LWT cask closure lid is analyzed for structural adequacy in accordance with the requirements of 10 CFR 71.73(c)(1) free drop (hypothetical accident condition). The cask is assumed to be inverted, with the lid downward, when dropped through a distance of 30 feet onto a flat, unyielding, horizontal surface. The structural evaluation is performed by classical elastic analysis methods.

2.6.7.5.2 Analysis Description

Geometry

The closure lid geometry is shown in Figure 2.6.7-20. The lid is bolted in position on the upper end of the cask. The lid material is Type 304 stainless steel. The temperature-dependent material properties for Type 304 stainless steel, which are presented in Section 2.3, are used in this analysis.

Loadings

During impact, the cask cavity contents are considered to apply an internal inertia pressure on the interior surface of the lid in the outward normal direction. The impact limiter applies an external inertia pressure on the exterior lid surface in the inward normal direction; however, this pressure is conservatively ignored in this analysis. Each bolt is torqued to a preload force of 21,000 pounds. The lid is also loaded with an assumed 50-psig internal pressure for the 130°F ambient temperature hot case.

Displacement Boundary Conditions

The closure lid is restrained from vertical and rotational deformation at the 17.875-inch bolt circle diameter by the preloaded lid bolts.

Detailed Analysis

For the loading and boundary conditions described, the structural behavior of the closure lid may be assessed by superposition of maximum stresses from Section 2.6.1, which includes consideration of thermal effects, bolt preload, and internal pressure, with the maximum stresses produced by the inertia loading. The maximum $P_m + P_b$ component stresses from Section 2.6.1 (Table 2.6.1-2) are:

S_x = -3060 psi; S_y = - 260 psi; S_z = 100 psi; S_{xy} = 180 psi

The free body diagram of Figure 2.6.7-21 can be evaluated by applying formulas from Case 6 (Roark, page 217) for a uniformly loaded circular plate.

The total deceleration force of the contents, F_D = 4000 lbf × 60 g deceleration = 240,000 lbf, creates a pressure, W, on the lid interior surface:

$$W = \frac{240{,}000}{\pi(8.938)^2} = 956 \text{ psi}$$

The maximum radial, tangential, and vertical stresses on the lid are:

$$S_r = \frac{3Wa^2}{4t^2}$$

$$= 895 \text{ psi}$$

$$S_t = \frac{3Wa^2\gamma}{4t^2}$$

$$= 246 \text{ psi}$$

$$S_v = -W$$

$$= -956 \text{ psi}$$

where:

a = 8.938 inches

γ = 0.275

t = 8.0 inches

Conservatively combining these stresses with $P_m + P_b$ stresses from Section 2.6.1 (Table 2.6.1-2), the total $P_m + P_b$ component stresses on the lid are:

S_x = -3955 psi; S_y = - 1216 psi; S_z = 346 psi; S_{xy} = 180 psi

For small S_{xy}, the stress intensity becomes S.I. = S_z - S_x = 4301 psi. Since the maximum cask lid temperature is less than 300°F for the 130°F ambient temperature hot case (Section 3.4.2), the closure lid allowable $P_m + P_b$ stress is 72,000 psi (3.6 S_m). Therefore, the minimum margin of safety is +Large; thus, containment is maintained.

2.6.7.5.3 Conclusion

It is demonstrated by use of a conservative loading that the minimum margin of safety is +4.23 and containment is maintained. Therefore, the NAC-LWT cask lid satisfies the requirements of 10 CFR 71 for consideration of the closure lid impact in the 30-foot free drop accident.

2.6.7.6 Bolts - Closure Lid (Normal Conditions of Transport)

The NAC-LWT cask closure lid is bolted to the cask body top forging with twelve 1 - 8 UNC bolts fabricated from SA-453, Grade 660 high alloy steel. The threaded portion of the bolt engages the cask body a minimum of 1.875 inches. In accordance with the free drop provisions of the normal conditions of transport, 10 CFR 71.71(c)(7), this bolted closure has been carefully evaluated for structural adequacy and found to satisfy all regulatory requirements and design criteria. Details of this analytic evaluation follow.

The simultaneous loads that may be imposed upon the cask closure bolts include: pressure loads, thermal differential expansion loads, pre-loads and inertial loads arising from impact responses. For a given set of initial conditions, the pressure loads, thermal loads and pre-loads all remain constant. Inertial impact loads, however, vary with impact orientation and bolt location. Lateral impact loads acting upon the lid are directly related to the mass of the lid and the lateral impact acceleration. Longitudinal impact loads acting on the lid are proportional to the longitudinal impact acceleration, as well as, the mass of the lid and the payload within the containment cavity.

In general, these lid impact loads impose unequal individual forces, or loadings, in the closure bolts. This NAC-LWT cask evaluation conservatively assumes a set of impact forces that induce maximum containment closure separation forces and bolt loadings. With this conservative assumption, the external impact force is presumed to be located at a point where it cannot restrain those forces that tend to separate the cask lid from the cask body. This assumption locates the external impact force at the lower corner of the lid-body interface. With this assumption the lower corner of the lid is assumed to be pinned (by the impact forces), and bolt tension forces are assumed to vary linearly from zero at this pinned lower corner to a maximum value at the opposite, or upper, corner of the lid.

A complete range of impact orientations is evaluated, from an end impact at 0 degrees to a flat side impact at 90 degrees, and at 5-degree increments in between. Loads are derived from the normal impact accelerations summarized within Table 2.6.7-34. Where necessary, impact accelerations have been interpolated at 5-degree increments from those values given in Table 2.6.7-34.

The details of this analytic evaluation are described and performed within Section 2.10.9 for both normal conditions of transport and hypothetical accident conditions. Normal conditions of transport results are summarized in Table 2.6.7-35 and Table 2.6.7-36, corresponding to a "hot" initial condition and a "cold" initial condition, respectively. The hot initial condition bolt temperature is taken at 227°F, as summarized in Table 3.4-2. The cold initial condition bolt temperature is assumed to be -20°F, per regulatory requirements. Physical properties for the SA-453, Grade 660 bolts are conservatively taken at 300°F and at room temperature (70°F) for hot and cold conditions, respectively. As defined within Table 2.1.2-1, the allowable bolt stress is taken as S_y, leading to allowable direct tension stresses of 81.9 and 85.0 ksi, at 300°F and 70°F, respectively. Based on this thorough evaluation, the closure bolts incur a maximum stress intensity of 61,012 psi, which results in a minimum margin of safety of 34 percent. See Table 2.6.7-35 (at 5°):

$$MS = 81.9/61.042 - 1$$
$$= +0.34$$

Bolt engagement may be evaluated by computing shear stresses within the SA-336, Type 304, end forging material. At 300°F, the allowable shear stress is 0.5 S_y, or 11.25 ksi, according to Tables 2.1.2-1 and 2.3.1-1. The maximum tensile load is found as the product of the maximum bolt stress intensity, noted above, and the bolt stress area; that is, (61,042 psi)(0.6051) = 36,937 pounds. The shear area per inch of engagement for a 1 - 8 UNC internal thread is 2.325 in^2/in ("Table Speeds Calculation of Strength of Threads," pp. 41-49). The resultant shear stress and margin of safety within the top body forging is:

$$\tau = P/A = (36,937)/[(2.325)(1.875)]$$
$$= 8473 \text{ psi}$$
$$MS = 11.25/8.473 - 1$$
$$= +0.33$$

Using consistently conservative assumptions, the NAC-LWT cask lid bolted closure can be shown to satisfy the performance and structural integrity requirements of 10 CFR 71.71(c)(7) for normal conditions of transport.

2.6.7.7 Neutron Shield Tank

2.6.7.7.1 Introduction

The neutron shield tank is welded to, and concentric with, the NAC-LWT cask outer shell. The tank consists of eight cells. The neutron shield fluid flows freely through holes in the longitudinal stiffeners between these cells. During thermal expansion or contraction, fluid passes through the valve assembly into or out of the expansion tank, which is external to and concentric with, the shield tank. Table 2.6.7-37 summarizes the results of the structural analyses described below. The table shows positive margins of safety, demonstrating that each component of the neutron shield tank satisfies the requirements of the normal operations conditions 1-foot free drop as described in 10 CFR 71.71. Classical analysis techniques are used to demonstrate that each tank component withstands the hydrodynamic loads from a 1-foot side or end drop in combination with internal tank pressure. Similarly, classical analyses show that the shield/expansion tank does not rupture, nor does the check valve sustain damage during the penetration test.

The shield tank wall has a mean diameter of 39.04 inches, is located approximately 23 inches below the top edge of the upper end casting, and extends 164 inches longitudinally. Constructed entirely of Type 304 stainless steel, the tank external shell and eight longitudinal stiffeners are 0.24-inch thick plate. Each end of the tank is a 0.50-inch thick end plate. Equally spaced between stiffeners are eight 0.24-inch thick gusset plates, which provide additional support to the end plates.

A 56 percent by volume ethylene glycol and water solution provides the neutron shielding. The shield tank fluid volume (excluding stiffeners) is 84,742 cubic inches or approximately 370 gallons (3,280 pounds) of fluid. At the upper end, concentric with the shield tank, is the expansion tank. The expansion tank is 46 inches long and is constructed from 0.32-inch thick stainless steel plate; there are eight cells divided by equally spaced plate stiffeners with holes in them, which enables the fluid to flow from chamber to chamber. The expansion tank empty volume is 13,245 cubic inches. It is filled with 11.5 gallons (103 pounds) of solution initially, leaving an expansion volume of 10,589 cubic inches. At the bottom of the expansion tank is a siphon tube, which goes around the shield tank and exits at its top. Volumetric expansion forces fluid through the siphon tube. During heating, the solution in the shield tank expands into the expansion tank avoiding uncontrolled pressurization of the shield/expansion tank. A pressure relief valve in the shield tank assures that the tank structure is protected against over pressurization. The pressure relief valve is set to begin relieving pressure at 165 psig. Initially, the expansion tank is filled with 11.5 gallons of fluid to assure that the shield tank remains filled at -40°F. A cross section of the upper end of the cask with pertinent dimensions is shown in Figure 2.6.7-22.

2.6.7.7.2 Structural Criteria

The neutron shield tank and expansion tank analyses use 10 CFR 71 and Regulatory Guide 7.8 to determine load/ambient conditions to bound other load conditions. In this way, the shield/expansion tank components are conservatively analyzed for the most severe structural loads at maximum temperatures; thus, the material properties and allowable stresses have minimum values.

The 10 CFR 71 requires that all transport packages weighing more than 30,000 pounds be evaluated to determine the consequences of a free fall through a distance of 1-foot onto a horizontal, unyielding surface for normal operation; cask orientation during the fall shall be such that maximum damage is inflicted upon the cask. End and side drop g loads are the most severe normal operating loads that the cask sustains; analyses of the shield and expansion tanks are based on the end and side drop loads. All other cask drop orientations produce less severe g loads.

Table 2 in Regulatory Guide 7.8 defines three initial ambient states that guide the analyses. The two extreme cases used to envelope analyses are:

1. 100°F ambient temperature, with maximum insolation, decay heat, internal pressure, weight, and minimum external pressure
2. 20°F ambient temperature, with no insolation or decay heat, minimum internal pressure, weight, and external pressure.

These conditions are used to evaluate the shield tank fluid temperatures (Actually, Sections 3.4.2 and 3.4.3 results, which are based on the more limiting ambient temperatures of 130°F and -40°F are used). With the fluid temperatures established, it is then possible to calculate the shield/expansion tank pressures for the extreme cases and the resulting amount of fluid flowing between the shield tank and the expansion tank (for expansion tank sizing). Table 2.6.7-38 summarizes the calculated shield tank fluid temperatures used in analyzing the shield tank structure.

Since the functional and structural adequacy of the neutron shield and expansion tanks depend on linear elastic evaluations, the allowable stress criteria is selected as the material yield strength. All calculated stresses are less than this criteria. From Table 2.6.7-38, the highest average fluid temperature is 227°F; therefore, material properties for 250°F are used in the analyses. The evaluation of the shield/expansion tank and the resulting conclusions are conservative.

2.6.7.7.3 Neutron Shield and Expansion Tank Loads

Structural, hydrostatic/hydraulic pressure and expansion pressure are the three components of shield tank loads. Structural loads result from decelerating the cask structure. Hydrostatic and hydraulic loads (water hammer) result from the shield tank fluid decelerating against the shield tank structure. Expansion pressure loads are generated when the fluid expands during heating. An explanation of how each type of load is calculated follows.

Structural loads are loads imposed on the structure by the weight of the structure itself. The stainless steel materials from which the cask is fabricated all have mass and are acted upon by gravity and the normal operations conditions 1-foot drop deceleration. Shield tank structural components weigh approximately 2,116 pounds. Expansion tank components weigh approximately 610 pounds. These loads are included in the analysis of the tanks.

Hydrostatic pressure is the pressure at a given depth within a fluid caused by the mass of the fluid being accelerated by gravity. Hydraulic pressure is the hydrostatic pressure acted upon by accelerations other than gravity. To determine the hydrostatic pressure of fluid acting on the plate, the following formula is used:

$$p = \rho g h$$

where:

ρ = mass density of fluid (lbm/in^3)

g = acceleration due to gravity (in/sec/sec)

h = height of fluid above point considered (in)

When the cask is vertical, the maximum fluid height in the shield tank is 164 inches, which is equivalent to 6.3 psig under the acceleration of gravity (1 g). When the cask is in the horizontal position, there is a 39-inch maximum fluid height (diameter of shield tank) or 1.56 psig (1 g). The presence of the expansion tank around the shield tank is conservatively neglected, because the fluid pressure acting on the exterior of the shield tank reduces the forces acting on the shield tank components. During a 1-foot end drop (normal operations conditions), the cask undergoes a 15.8 g deceleration (Section 2.6.7.4). This results in a hydraulic pressure of 100 psig (6.3 psig × 15.8 g) at the bottom of the shield tank. Similarly, during the side drop, the pressure at the lowest point on the shield tank is 38 psig (1.56 psig × 24.3 g). The maximum hydrostatic and hydraulic pressures for the end and side drops and the location of the maximum pressure for the shield tank analyses are shown in the following sketches.

1-Foot End Drop (15.8 g)

Maximum Hydrostatic Pressure	Maximum Hydraulic Pressure
6.3 psig	100 psig

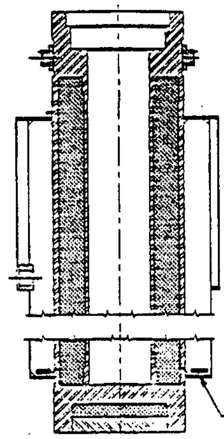

Vertical Orientation

1-Foot Side Drop (24.3 g)

Maximum Hydrostatic Pressure	Maximum Hydraulic Pressure
1.56 psig	38 psig

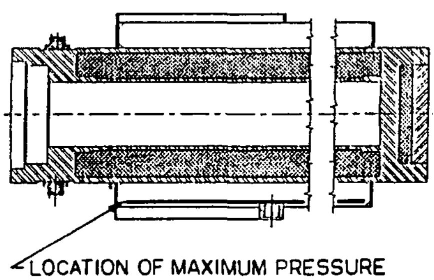

Horizontal Orientation

The g loads for various drop orientations and how they were calculated are explained in Section 2.6.7.4.

Once the shield/expansion tank is filled, it is a sealed compartment, which will not permanently deform under normal transport conditions. The neutron shield tank solution expands or contracts when heated or cooled. During heating the liquid expansion causes fluid to flow into the expansion tank, compressing the air in the expansion tank and causing the pressure to increase. Similarly, as the cask fluid temperatures reach 40°F, there is sufficient fluid in the expansion tank to always keep the neutron shield tank completely filled.

The neutron shield tank is completely filled in the upright configuration, when the fluid and ambient conditions are at 68°F. The 56 percent by volume ethylene glycol and water solution has a density of 67.07 lbs/ft^3 at 68°F. After the neutron shield tank is filled, 11.5 gallons of solution are poured into the expansion tank. Both tanks are then sealed.

The normal transport condition of maximum decay heat load, 100°F ambient temperature and maximum insolation results in an average (natural and forced mixing of fluid is assumed) shield tank fluid temperature of 227°F. The volume of fluid that enters the expansion tank as the temperature increases from 68°F to 227°F is:

$$\Delta V = V_1 \left(\frac{\rho_1}{\rho_2} - 1 \right) = 5539 \text{ in}^3$$

where:

ρ_1 = 67.07 lb/ft^3 = density of 56 percent ethylene glycol and water solution at 68°F

ρ_2 = 63.07 lb/ft^3 = density of 56 percent ethylene glycol and water solution at 230°F

V_1 = 87,398 lb/in^3 = volume of fluid in the expansion and shield tank at 68°F

ΔV = volume of fluid entering the expansion tank

Then the increased uniform air pressure in the expansion tank at 230°F is:

$$P_2 = P_1 \left(\frac{V_1 T_2}{T_1 V_2} \right) = 40.3 \text{ psia } (25.6 \text{ psig})$$

where:

P_1 = 14.7 psia

V_1 = 10,589 in^3 (expansion tank air volume at 68°F)

T_1 = 528°R = 68°F

T_2 = 690°R = 230°F

V_2 = 10,589 in^3 - 5539 in^3 - 5050 in^3 (expansion tank air volume at 230°F)

The same analysis procedure was used to calculate the pressures at other significant normal operating states; these pressures are presented in Table 2.6.7-39. Properties for the 56 percent by volume ethylene glycol and water solution are presented in Table 3.2-5. Two normal operating conditions are presented in Table 2.6.7-39, and are helpful in understanding how the cask operates, but are all bounded by the pressure relief valve release pressure (PRVR) shown in Table 2.6.7-39. The PRVR pressure is used to establish the structural loads for shield and expansion tank analyses.

Thus, the magnitude of the expansion pressure is determined as discussed previously by the volume of fluid added to the expansion tank during the initial filling. It is assumed that 11.5

gallons of fluid are added to the expansion tank, 0.5 gallons more than specified. This results in a maximum expansion pressure of 26 psig.

In addition to the expansion pressure acting radially outward, 10 CFR 71, Subpart F, requires that the cask be able to sustain a reduced external pressure. The cask is initially filled and pressurized at atmospheric pressure (14.7 psia). When the external pressure is reduced to 3.5 psia, there is a relative increase in internal pressure of 11.5 psig (rounded to 12 psig). The reduced external pressure load has been included in the analysis as an increase in internal pressure.

The calculated pressures for the end drop load condition are as follows:

Reduced external pressure	12 psig
Hydraulic pressure	100 psig
Expansion pressure	26 psig
TOTAL	138 psig

The calculated pressures for the side drop load condition are as follows:

Reduced external pressure	12 psig
Hydraulic pressure	38 psig
Expansion pressure	26 psig
TOTAL	76 psig

These pressures are conservatively assumed to add algebraically and represent the highest pressure expected at a point on the shield/expansion tank structure. All other pressures within the shield/expansion tank are less because the hydraulic pressure is a function of fluid depth.

2.6.7.7.4 Neutron Shield Tank Structural Analyses

To simplify analysis of the shield tank structure, the use of symmetry, superposition and analysis of worst case loads are employed to reduce the number of calculations to be performed. Major shield tank structural components are shown in Figure 2.6.7-23. Analyses performed and resulting conclusions for one location of the shield tank are directly applicable to the same relative location elsewhere on the shield tank structure. For reasons stated earlier, the normal operating conditions 1-foot end drop loads envelope all other normal operations conditions drop orientations, and is the only loading condition that is considered in the following analyses. Moreover, the bottom end drop g load is more severe than the top end drop, and is used in both the top and bottom end drop analyses. The shield tank analysis is performed with the shield tank pressure equal to 180 psig, a pressure 42 psig higher than the calculated 138 psig for the end drop (which envelops the side drop condition).

The bottom end plate, shield tank shell, gussets, top end plate, and welds are the major components of interest in the shield tank evaluation for normal transport conditions.

To ensure a conservative analysis of the neutron shield and expansion tank structure, several simplifying assumptions are made for all analyses performed (other assumptions are stated with each analysis). The allowable stress is taken as the yield strength of Type 304 stainless steel at 250°F, which is 23,750 psi. This is conservative since the maximum calculated shield/expansion tank normal operating temperature is 227°F.

Finally, the edge restraint of the structural components analyzed is considered to be simply supported. The smallest welds are considered in the analyses; a larger weld assures a conservative analysis.

Weld Allowable Stresses

The shield and expansion tanks are constructed primarily from 0.24-inch thick Type 304 stainless steel plate. The plates are welded together using 0.188-inch fillet welds, using Type 308 weld material. From the Metals Handbook, 9th Edition, Volume 3, page 20, the ultimate tensile strength is 75.0 ksi. The allowable strength for shield tank fillet welds is:

$$S_{ALL} = (0.3)(75{,}000)$$
$$= 22{,}500 \text{ psi}$$

or:

$$f_{ALL} = (0.707)(22{,}500)\omega$$
$$= 15{,}900\omega \text{ lb/in}$$

where:

f_{ALL} = fillet allowable (lb/in)

ω = fillet weld size (in)

The only size fillet weld considered in the shield tank analysis is a 0.188-inch fillet. Therefore, the 0.188-inch fillet weld has an allowable strength of:

$$f_{ALL} = (15{,}900)(0.188 \text{ in})$$
$$= 2980 \text{ lb/in}$$

Structural Loads

Shield tank and end plate loads are considered in the neutron shield tank analysis. The weight of a unit depth of the 0.24-inch thick shield tank plate material is considered to be located at the mass centroid of the plate assembly. The mass centroid is 6.13 inches from the outer shell, as shown in the following analysis:

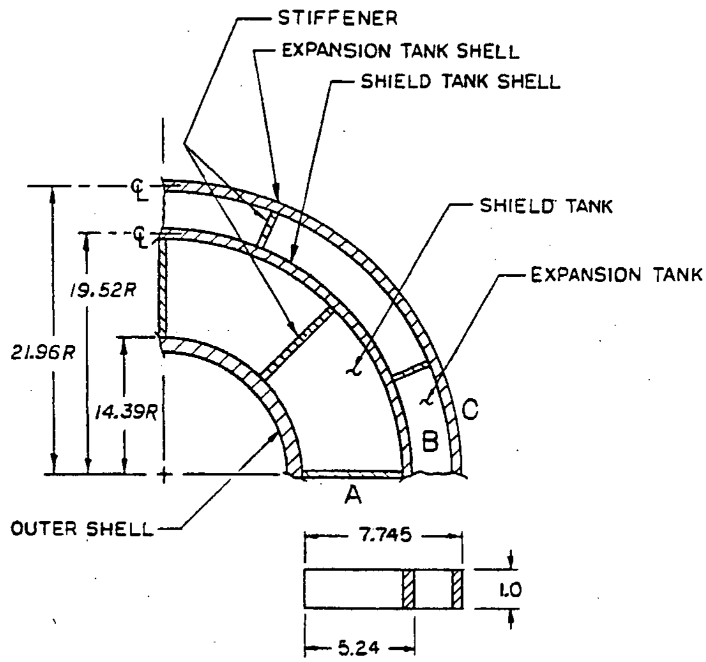

Quarter Section - NAC LWT Cask

Two "A" plates weigh 1.051 pounds with a mass centroid at 3.87 inches from the outer shell.
Two "B" plates weigh 2.005 pounds with a mass centroid at 5.12 inches from the outer shell.
Two "C" plates weigh 3.032 pounds with a mass centroid at 7.59 inches from the outer shell.
The total weight of the plates is 6.09 pounds.

The mass centroid is located at:

$$\bar{x} = \frac{(1.051\ \text{lb})(3.873\ \text{in}) + (2.005\ \text{lb})(5.12\ \text{in}) + (3.032\ \text{lb})(7.59\ \text{in})}{5.643\ \text{lb}}$$

$$= 6.134\ \text{in}$$

The weight of the neutron shield tank structural plates is considered to act at 6.09 inches from the outer shell. The weight of one stiffener and shield/expansion tank shell section is 3.54 pounds.

The shield tank end plates are 0.5-inch thick stainless steel plate. To determine the structural load, the weight of the plate was divided by its area. The resulting structural load is 3 pounds/square inch.

Shield Tank Shell

The shield tank shell is analyzed as a thin-walled tube, taking no credit for the eight radial stiffeners, which run the length of the tank. Using Case 1 (Roark, page 298), the meridional and hoop stresses are calculated:

$$S_1 = \frac{pR}{2t} = 7414 \text{ psi}$$

where:

$p = 180$ psig

$R = 19.44$ inches

$t = 0.24$ in

and

$$S_2 = \frac{pR}{t} = 14{,}827 \text{ psi}$$

Von Mises yield criterion is used to calculate an equivalent stress, S_e, which is compared to the yield strength of stainless steel.

$$S_e = \frac{1}{\sqrt{2}}\left[(S_1 - S_2)^2 + (S_2 - S_3)^2 + (S_3 - S_1)^2\right]^{0.5}$$

$$= 12{,}841 \text{ psi}$$

where:

$S_1 = 7414$ psi

$S_2 = 14{,}827$ psi

$S_3 = 0$ psi

then

$$M.S. = \frac{S_{ALL}}{S_e} - 1 = \underline{+0.07}$$

where:

$S_{ALL} = (0.577)(23{,}750 \text{ psi})$

$= 13{,}700$ psi

Stiffener

A 1-inch longitudinal section of the neutron shield tank is analyzed. The total pressure load (180 psi) acts equally between stiffeners as shown in Figure 2.6.7-24. No credit is taken for support from the end plates or the expansion tank end plate. The load acting on the stiffener (L = 2772 pounds) is the area of the tank shell 15.4 square inches (15.4 inches × 1 inch) multiplied by the total end drop pressure, 180 psi. The cross sectional area, A_p, of a 1-inch section of the stiffener plate is 0.24 square inches (0.24 inch × 1.0 inch). The tensile stress acting on the stiffener is calculated:

$$S_T = \frac{L}{A_p} = 11{,}746 \text{ psi}$$

then

$$M.S. = \frac{S_{ALL}}{S_T} - 1 = \underline{+0.17}$$

where:

S_{ALL} = 13,700 psi (Section 2.6.7.7.4)

The stiffeners are the structural members locating the shield tank shell and providing support for the end plates (similar to the gussets) during end drops. This analysis demonstrates that the stiffeners have adequate strength to withstand the maximum pressure in the shield tank. The analysis in Section 2.6.7.7.4 shows that the shield tank shell has adequate strength to withstand the maximum pressure in the shield tank. All other drop orientations offer less severe structural loads on both the stiffeners and tank shell. Lightening holes in each stiffener do not affect the structural integrity of the shield tank and stiffeners. Lightening holes are located away from the ends of the stiffeners where the hydraulic component of the pressure load is less severe.

Stiffener Weld

A unit section (1 inch longitudinal) of stiffener weld is analyzed. Two loads act on the weld attaching the stiffener to the cask outer shell. The drop pressure load acting on the stiffener is L = 2772 pounds (see section titled "Stiffener"). In addition to the pressure load, the structural load (L_s) is calculated concentrating the mass of the tank (stiffeners and shell) unit section (see section titled Structural Loads). The structural pressure loads and welds being examined are shown in Figure 2.6.7-25. Treating the two 1-inch welds as lines and determining the weld loading using methodology found in Design of Welded Structures (Blodgett, Section 7.4):

Tensile Load

$f_t = 2772/2$

$= 1{,}386$ lb/in

where:

L = 2,772 lbs

Shear Load

$f_s = 55.9/2$

$= 28.0$ lb/in

where:

$L_s = 3.54$ lb x 15.8 g

$= 55.9$ lbs

15.8 g = end drop g load (Section 2.6.7.4)

The end drop structural load produces a bending moment on the weld group (Figure 2.6.7-25). The bending moment (M) is 343 inch-pounds (6.13 inches × 55.9 pounds). The section properties of the weld group are calculated from Blodgett, Table 5, page 7.4-7,

$$S_\omega = \frac{d^2}{3}$$

$$= 0.33 \text{ in}^2$$

where:

d = 1 in

Bending Load

$$f_b = \frac{M}{S_\omega}$$

$$= 343/0.33$$

$$= 1038 \text{ lb/in}$$

The resultant load on the weld group is calculated:

$$f_r = \sqrt{f_1^2 + f_2^2}$$

$$= 2424 \text{ lb/in}$$

where:

$f_1 = f_s = 28.0$ lb/in

$f_2 = f_t + f_b$

$= 2{,}424$ lb/in

The allowable weld load is f_{ALL} = 2,980 lb/in; therefore, the margin of safety is:

$$M.S. = \frac{f_{ALL}}{f_r} - 1 = \underline{+0.23}$$

Gusset Weld

It is assumed that the end drop load on the end plate is shared equally between the stiffeners and gussets (Figure 2.6.7-26). The fillet weld attaching the gusset to the cask outer shell and end plate is 0.188 inch and is on both sides of the gusset. Bending and shear stresses on the weld group A are calculated in the following analyses. Since the gussets and stiffeners share the end drop load, the end plate area, which the gusset must support, is calculated:

$$A = [\pi(R_o^2 - R_i^2) - (16)(T_{PLT})(R_o - R_i)]/16$$

$$= 33.95 \text{ in}^2$$

where:

R_o = 19.6 inches

R_i = 14.3 inches

T_{PLT} = 0.25 in

The distributed load is composed of the end drop pressure load (180 psig) and a structural load (3 psig) equivalent to the end plate weight. The concentrated load (L) is calculated by multiplying the area (A) by the sum of the distributed loads (183 psig): L = 6,213 pounds. Therefore, the moment acting on weld group A is:

$$M = L\left(\frac{5.1}{2}\right)$$

$$= 15{,}843 \text{ in-lb}$$

The section properties of the weld group are calculated from Blodgett, Table 5, page 7.4-7:

$$S_\omega = \frac{d^2}{3}$$

$$= 12 \text{ in}^2$$

where:

d = 6 inches

Bending Load

$$f_b = \frac{M}{S_\omega}$$

$$= 1320 \text{ lb/in}$$

Shear Load

$$f_s = \frac{L}{W_{LEN}}$$

$$= 518 \text{ lb/in}$$

where:

L = 6,213 lbs

$W_{LEN} = 2 \times 6$ inches

= 12 inches

The resultant load on the weld group is calculated by:

$$f_r = \sqrt{f_1^2 + f_2^2}$$

$$= 1418 \text{ lb/in}$$

where:

$f_1 = f_s = 518$ lb/in

$f_2 = f_b = 1320$ lb/in

The allowable weld load is $f_{ALL} = 2980$ lb/in; therefore, the margin of safety is:

$$M.S. = \frac{f_{ALL}}{f_r} - 1 = \underline{+1.10}$$

Bottom End Plate

It is assumed that the portions of the end plate between a gusset and the adjacent stiffener can be modeled by a rectangular plate of the appropriate dimensions. The width (b) of the plate is the difference between radii of the cask outer shell and the shield tank shell as shown in Figure 2.6.7-27. The length (a) of the plate is the average of the inner and outer arc lengths, 6.7 inches

((7.7 inches + 5.6 inches)/2). Using Case 36 (Roark, page 225), the maximum bending stress on the 0.5-inch thick end plate is:

$$S_b = \beta \frac{wb^2}{t^2}$$

$$= 8{,}525 \text{ psi}$$

where:

$\beta = 0.4146$

w = 183 psi (see section titled "Gusset Weld")

b = 5.3 inches

t = 0.5-in thick

The margin of safety is:

$$M.S. = \frac{S_{ALL}}{S_B} - 1 = \underline{+1.79}$$

where:

$$S_{ALL} = S_{y_{250°F}}$$

$$= 23{,}750 \text{ psi}$$

Gusset Plate Cross Section

The plate was modeled as a large weld, with the throat in tension during an end drop. The end drop load (L) acting on the gusset is the load acting on the end plate between the gusset and adjacent stiffener. The gusset root cross section (R) is considered to be in tension (Figure 2.6.7-28). From the section titled "Gusset Weld," the load on the gusset root is L = 6213 pounds. The gusset root cross sectional area is calculated:

$$A_R = 0.707(h)(T_{PLT})$$

$$= 0.865 \text{ in}^2$$

where:

h = 5.1 in (shortest leg)

T_{PLT} = 0.24 in (thickness)

Calculating the tensile load:

$$S_T = \frac{L}{A_R}$$

$$= 7180 \text{ psi}$$

The margin of safety is:

$$M.S. = \frac{S_{ALL}}{S_T} - 1 = \underline{+LARGE}$$

where:

$S_{ALL} = 23{,}750$ psi

End Plate Welds

Peripheral weld group B (Figure 2.6.7-29) is considered to be in shear during an end drop. The end plate load is 6213 pounds, from the section titled "Gusset Weld." The area of weld material is:

$$A_W = 0.707\left(\frac{3}{16}[2(19.6 - 14.3) + 7.7] + \frac{3}{8}(5.6)\right)$$

$$= 3.9 \text{ in}^2$$

The tensile stress on weld group B is:

$$S_T = \frac{L}{A_W}$$

$$= 1593 \text{ psi}$$

The margin of safety is:

$$M.S. = \frac{S_{ALL}}{S_T} - 1 = \underline{+LARGE}$$

where:

$S_{ALL} = 23{,}750$ psi

Top End Plate - Normal Operations Conditions

In the analyses of the section titled "Bottom End Plate" and Section 2.6.7.8.2, the 0.5-inch thick bottom end plates are shown to be structurally adequate. This analysis shows that the top end plate, which is in effect equivalent to both bottom end plates welded together at the shield tank shell, is structurally adequate. Two bounding conditions are considered. The first condition considers the shield tank top end plate loaded with a pressure of 180 psig and the expansion tank top end plate unloaded. Using Case 38 (Roark, page 113), considering a unit strip of top end plate, where the two end points are considered pinned, the maximum bending stress is 10,272 psi, and the margin of safety equals +0.33. The second condition considers both the shield and expansion tank end plates loaded at 180 psig. Again using Case 38, the bending stress equals 11,172 psi, resulting in a margin of safety of +0.23. The maximum normal operations conditions pressure in the expansion tank is 162 psig; therefore, the top end plate is adequate for the normal operations conditions.

2.6.7.8 Expansion Tank

The expansion tank is located at the upper end of the cask and is concentric with the shield tank. As its name implies, the expansion tank provides a location for fluid to expand into during fluid heating; thus, protecting both the neutron shield tank and the expansion tank from over-pressurization during normal operations conditions. A description of the expansion tank, structural criteria, and structural loads is presented in Sections 2.6.7.7.1 through 2.6.7.7.3. Table 2.6.7-40 summarizes the results of the structural analyses described in the following sections. The table shows adequate margins of safety for each component of the expansion tank examined. Therefore, the normal operations conditions requirements of 10 CFR 71 are satisfied.

To simplify analysis of the expansion tank structure, the use of symmetry, superposition, and worst case loads are employed to reduce the number of calculations to be performed and yet provide a thorough analysis. Major expansion tank structural components are shown in Figure 2.6.7-30. Analysis of the expansion tank uses the same format and simplifying assumptions as were used in the neutron shield tank structural analysis.

2.6.7.8.1 Expansion Tank Shell

The expansion tank shell is analyzed as a thin-walled tube, taking no credit for the eight radial stiffeners, which run the length of the tank. Using Case 1 (Roark, page 298), the meridional and hoop stresses are calculated:

$$S_1 = \frac{pR}{2t}$$

$$= 6269 \text{ psi}$$

$$S_2 = \frac{pR}{t}$$

$$= 12{,}537 \text{ psi}$$

where:

p = 180 psig

R = 21.94 inches

t = 0.32 in

Von Mises yield criterion is used to calculate an equivalent stress (S_e), which is compared to the yield strength of Type 304 stainless steel.

$$S_e = \frac{1}{\sqrt{2}} \left[(S_1 - S_2)^2 + (S_2 - S_3)^2 + (S_3 - S_1)^2 \right]^{0.5}$$

$$= 10,857 \text{ psi}$$

where:

$S_3 = 0$ psi

then

$$M.S. = \frac{S_{ALL}}{S_e} - 1 = \underline{+0.26}$$

where:

$S_{ALL} = 0.577$ (23,750 psi)
= 13,700 psi

2.6.7.8.2 Bottom End Plate

It is assumed that the sections of end plate between stiffeners can be represented by a rectangular plate of appropriate dimensions. The width (b) of the plate is the difference between radii of the neutron shield tank and expansion tank shells, as shown in Figure 2.6.7-31. The length (a) of the plate is the average of the inner and outer arch lengths, a = 16.4 inches ((17.3 + 15.4)/2). Using Case 36 (Roark, page 225), the maximum bending stress on the 0.5-inch thick end plate is:

$$S_{max} = \beta \frac{wb^2}{t^2}$$

$$= 3375 \text{ psi}$$

where:

$\beta = 0.75$
w = 180 psig
b = 2.5 inches
t = 0.5 in

then

$$M.S. = \frac{S_{ALL}}{S_{max}} - 1 = \underline{+LARGE}$$

where:

S_{ALL} = 23,750 psi (S_y at 250°F)

2.6.7.8.3 Stiffener

The drop load is assumed to be distributed over all stiffeners equally. It is further assumed that the stiffener examined is in tension resulting from the drop load, as shown in Figure 2.6.7-32. The analysis shown below is for a 1-inch section (longitudinal) without credit for end plate welds. The drop pressure load is L = 3,114 pounds (17.3 in^2 x 180 psi). Additionally, the stiffener must support itself and the expansion tank shell during a drop, which adds an additional 45 pounds of structural load, bringing the total load (L) on the stiffener to 3,159 pounds. The cross sectional area of the 1-inch section analyzed is 132 in^2.

$$S_T = \frac{L}{A}$$

$$= 10{,}029 \text{ psi}$$

The margin of safety is:

$$M.S. = \frac{S_{ALL}}{S_T} - 1 = \underline{+0.37}$$

where:

S_{ALL} = 0.577(23,750) psi
= 13,700 psi

2.6.7.8.4 Stiffener Weld

This analysis of a unit section (1-inch longitudinal) of expansion tank shell assumes that the drop load is equally distributed among all stiffeners. The load acting on the weld attaching the stiffener to the adjacent shield tank stiffener equals the load acting on the stiffener, L = 3,114 pounds (Section 2.6.7.8.3). The weld is a 0.188-inch fillet, both sides with a total throat area, A_w = 0.265 in^2. The tensile stress acting on the weld is:

$$S_T = \frac{L}{A_w}$$

$$= 11{,}750 \text{ psi}$$

The resulting margin of safety is:

$$M.S. = \frac{S_y}{S_T} - 1 = \underline{+0.17}$$

where:

$S_y = 0.577(23{,}750)$ psi

$= 13{,}700$ psi

2.6.7.9 Upper Ring/Outer Shell Intersection Analysis

Membrane and bending stresses are induced in the upper ring/outer shell intersection region of the cask body. These stresses are calculated using a detailed finite element model (Figure 2.6.7-33) and the ANSYS PC-Linear computer program.

The upper ring/outer shell intersection region is conservatively analyzed utilizing an axisymmetric model, axisymmetric loading and minimum ring cross section properties. The actual loading occurs only at the two lifting trunnions, and the minimum ring cross section occurs only at four 90-degree locations around the ring circumference. The model is restrained in the longitudinal direction by roller boundary conditions on the inner and outer shells (Figure 2.6.7-34) located 10 inches below the upper ring/outer shell intersection (attenuation length = 2.5 $(Rt)^{0.5}$ = 9.81 inches). A fine mesh grid is used in the model in regions where peak stresses caused by concentration effects are expected. The following assumptions are made in this analysis:

1. The stiffness and support of the lead shell are not included.
2. The support/restraint of the upper ring provided by the closure lid and bolts is not included.
3. A uniform average temperature of 300°F is used in the analysis.
4. ANSYS STIF42 isoparametric quadrilateral elements adequately represent the cask geometry.

The sections analyzed as critical are shown in Figure 2.6.7-35. Section c-c is critical for P_m stress, and section a-a is critical for $P_m + P_b$ stress.

Applied Loads

The normal operations lifting trunnion loads used in this analysis are:

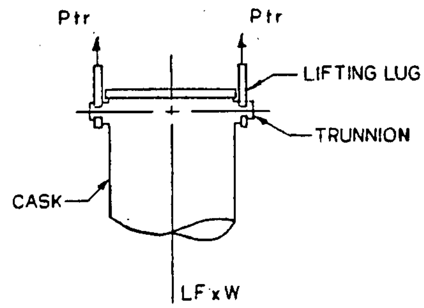

Lifting Load On Trunnions

Load Factor (LF) = 1.15

Cask Weight (W) = 52,000 lbs

P_{tr} = (LF)(W/2) = (1.15)(52,000/2) = 29,900 lbs

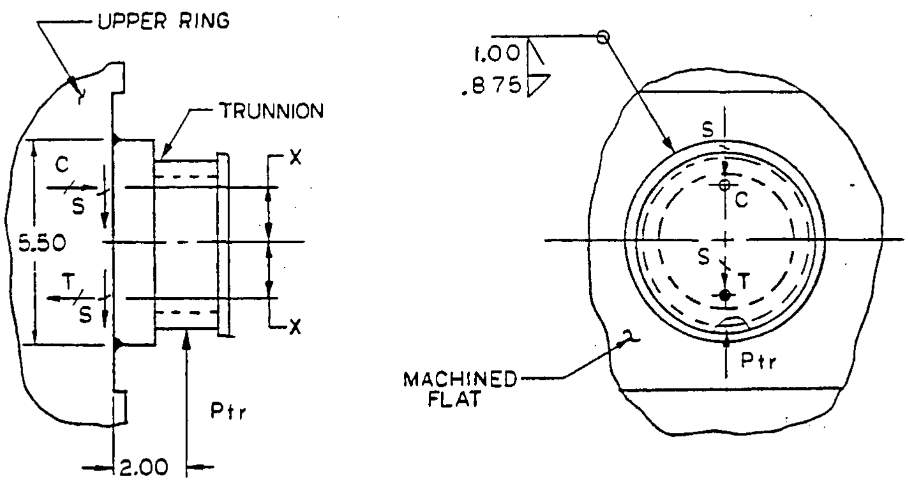

Lifting Trunnion Load Geometry

The concentrated loads were used to represent the distributed loads in the trunnion weld.

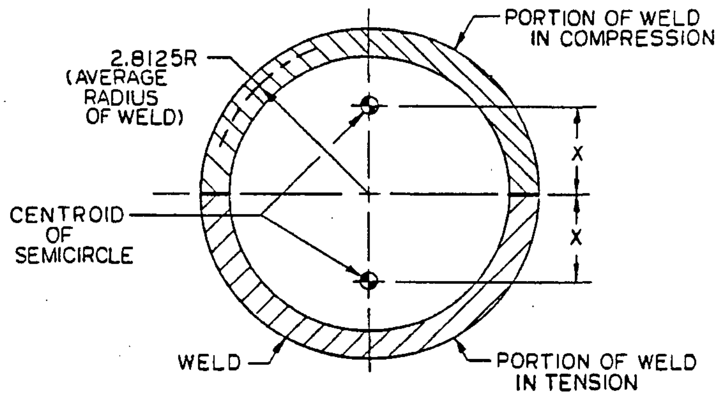

Trunnion Weld Group Centroid

To determine the trunnion weld group centroid:

$x = 0.6366\ R_{avg}$

$= 0.6366\ (2.8125)$

$= 1.790$ inches

$T = C = y\ (P_{tr}/2x)$

$= 2.00\ (29{,}900) / 2\ (2.8125)$

$= 16{,}704$ lbs

$S = P_{tr}/2$

$= 29{,}900/2$

$= 14{,}950$ lbs

Assume these loads are uniform over the trunnion weld diameter:

$T_u = C_u = 16{,}704/2(2.8125)$

$= 2969.6$ lb/in

$S_u = 14{,}950/2(2.8125)$

$= 2657.8$ lb/in

The ANSYS program requires that the loads for an axisymmetric model be input as load/radian:

Radians enclosed in 1 inch of circumference = 1/radius = 11/13.94 = 0.0717

$T_r = C_r = (2969.6)/0.0717$

$= 41{,}396.22$ lb/rad

$S = 2657.8/0.0717$

$= 37{,}049.73$ lb/rad

Calculated Stress Summary - Normal Operations Conditions

As anticipated, the maximum stresses occur at the upper ring/outer shell intersection, in the region of the machined flat and the internal radius of the outer shell. This analysis conservatively considers an outer shell thickness of 1.12 inches (actual shell thickness is 1.20 inches).

Stress peaking is present at the intersection of the outside surface of the outer shell with the upper ring because of stress concentration effects. The three sections through this region were investigated to determine the maximum stress intensity.

Section	Node	ANSYS Output Stress Summary			
		Radial S_x (ksi)	Axial S_y (ksi)	Hoop S_z (ksi)	Shear S_{xy} (ksi)
	66	1.6	7.3	2.9	-0.6
a-a	65	-0.1	4.9	1.9	-0.4
	64	-2.6	-0.4	-0.2	0.8
	66	1.6	7.3	2.9	-0.6
b-b	61	-0.7	5.1	1.6	0.5
	56	1.1	1.8	0.6	0.6
	66	1.6	7.3	2.9	-0.6
c-c	61	-0.7	5.1	1.6	0.5
	56	-0.2	4.5	0.6	0.6

The P_m and the $P_m + P_b$ stress components are determined by linearization of the ANSYS output stress components across sections a-a, b-b, and c-c. The principal stresses are calculated using the classical stress transformation law (Table 2.6.7-41).

The total normal operations lifting condition component stresses, principal stresses, and stress intensities at the critical section are calculated by combining the principal stresses from lifting, section b-b, with the internal pressure hot case (Table 2.6.1-1 and Table 2.6.2-2).

The P_m principal stress summary is:

	Principal Stresses (ksi)		
Load Condition	S_1	S_2	S_3
Lifting	5.5	-0.3	2.0
Internal Pressure	2.9	0.4	-0.4
Total	8.4	0.1	1.6

P_m stress differences are: S_{12} = 8.3 ksi, S_{23} = -1.5 ksi, and S_{31} = -6.8 ksi.

P_m stress intensity is S_i = 8.3 ksi.

Allowable stress intensity is S_a = 1.0 S_m = 20.0 ksi (Table 2.3.1-1).

$$M.S. = \frac{S_a}{S_i} - 1 = \underline{+1.41}$$

The $P_m + P_b$ principal stress summary is:

	Principal Stresses (ksi)		
Load Condition	S_1	S_2	S_3
Lifting	9.1	-2.7	4.0
Internal Pressure	4.2	1.5	0.2
Total	13.3	-1.2	4.2

The $P_m + P_b$ stress differences are: S_{12} = 14.5 ksi, S_{23} = -5.4 ksi, and S_{31} = -9.1 ksi.

The $P_m + P_b$ stress intensity is S_i = 14.5 ksi.

Allowable stress intensity is S_a = 1.5 S_m = 30.0 ksi.

$$M.S. = \frac{S_a}{S_i} - 1 = \underline{+1.07}.$$

The maximum peak stress, S_y = 7.3 ksi, is less than 1.5 S_m; therefore, a fatigue evaluation is not required.

2.6.7.10 PWR/BWR Rod Transport Canister Assembly Analysis

2.6.7.10.1 Discussion

The NAC-LWT PWR/BWR Rod Transport Canister is analyzed for structural adequacy in accordance with the requirements of 10 CFR 71 for a 1-foot drop (normal transport condition). The structural evaluation is performed by classical elastic analysis methods. The components evaluated include the can weldment, internal spacer, 4×4 and 5×5 inserts (rod holder), PWR insert, BWR fuel assembly lattice spacer and can weldment spacer. In the 5×5 insert configuration, four of the tubes comprising the insert may be replaced with a single larger tube to accommodate an oversize nonfuel-bearing component (e.g., a single BWR water rod or a CE guide tube). Evaluations are performed for the inserts being comprised of 16 or 25 tubes to accommodate the fuel rods and these evaluations are considered to bound the insert configuration containing a single BWR water rod. The presence of the BWR water rod reduces the inertial loading due to contents, as well as employs a larger cross-section for the BWR water rod as compared to four smaller tubes containing fuel rods.

2.6.7.10.2 Analysis Description

Geometry

The geometry of the can assembly is shown in Drawing 315-40-098. Note that the tube component of the can assembly is fabricated from a 6-in.×6-in.×0.5-in.-thick tube that is machined to the final dimensions of 5.5-in.×5.5-in.×0.25-in.-thick. The can assembly is positioned within the basket during transport of the cask. If the cask is equipped with a PWR basket, the PWR insert is required to provide correct positioning within the basket. The can assembly is constructed of Type 304 stainless steel with the exception of the PWR insert, which is constructed of 6061 Aluminum.

Loadings

The magnitude of the impact force varies according to the drop height and drop orientation. As calculated in Section 2.6.7.4, the g-loads for the 1-foot end and side drops are 15.8 and 24.3g, respectively.

Detailed Analysis

The maximum temperatures of the components are shown below. For the can weldment and components outside the can weldment, the temperatures are significantly below 700°F, which are within the 800°F design limits. For the tubes supporting the fuel pins, the maximum temperatures are determined to be 925°F. The tubes, which are only used with the insert for the high burnup pins, are shown to be acceptable using ASME Code, Section III, Division I, Subsection NH, which specifies allowable stresses above 800°F. The remaining components are shown to be acceptable using the stress allowable in ASME Code, Section III, Subsection NB.

Thermal Stresses

To evaluate effects of the calculated temperatures within the can assembly, the nominal dimensions of the can are used to calculate the resulting thermal expansions. The coefficient of thermal expansion for ASME SA 240 Type 304 stainless steel is 9.0×10^{-6} in./in.-°F. All components of the can assembly are constructed of Type 304 stainless steel, except for the PWR insert. The PWR insert is made of 6061 Aluminum with a coefficient of thermal expansion of

13.5E-6 in/in-°F. The following temperatures are used in the thermal expansion calculation and material property definitions.

Component Name	Maximum Operating Temperature (°F)	Temperature Used for Calculation (°F)
Aluminum PWR Insert	394	400
Can Weldment	538	575
5 × 5 Insert	885	925

Since the 5 × 5 insert is larger than the 4 × 4 insert, it is bounding for the thermal expansion calculations. The nominal gap between the insert and internal spacer is 3.56 – 3.44 = 0.12 inch. The growth of the insert is 3.44 × 9.0 E-6 in/in-°F × (925-70)°F = 0.027 inch. Since the growth of the insert is less than the nominal gap, no interference will occur.

The nominal gap between the internal spacer and can shell is 5.0 – 4.94 = 0.06 inch. The growth of the internal spacer is 4.94 × 9.0 E-6 in/in-°F × (575-70)°F = 0.023 inch. Since the growth of the internal spacer is less than the nominal gap, no interference will occur.

The nominal gap between the can shell and PWR insert is 5.75 – 5.5 = 0.25 inch. The growth of the can shell is 5.5 × 9.0 E-6 in/in-°F × (575-70)°F = 0.025 inch. Since the growth of the can shell is less than the nominal gap, no interference will occur.

Because the differential thermal expansion causes no interference or binding, no further thermal stress evaluation is required.

Can Weldment

The can weldment is contained within the basket assembly and not subjected to bending stresses in the side-drop case.

For the end drop, the can weldment is loaded by its own weight. The can contents bear against the bottom or top of the can assembly, depending on drop orientation.

LWT Can Body Compressive Stress

Under normal operating conditions the tube is evaluated for a 15.8 g acceleration for the end drop. The compressive load (P) on the tube is the combined weight of the lid and tube times the appropriate g factor.

The compressive stress (S_c) in the tube body is:

$$S_c = \frac{P}{A} = \frac{4{,}898 \text{ lb}}{4.98 \text{ in}^2} \cong 984 \text{ psi}$$

where:

$A = \pi (0.75^2 - 0.5^2) + 4 \times 4.0 \times 0.25 = 4.98 \text{ in}^2$

P = 310 × 15.8 = 4,898 lbs (conservatively, the weigh of the tube, lid, and bottom plate is used)

The margin of safety (MS) is then:

$$MS = \frac{S_m}{S_c} - 1 = \frac{17{,}300 \text{ psi}}{984 \text{ psi}} - 1 = +16.6.$$

LWT Can Body Bearing Stress

For the bottom end drop, the can base feet are subjected to a bearing stress. The compressive load (P) on the base is the combined weight of the can assembly, fuel and insert, and the internal spacer times the appropriate g factor.

P = [310 (can weldment) + 350 (fuel) + 75 (tube insert) + 240 (internal spacer)] × 15.8 = 15,405 lbs

The compressive stress (S_c) in the feet is:

$$S_c = \frac{P}{A} = \frac{15{,}405}{2.8} \cong 5{,}502 \text{ psi}$$

where:

$A = 4 \times 0.5 \times (2.0 - 0.6) = 2.8 \text{ in}^2$

The margin of safety (MS) for bearing is then:

$$MS = \frac{S_m}{S_c} - 1 = \frac{17{,}300 \text{ psi}}{5{,}502 \text{ psi}} - 1 = +2.14$$

Can Internal Pressure

Can weldment internal pressure is considered insignificant in the end-drop and side-drop cases because it will tend to reduce the compressive loads on the can tube sides.

The effect of internal pressure is evaluated for the bending stress that the pressure imposes on the can weldment sides. Conservatively, a one-inch-wide section of the tube wall, equal in length to the outside dimension of the tube (L = 5.5 in.) is analyzed as a cantilevered beam with a uniform load.

The maximum moment (M) is determined by the following relation:

$$M = \frac{wL^2}{12} = \frac{(85 - 14.7)(5.5^2)}{12} \cong 177.2 \text{ in.-lb}$$

where w is the maximum differential pressure across the can wall due to the maximum normal temperature (assumes that the cask internal pressure is atmospheric). The 85 psia envelopes the pressure reported in Section 3.4.4.2.

The combined stress (σ) in the 0.25-inch thick tube wall is:

$$\sigma = \frac{Mc}{I} + \frac{wL}{t}$$

$$= \frac{(177.2)(0.125)}{0.0013} + \frac{(85 - 14.7)(5.5)}{0.25} \cong 18{,}600 \text{ psi}$$

The margin of safety (MS) is:

$$MS = \frac{1.5 S_m}{\sigma} - 1 = \frac{25.35 \text{ ksi}}{18.6 \text{ ksi}} - 1 = +0.36 \text{ for the normal condition}$$

Can Lid Bolt Analysis

The tensile force (F_p) on each lid bolt due to internal pressure is:

$$F_p = \frac{PA}{n} = \frac{(85 - 14.7)(3.75^2)}{8} \cong 123.6 \text{ lbs}$$

where

P = the pressure differential across the can wall at maximum normal temperature (assumes cask internal pressure is atmospheric)

A = 3.75 in × 3.75 in, the area of the can lid exposed to pressure

n = 8, number of bolts

The total tensile force on each lid bolt is F_p + the initial preload force, F_i = 635 lbs

The lid bolt tensile stress (σ) is:

$$\sigma = \frac{F_p + F_i}{A_t} = \frac{758.6}{0.049} = 15{,}480 \text{ psi}$$

where

A_t = 0.049 in.^{2}, the bolt tensile stress area $\frac{\pi}{4}(0.25^2)$

The margin of safety (MS) for the normal condition is:

$$MS = \frac{S_y}{\sigma} - 1 = \frac{18.8 \text{ ksi}}{15.48 \text{ ksi}} - 1 = +0.21$$

Can Tube Buckling

The tube is evaluated, using the Euler formula, to determine the critical buckling load (P_{cr}):

$$P_{cr} = \frac{K\pi^2 EI}{L^2} = \frac{3.26\pi^2 (24.4\times10^6)(24.2)}{(165.5)^2} = 0.698 \times 10^6 \text{ lbs}$$

where:

$E = 24.4 \times 10^6$ psi at 750°F

$I = \dfrac{5.5^4 - 5.0^4}{12} = 24.2 \text{ in}^4$

L = tube body length (165.5 inches)

Because the maximum compressive load (310 × 15.8 = 4,898 lbs) is much less than the critical buckling load (698×10^3 lbs), the tube has adequate resistance to buckling.

Internal Spacer

The internal spacer body is contained within the can assembly and not subjected to bending in the side drop condition.

The compressive stress in the internal spacer rails during the side drop is determined as follows:

$$\sigma_b = \frac{Wg}{A} = \frac{665 \text{ x } 24.3}{123.7} \cong 130.6 \text{ psi}$$

where:

W = total load = 350 (fuel) + 240 (internal spacer) + 75 (4x4 insert) = 665 lbs

g = 24.3 (normal condition side drop)

A = 123.7 in^2 cross-sectional area of spacer rails, 4 × 0.188 × (165.25 – 2 × 0.38)

The resulting margin of safety is large.

Internal Spacer Compressive Stress

For the end drop, the internal spacer shell is loaded by its own weight. The insert rail stiffness is conservatively neglected in the strength.

Under normal operating conditions, the spacer is evaluated for a 15.8 g acceleration. The compressive load (P) on the shell is due to the weight of the internal spacer. The entire weight of the internal spacer times the appropriate g factor will be used to calculate the compressive load.

P = 240 × 15.8 = 3,792 lbs

The compressive stress (S_c) in the internal spacer body is:

$$S_c = \frac{P}{A} = \frac{3,792}{1.69} \cong 2,244 \text{ psi}$$

where:

$$A = (3.936^2 - 3.56^2) - 12 \times 0.5 \times 0.188 = 1.69 \text{ in}^2$$

The margin of safety (MS) is then:

$$MS = \frac{S_m}{S_c} - 1 = \frac{17,300}{2,244} - 1 = +6.71$$

Internal Spacer Buckling

The shell is evaluated, using the Euler formula for an axially distributed load, to determine the critical buckling load (P_{cr}):

$$P_{cr} = \frac{K\pi^2 EI}{L^2} = \frac{3.26\pi^2 (24.4\times10^6)(6.615)}{(165.25)^2} = 0.19 \times 10^6 \text{ lbs}$$

where:

$E = 24.4 \times 10^6$ psi at 750°F

$$I = \frac{3.936^4 - 3.56^4}{12} = 6.615 \text{ in}^4$$

L = spacer body length (165.25 inches)

Because the maximum compressive load ($240\times15.8 = 3,792$ lbs) is much less than the critical buckling load (190×10^3 lbs), the internal spacer has adequate resistance to buckling.

4×4 and 5×5 Inserts

The 4×4 and 5×5 inserts are contained within the internal spacer. The 4×4 inserts are supported by straps on 10-inch spacing. These straps provide a clearance of 0.31 inches and will allow bending of the tubes to occur. The 5×5 insert tubes are evaluated for a diametrically opposed load due to the weight of the adjacent tubes during the side drop.

The 4×4 insert lower tube will be evaluated as a fixed-fixed beam over a 10-inch span. The weight of the 3 tubes above (as well as lower tube self-weight) will be considered in the analysis. The stiffness of the tubes above the lower tube will conservatively be neglected. The combined weight (P) of the fuel pins and insert tubes are considered as a uniformly distributed load over the 10-inch span. In addition, the weights are scaled by the appropriate deceleration factor depending on the drop orientation and condition being evaluated.

The maximum bending stress (f_b) is determined as follows:

$$f_b = \frac{Wlg}{12Z} = \frac{5.8(10.0)24.3}{12x0.0092} \cong 12{,}766 \text{ psi}$$

where:

W = load on 10-inch section = (14 + 9.5) x 4 x 10/163.0 = 5.8 lbs

l = 10 inches (span of tube)

g = 24.3 (normal condition side drop)

Z = π/32 (0.6875^4-0.6315^4) / 0.6875 = 0.0092 in^3 (section modulus of the tube)

The margin of safety (MS) is:

$$MS = \frac{1.5S_m}{\sigma_{max}} - 1 = \frac{1.5(12{,}050)}{12{,}766} - 1 = +0.42$$

The bending moment due to the diametrically opposed line load on the 5×5 insert is calculated by the following:

$$M_b = \frac{WRg}{\pi} = \frac{70/163.0 \times 0.344 \times 24.3}{\pi} \cong 1.143 \text{ lb} - \text{in}$$

where:

W = total load = 14 × 4 + 70/5 = 70 lbs

g = 24.3 (normal condition side drop)

R = 0.6875/2 = 0.344 in (radius of insert tube)

The resulting bending stress is:

$$f_b = \frac{6M_b}{t^2} = \frac{6 \times 1.143}{0.028^2} \cong 8{,}745 \text{ psi}$$

The margin of safety (MS) is:

$$MS = \frac{1.5\ S_m}{\sigma_{max}} - 1 = \frac{1.5(12{,}050)}{8{,}745} - 1 = +1.07$$

<u>4×4 and 5×5 Insert Tube Compressive Stress</u>

Under normal operating conditions, the tube is evaluated for a 15.8 g acceleration. The compressive load (P) on the shell is due to the weight of the tube. The entire weight of the tube is calculated as:

P = π/4 (0.6875^2-0.6315^2) x 163.0 x 0.288 = 2.72 lbs

The compressive stress (S_c) in the tube body is:

$$S_c = \frac{P}{A} = \frac{2.72 \ x15.8}{0.058} \cong 741 \text{ psi}$$

where:

$$A = \pi/4\ (0.6875^2 - 0.6315^2) = 0.058 \text{ in}^2$$

The margin of safety (MS) is then:

$$MS = \frac{S_m}{S_c} - 1 = \frac{14{,}100}{741} - 1 = +18.0$$

PWR Insert

The PWR insert contains the can assembly for insertion into the PWR basket. The PWR insert comprises a square box section with smooth sides. Therefore, no bending stresses will be introduced in the side drop condition.

PWR Insert Bearing Stress

The bearing load (P) on the PWR insert is due to the weight of the loaded can assembly. The entire weight of the assembly times the appropriate g factor will conservatively be used to calculate the bearing load.

W = bearing load = [350 (fuel) + 310 (can) + 240 (internal spacer) + 75 (4x4 insert)] x 24.3 = 23,693 lbs

The compressive stress (S_c) in the tube body is:

$$S_c = \frac{P}{A} = \frac{23{,}693}{921.3} \cong 26 \text{psi}$$

where:

$$A = 5.5 \times 167.5 = 921.3 \text{ in}^2$$

The margin of safety (MS) is then:

$$MS = \frac{S_y}{S_c} - 1 = \frac{23{,}500}{26} - 1 = +\text{Large}$$

PWR Insert Body Compressive Stress

Under normal operating conditions, the tube is evaluated for a 15.8 g acceleration. The compressive load (P) on the body is due to the weight of the PWR insert. The entire weight of the PWR insert, times the appropriate g factor, will conservatively be used to calculate the compressive load.

$$P = 650 \text{ lb} \times 15.8 = 10{,}270 \text{ lbs}$$

The compressive stress (S_c) in the tube body is:

$$S_c = \frac{P}{A} = \frac{10{,}270}{39.2} \cong 262 \text{ psi}$$

where:

$$A = (8.5^2 - 5.75^2) = 39.2 \text{ in}^2$$

The margin of safety (MS) is then:

$$MS = \frac{S_y}{S_c} - 1 = \frac{23{,}500}{262} - 1 = +\text{Large}$$

PWR Insert Tube Buckling

The tube is evaluated, using the Euler formula, to determine the critical buckling load (P_{cr}):

$$P_{cr} = \frac{K\pi^2 EI}{L^2} = \frac{3.26\pi^2 (8.8\text{x}10^6)(343.9)}{(167.0)^2} = 3.86\times10^6 \text{ lbs}$$

where:

$$E = 8.8\times10^6 \text{ psi at } 400°\text{F}$$

$$I = \frac{8.5^4 - 5.75^4}{12} = 343.9 \text{ in}^4$$

L = tube body length (167.0 inches)

Because the maximum compressive load (650 x 15.8 = 10,270 lbs) is much less than the critical buckling load (3.86×10^6 lbs), the PWR insert has adequate resistance to buckling.

PWR Insert Assembly Bolts

The PWR insert is comprised of four short and four long aluminum plates joined with ½-13 UNC × 1.5-in. long socket head cap screws to form a hollow box. Each plate is secured to each adjacent plate using three screws.

The screws joining the plates are loaded in shear when the two lift tabs are used to lift the PWR insert and its payload. The controlling load path is through the lift tab attached to the shorter side plate and the three screws connecting the shorter side plate to the adjacent long plate. The distance from the line of load application (centerline of the lift tab) to the centerline of the 3-screw pattern is approximately 3.6 inches. Any internal moment created by this eccentricity is reacted by the strong-direction section modulus of the side plates and is effectively countered by the stiffness inherent in the overall symmetry of the box section. The screw shear stress (τ) in each of the 3 screws is:

$$\tau = \frac{P/2}{A} = \frac{900}{3(0.130)} = 2{,}308 \text{ psi}$$

where:

P = [310 (can weldment)+350 (fuel rods)+240 (internal spacer)+70 (5×5 insert)+650 (PWR insert)]×1.1 = 1,782 lbs, use 1,800 lbs for analysis. (Total lift weight with 10% dynamic load factor.)

A = screw cross-sectional area = $(0.4069^2 \text{ x } \pi)/4 = 0.130 \text{ in}^2$ (Thread minor diameter)

The safety factor (FS) is calculated using a shear allowable of $0.6S_m$ at 750°F.

$$FS = \frac{0.6(15{,}600)}{2{,}308} = 4.06 > 3$$

where

S_m = 15,600 psi for commercial austenitic stainless steel.

Therefore the design condition that lifting stresses have a load factor of 3 on the basis of yield strength is met.

Can Weldment Spacer

The can weldment spacer prevents the PWR basket, PWR insert, fuel, and can weldment from shifting during transport. The spacer (Drawing 315-40-125, Item 10) is placed on the top of the can weldment. The spacer is bolted to the bottom side of the lid and the cruciform stiffener functions as the spacer between the lid and can weldment. The maximum load applied to the spacer occurs during the top end drop. To bound both normal and accident conditions, stresses are compared using accident load conditions and are compared to allowable stresses for normal operating conditions. The stress in the spacer is:

$$\sigma = \frac{P \times g}{A} = \frac{1{,}945 \times 60}{8.4} = 13{,}893 \text{ psi}$$

where:

P= Conservative weight of the PWR basket, PWR insert, fuel, and can weldment = 1,945 lbs

g= Top end drop acceleration (60g)

A= Cross-sectional area of cruciform = $2 \times 7 \times 0.63 - 0.63^2 = 8.4 \text{ in}^2$

The margin of safety (MS) is:

$$MS = \frac{1.0 \times S_m}{\sigma} - 1 = \frac{17{,}500 \text{ psi}}{13{,}893 \text{ psi}} - 1 = +0.26$$

where:

S_m = The stress intensity of 304 stainless steel at 500°F

Because the height-to-diameter ratio (4.5/6.0 = 0.75) is less than one, the spacer has adequate resistance to buckling.

Using a bounding weight of 50.0 lbs for the spacer, the maximum shear stress on the 1/8-inch fillet weld corresponds to the hypothetical accident bottom end drop condition of 60g. The shear stress in the weld is computed as:

$$\tau = \frac{60 \times 50}{28.0 \times 0.707 \times 0.125} = 1{,}212 \text{psi}$$

where:

the perimeter of cruciform is 28.0 in [(7-0.625) × 4 + 0.625 × 4]

The margin of safety, based on the normal condition of transport allowable stress, is:

$$MS = \frac{0.6 S_m}{\tau} - 1 = \frac{0.6 \times 17{,}500}{1{,}212} - 1 = +7.66$$

The can weldment spacer is, therefore, determined to be structurally adequate for normal and accident conditions for the NAC-LWT cask.

Fuel Assembly Lattice Spacer

The BWR fuel assembly lattice fits into the PWR insert in place of the can assembly. The fuel assembly lattice holds up to 25 intact BWR fuel rods. To accommodate the fuel assembly lattice, the bottom plate of the PWR insert is removed. This allows the fuel assembly lattice to rest on the bottom of the cask. To prevent the PWR basket from shifting during transport, a spacer (Drawing 315-40-125, Item 12) is placed at the top of the fuel assembly lattice. The spacer is bolted to the bottom side of the lid and eight 1-inch diameter posts function as the spacer between the lid and PWR basket. The maximum load applied to the spacer occurs during the top end drop. To bound both normal and accident conditions, accident stresses are compared to the normal allowable stress. The stress in the spacer is:

$$\sigma = \frac{P \times g}{A \times Np} = \frac{400 \times 60}{0.785 \times 8} = 3{,}822 \text{ psi}$$

where:

P= Conservative weight of the PWR basket

g= Top end drop acceleration (Table 2.6.7-34)

A= Cross-sectional area of a post

Np = Number of posts

The margin of safety is:

$$MS= \frac{1.0 \times S_m}{\sigma} - 1 = \frac{17{,}500 \text{ psi}}{3{,}822 \text{ psi}} - 1 = +3.58$$

where:

S_m = The stress intensity of 304 stainless steel at 500°F

Buckling of the post is evaluated using the Euler formula. The critical buckling load (P_{cr}) is:

$$P_{cr} = \frac{K\pi^2 EI}{L^2} = \frac{0.25\pi^2 (25.8 \times 10^6)(0.0491)}{(13.4)^2} = 17{,}407 \text{ lbs}$$

where:

E = Modulus of elasticity = 25.8 × 10^6 psi at 500°F

I = Moment of inertia $= \frac{\pi \times d^4}{64} = 0.0491 \text{ in}^4$

d = Post diameter = 1 in

L = Post length = 13.38 inches

K = Euler buckling coefficient for fixed-free column = 0.25 (Marks, 9th Ed., p. 5-42)

Because the maximum compressive load (400/8 × 60 = 3,000 lbs) is less than the critical buckling load (17,407 lbs), the spacer has adequate resistance to buckling.

Figure 2.6.7-1 1-Foot Bottom End Drop with 130°F Ambient Temperature and Maximum Decay Heat Load

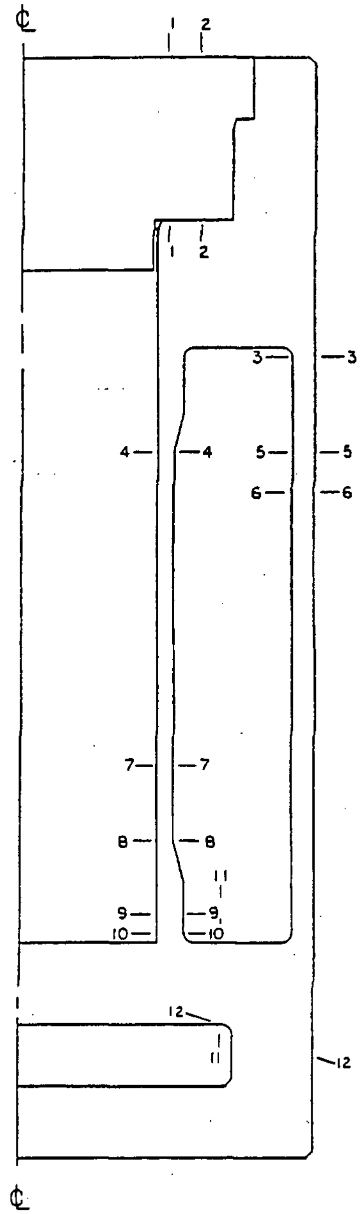

Figure 2.6.7-2 1-Foot Bottom End Drop with -40°F Ambient Temperature and Maximum Decay Heat Load

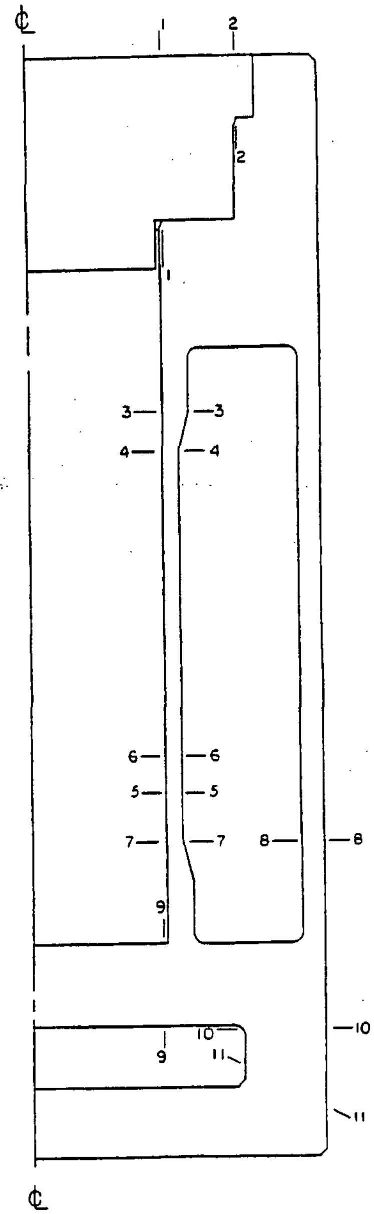

Figure 2.6.7-3 1-Foot Bottom End Drop with -40°F Ambient Temperature and No Decay Heat Load

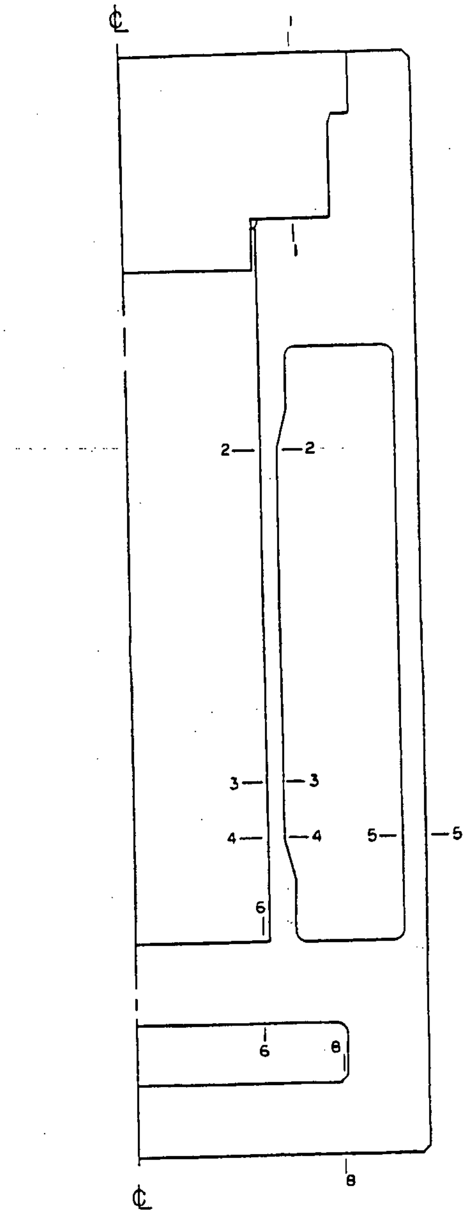

Figure 2.6.7-4 1-Foot Top End Drop with 130°F Ambient Temperature and Maximum Decay Heat Load

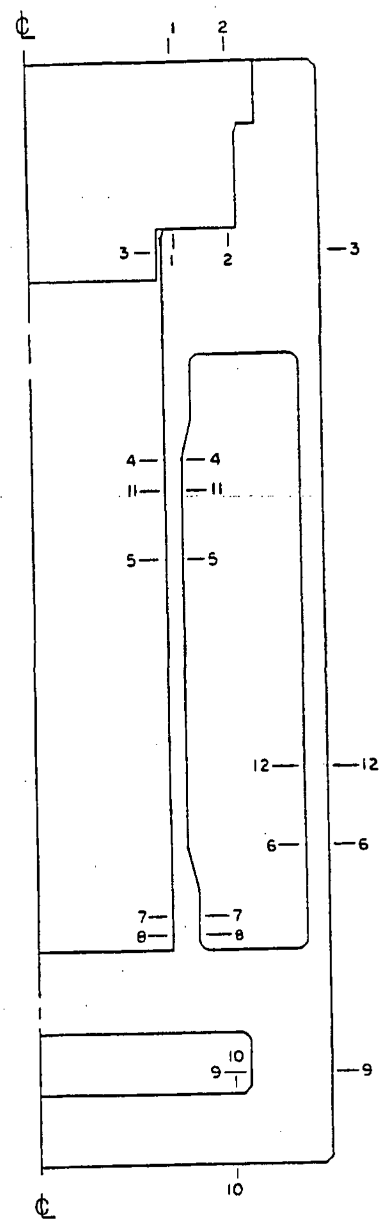

Figure 2.6.7-5 1-Foot Top End Drop with -40°F Ambient Temperature and Maximum Decay Heat Load

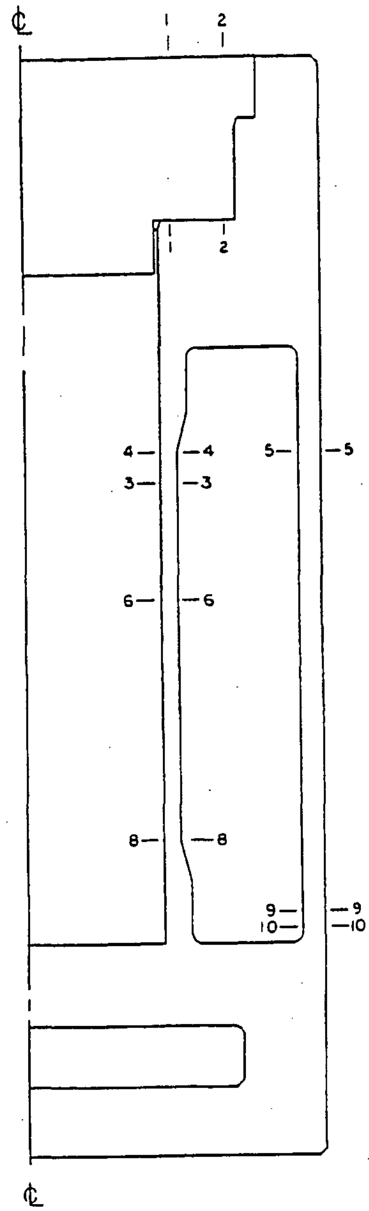

Figure 2.6.7-6 NAC-LWT Cask Critical Sections (1-Foot Side Drop with 100°F Ambient Temperature)

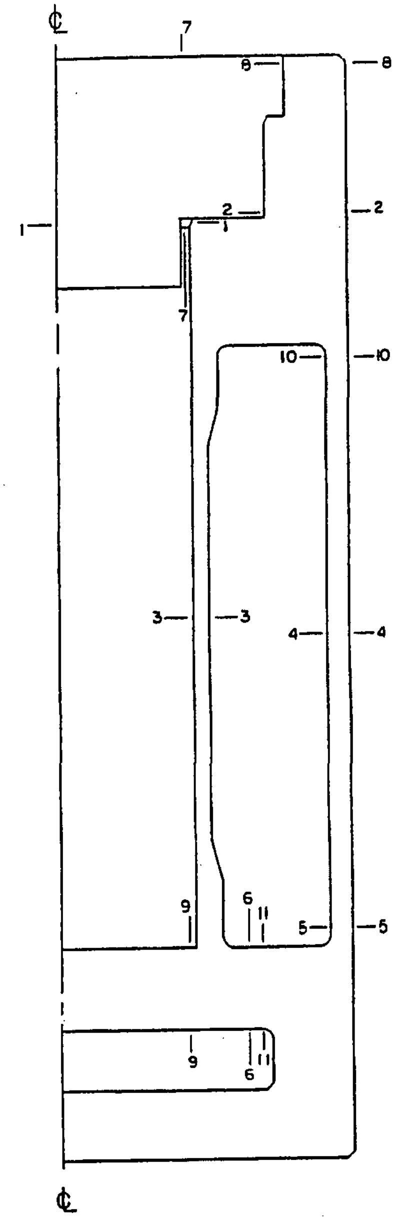

Figure 2.6.7-7 1-Foot Top Corner Drop with 130°F Ambient Temperature and Maximum Decay Heat Load - Drop Orientation = 15.74 Degrees

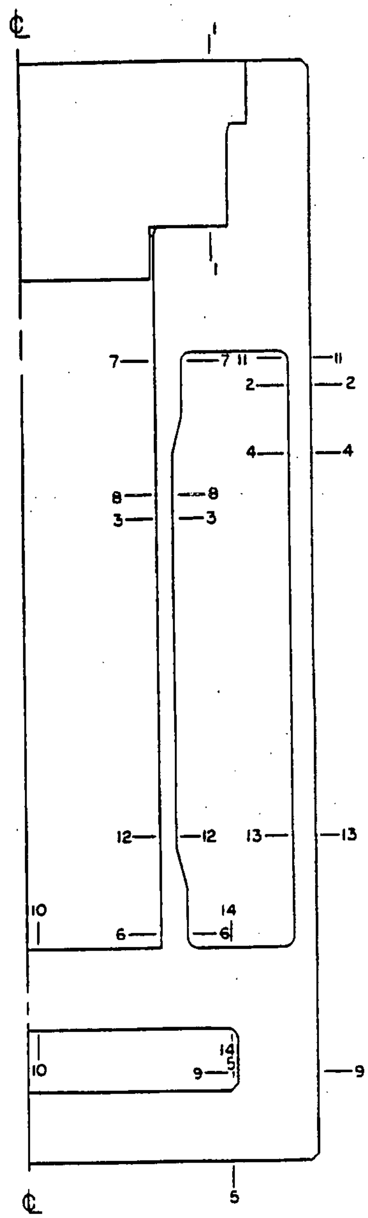

Figure 2.6.7-8 1-Foot Bottom Corner Drop with 130°F Ambient Temperature and Maximum Decay Heat Load - Drop Orientation = 15.74 Degrees

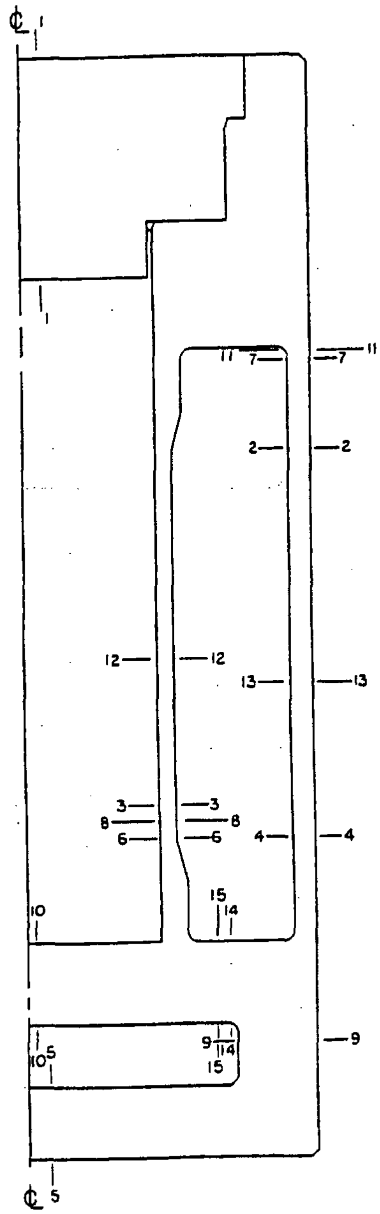

Figure 2.6.7-9 1-Foot Top Corner Drop with -40°F Ambient Temperature and No Decay Heat Load - Drop Orientation = 15.74 Degrees

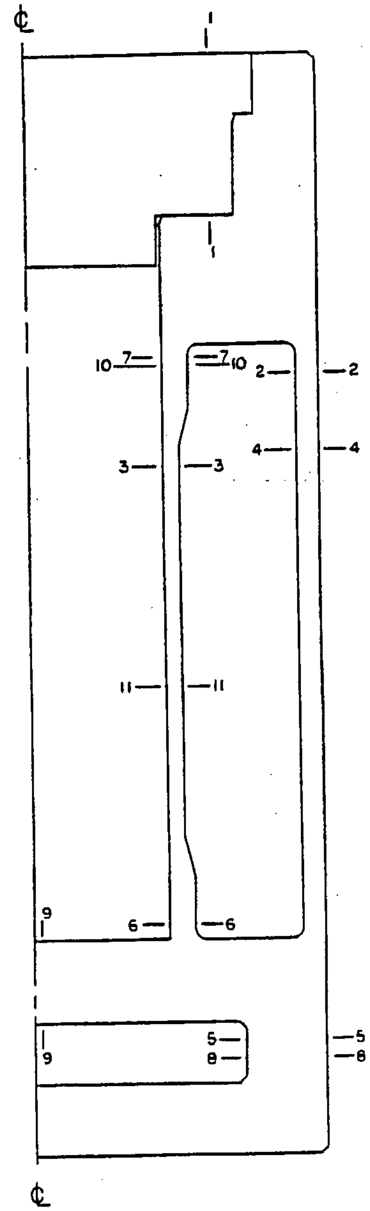

Figure 2.6.7-10 NAC-LWT Cask with Impact Limiters

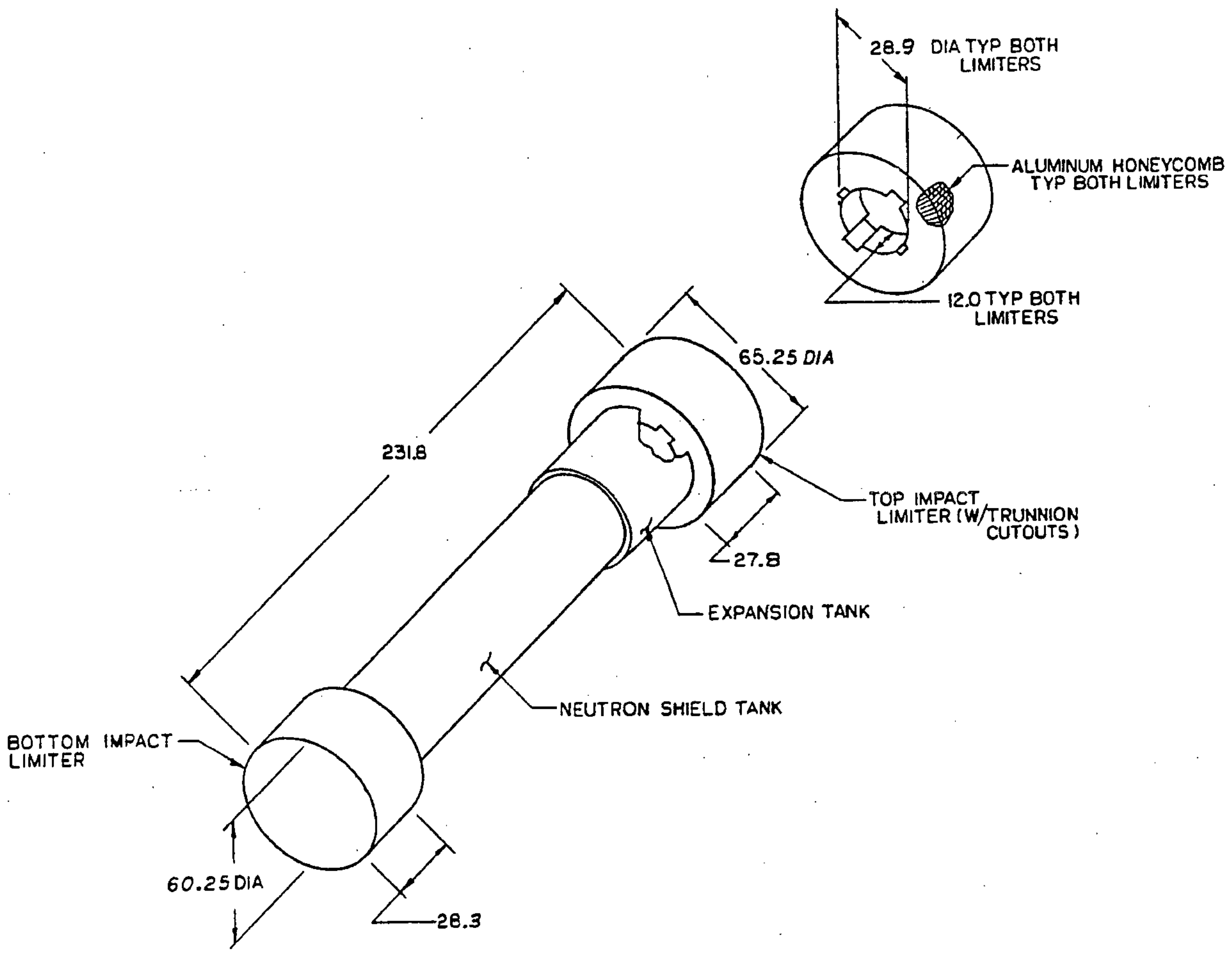

Figure 2.6.7-11 Cross-Section of Top Impact Limiter

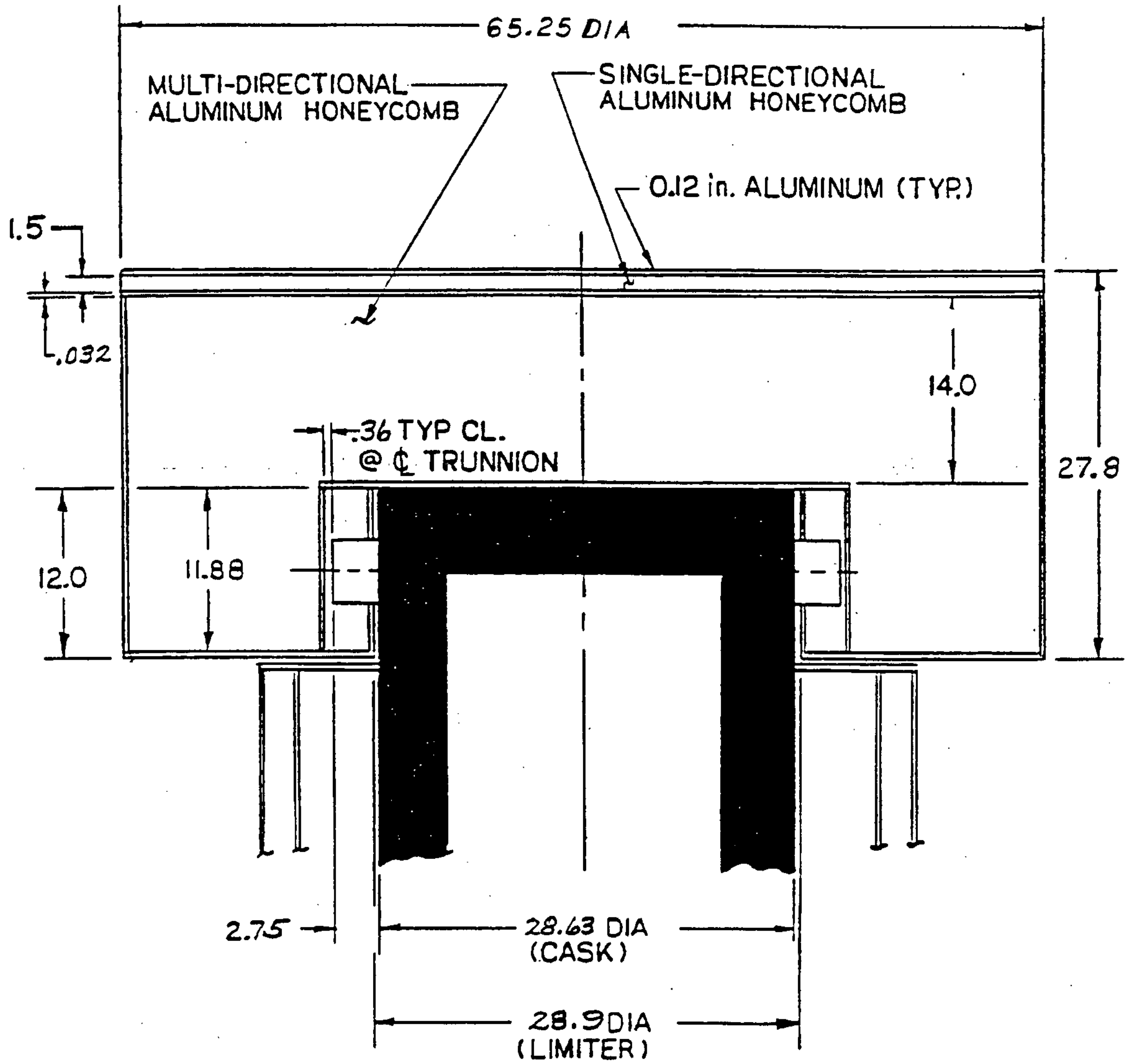

Figure 2.6.7-12 Load Versus Deflection Curve (Typical Aluminum Honeycomb)

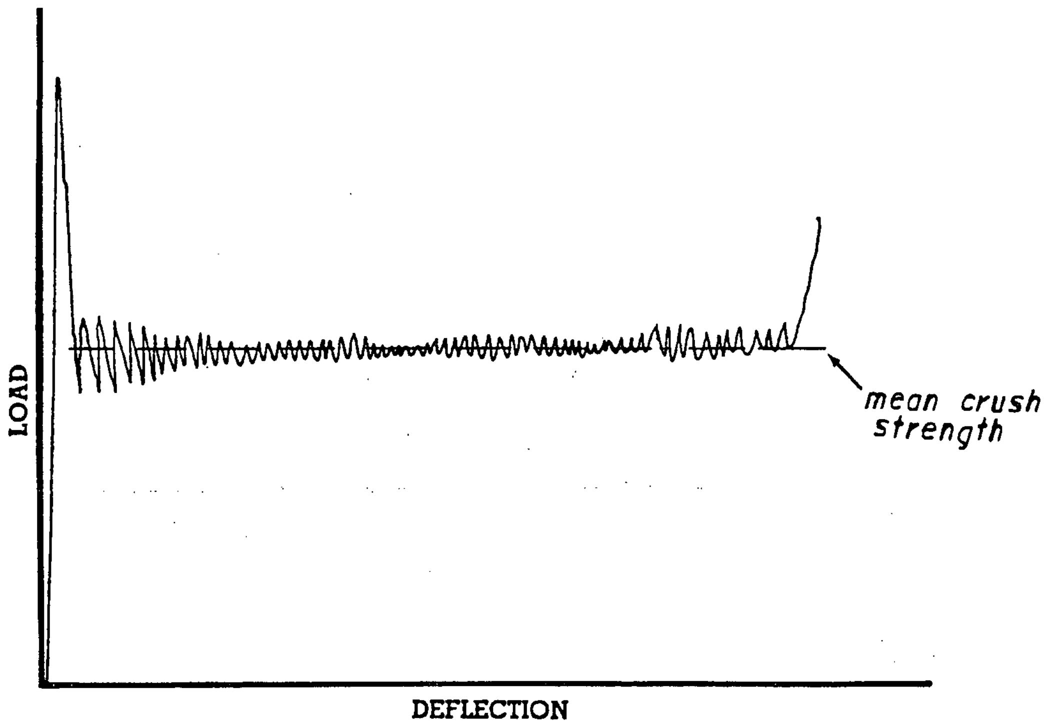

Figure 2.6.7-13 Quarter-Scale Model Limiter End Drop Cross-Section

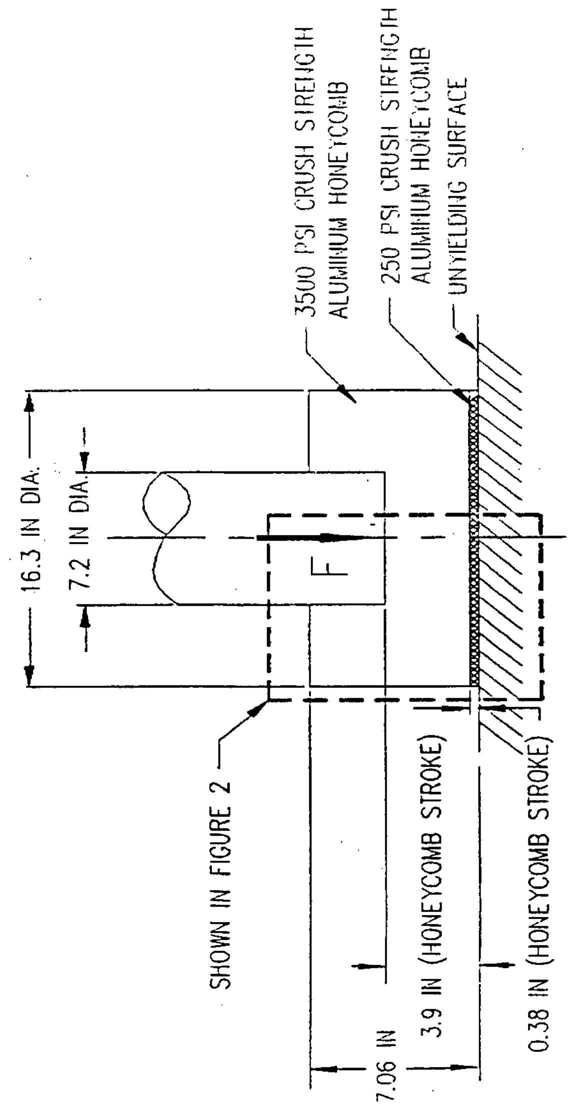

Figure 2.6.7-14 End Drop Impact Limiter Cross-Section

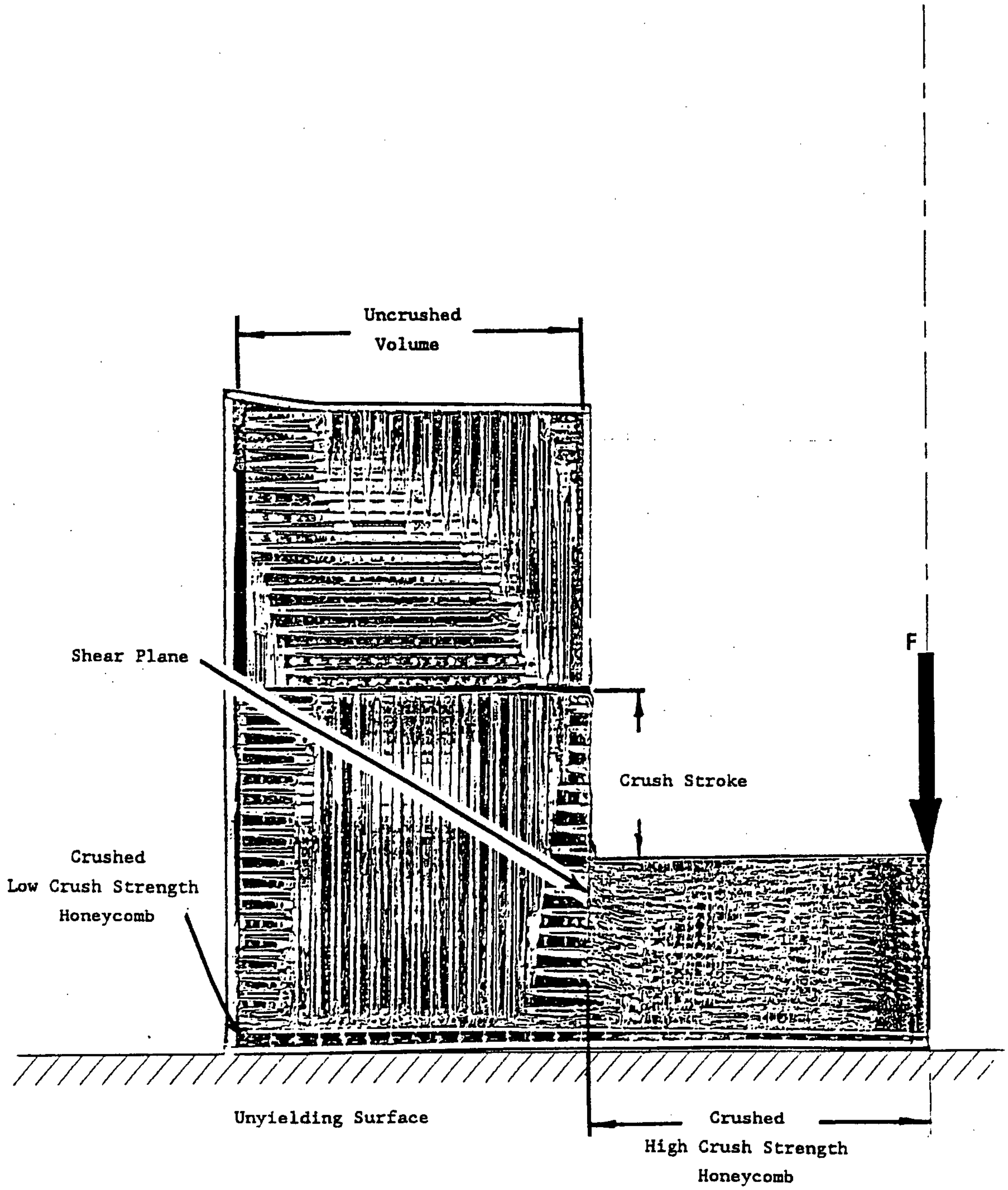

Figure 2.6.7-15 Impact Limiter Lug Detail

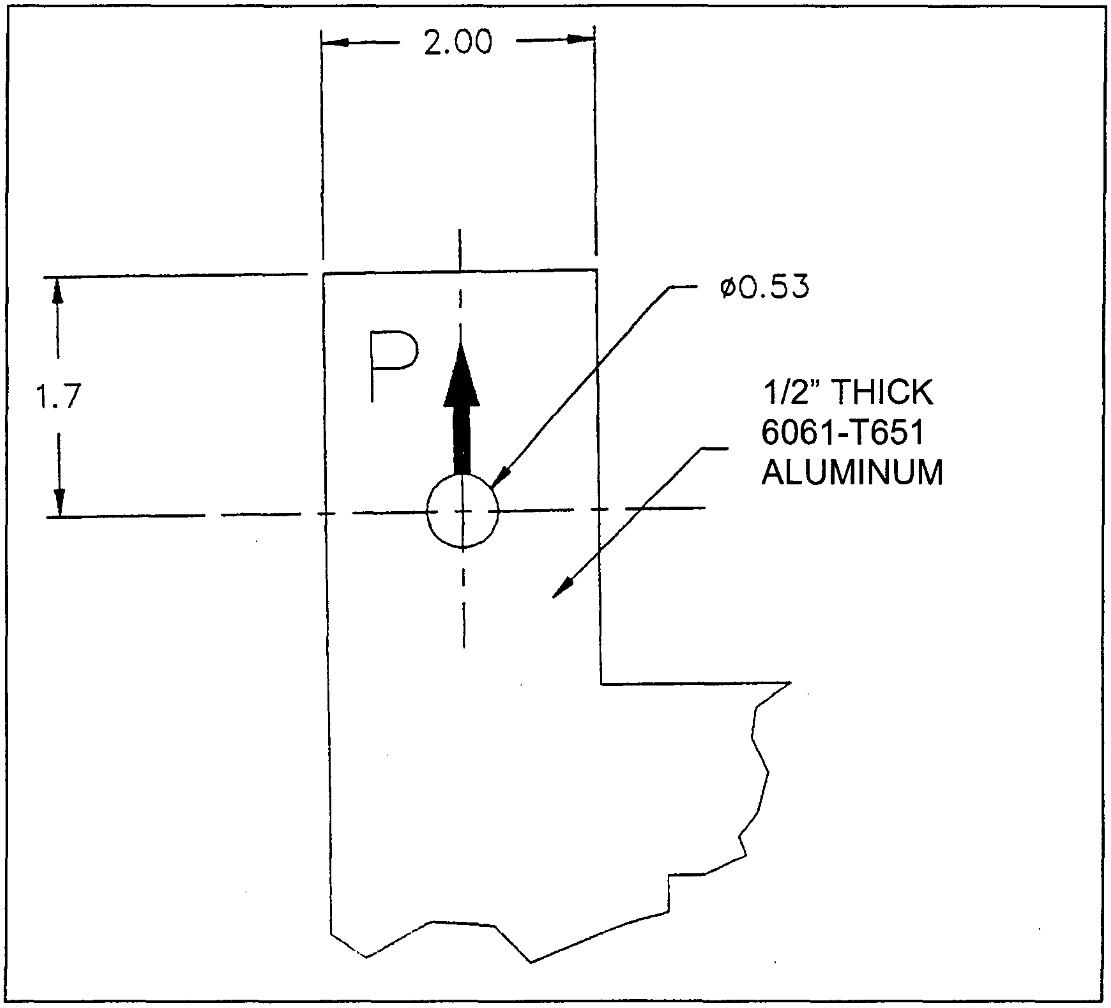

Figure 2.6.7-16 Cask Lug Detail

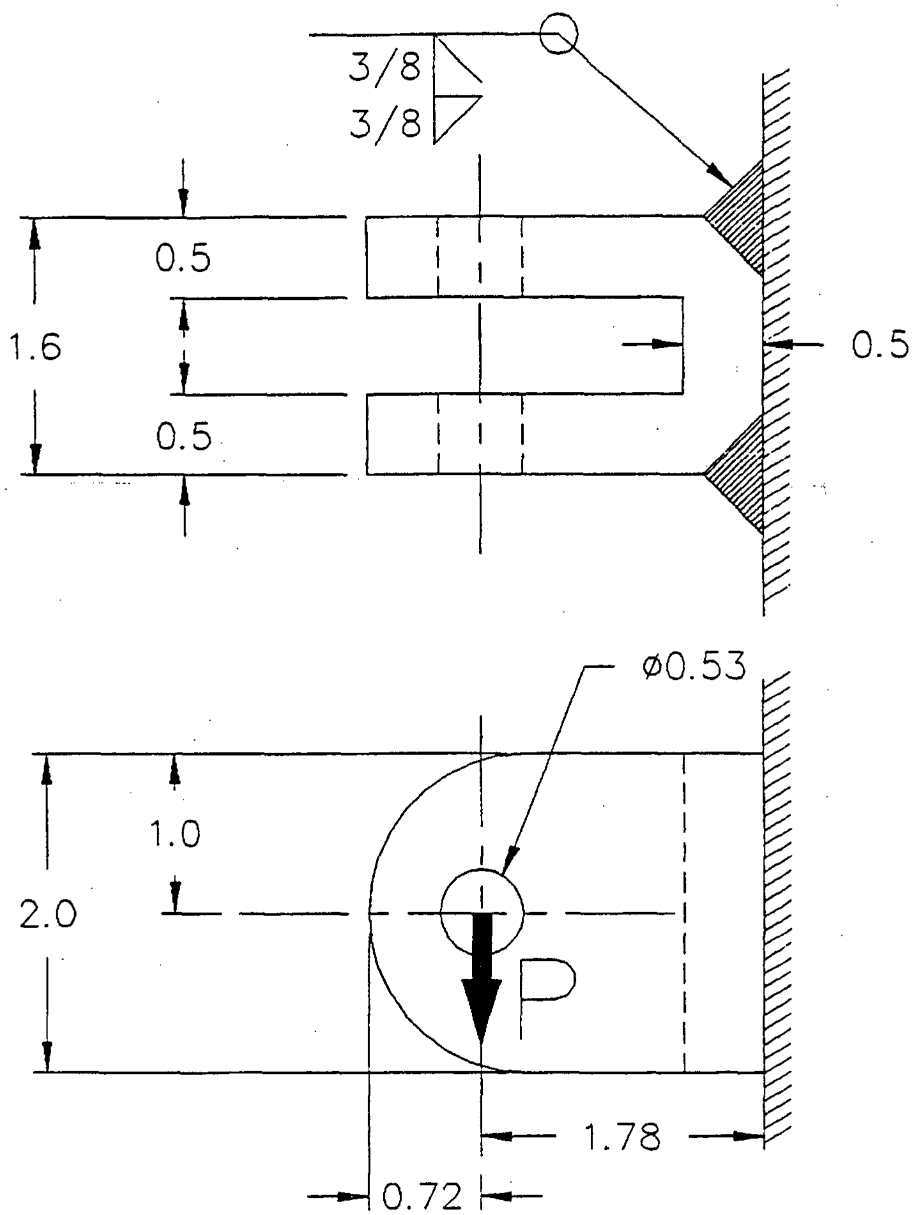

Figure 2.6.7-17 RBCUBED Output Summary – Center of Gravity Over Top Corner

Position	Crush Depth (in)	Crush Force, Fi (lb)	Package Velocity (in/sec)	Approximate Separation Moment (in-lb)
①	2	2.30×10^5	543.4	2.25×10^6
②	4	9.74×10^5	514.8	6.63×10^6
③	6	1.83×10^6	466.2	7.67×10^6
④	8	2.63×10^6	381.2	5.75×10^6

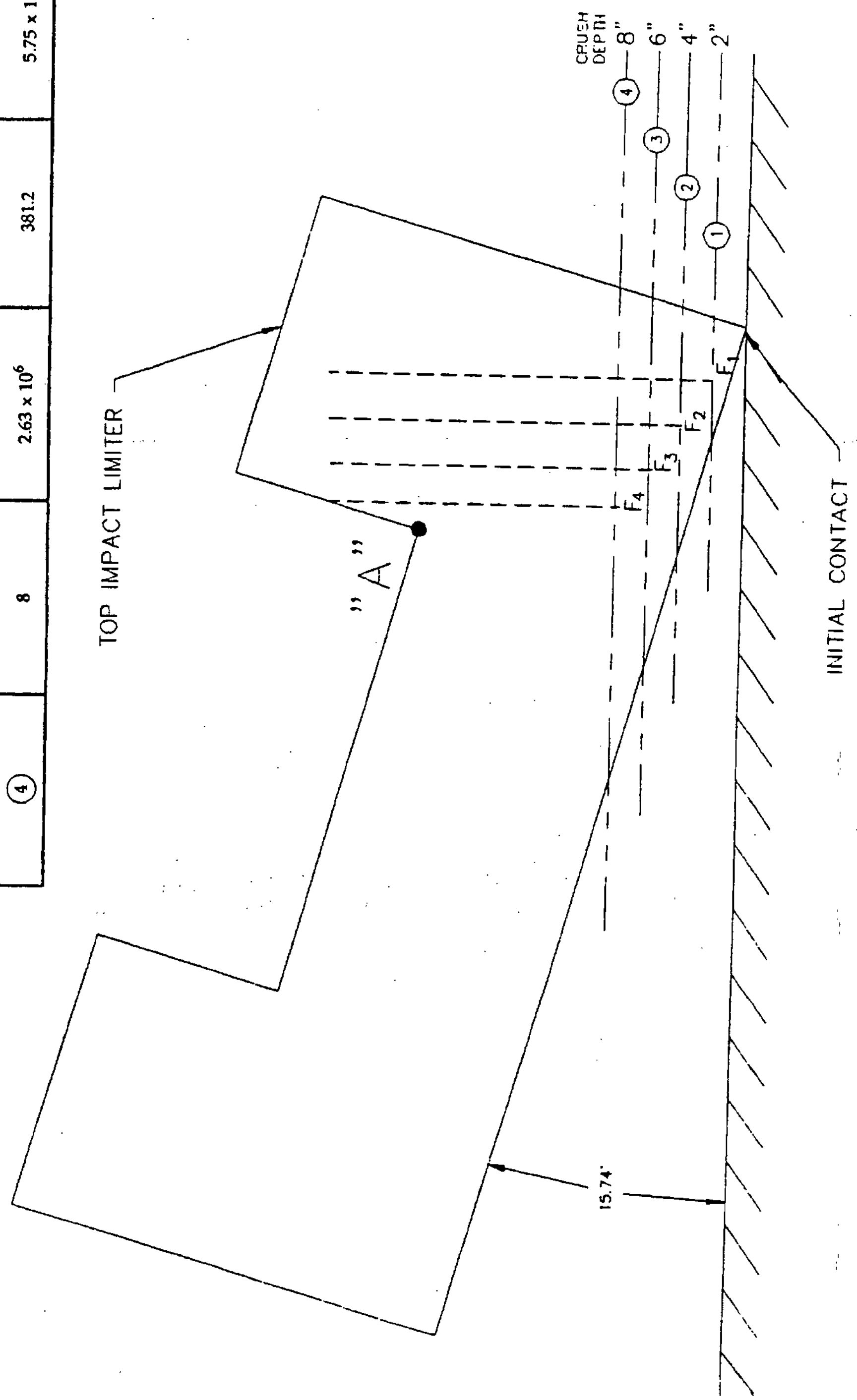

Figure 2.6.7-18 Free Body Diagram - Top Impact Limiter - Center of Gravity Over Corner

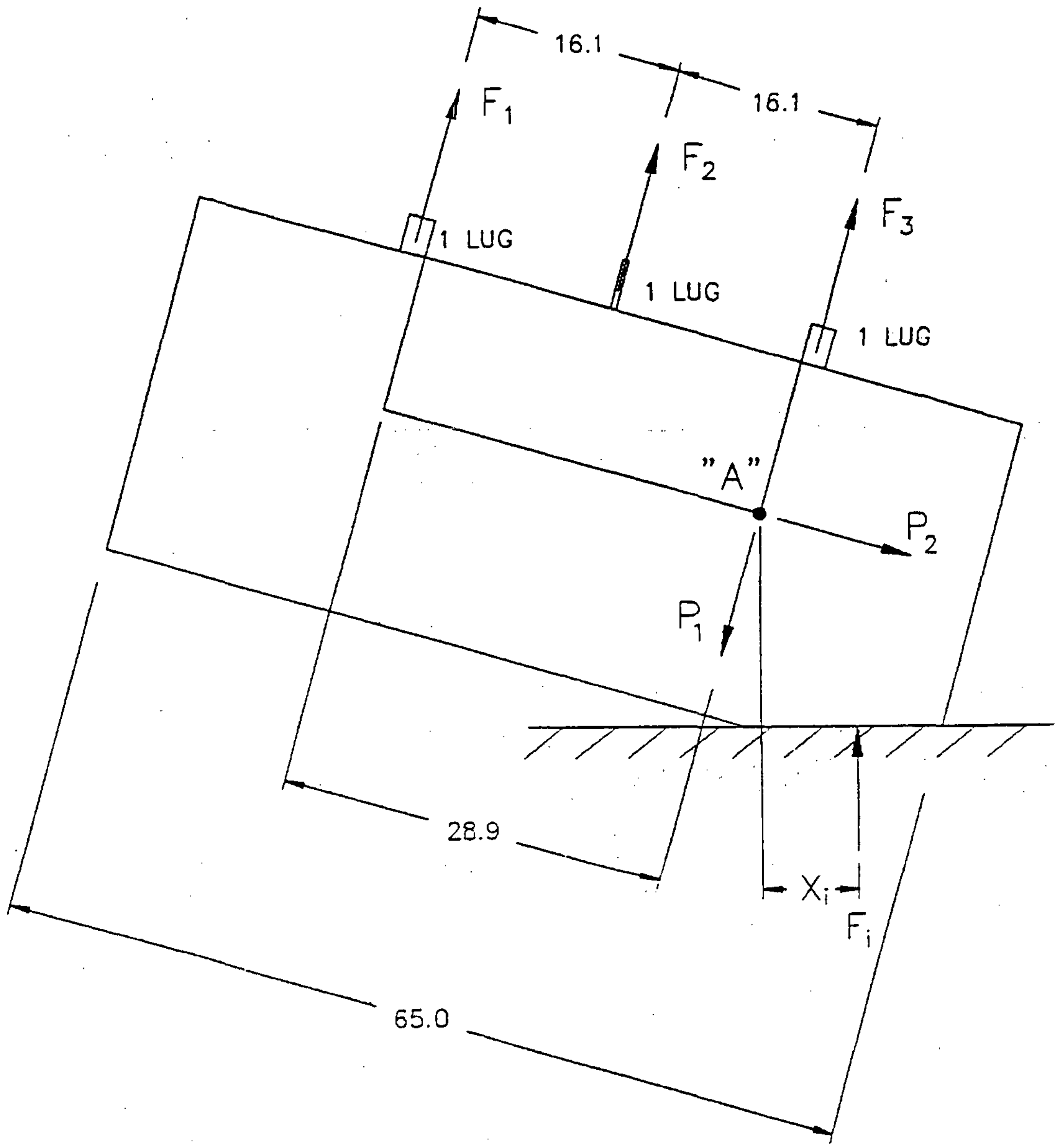

Figure 2.6.7-19 Free Body Diagram - Top Impact Limiter - Cask Wedging Forces

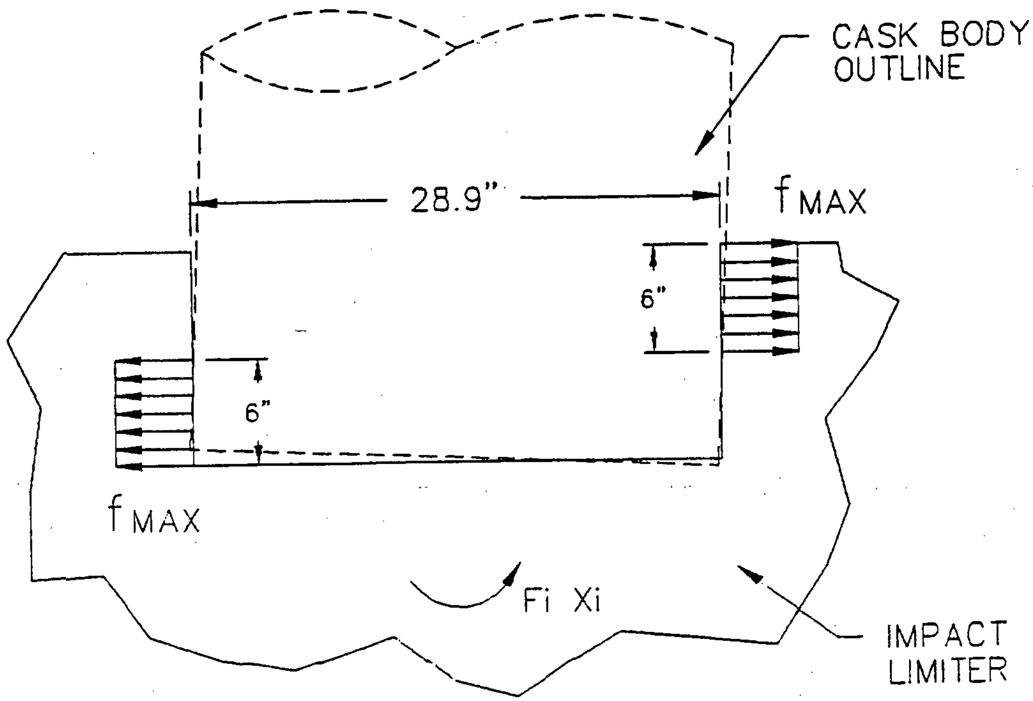

Figure 2.6.7-20 Cask Lid Configuration

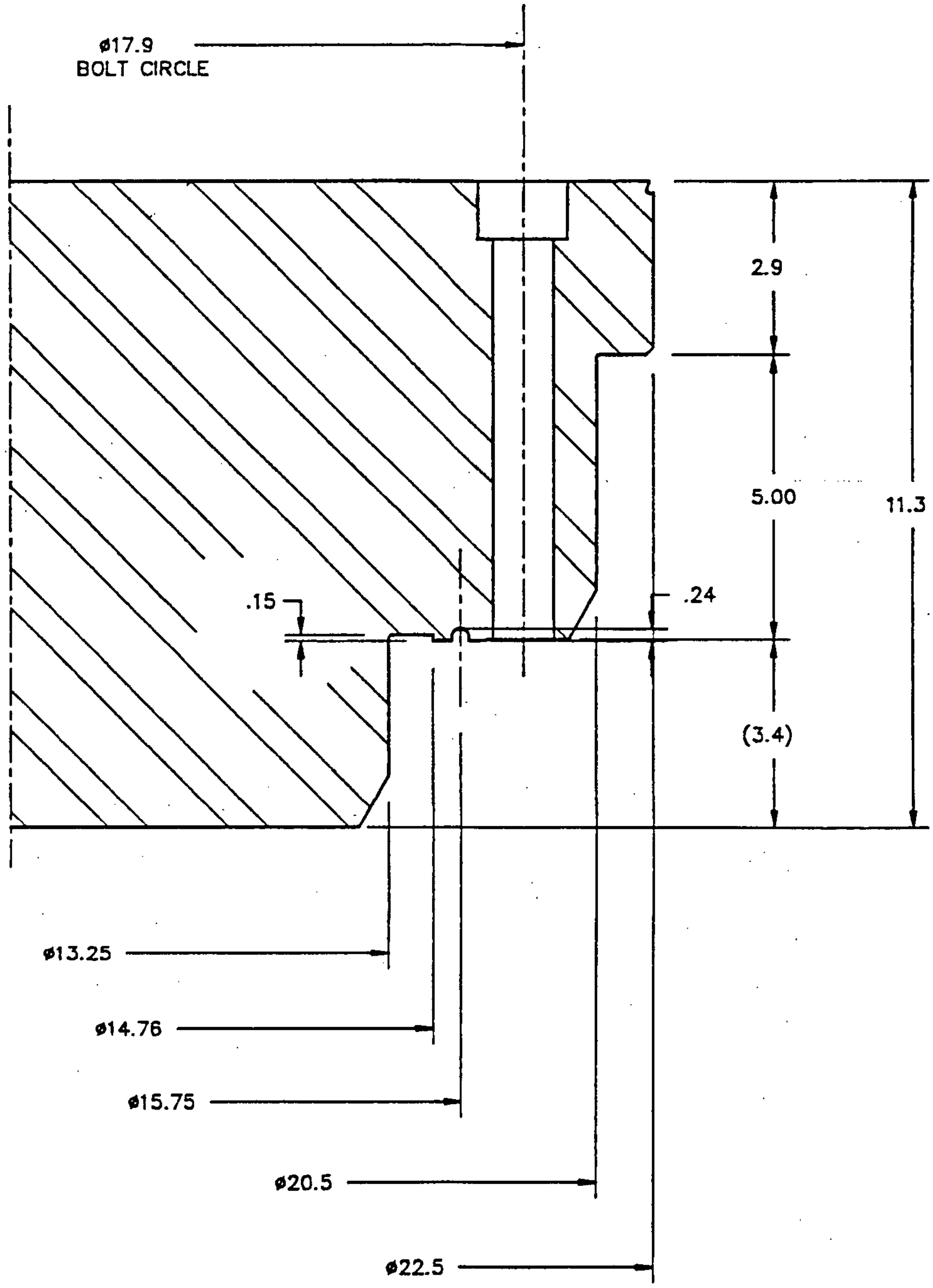

Figure 2.6.7-21 Closure Lid Free Body Diagram

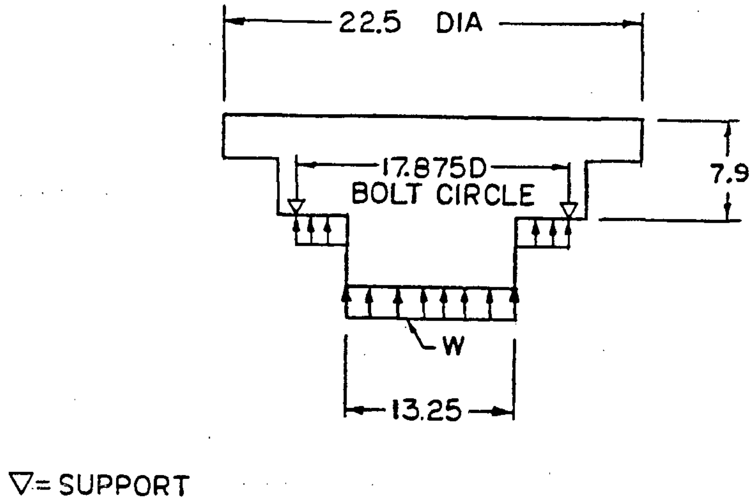

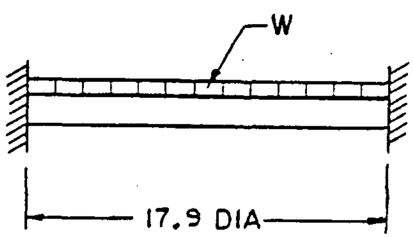

Figure 2.6.7-22 NAC-LWT Cask Cross-Section

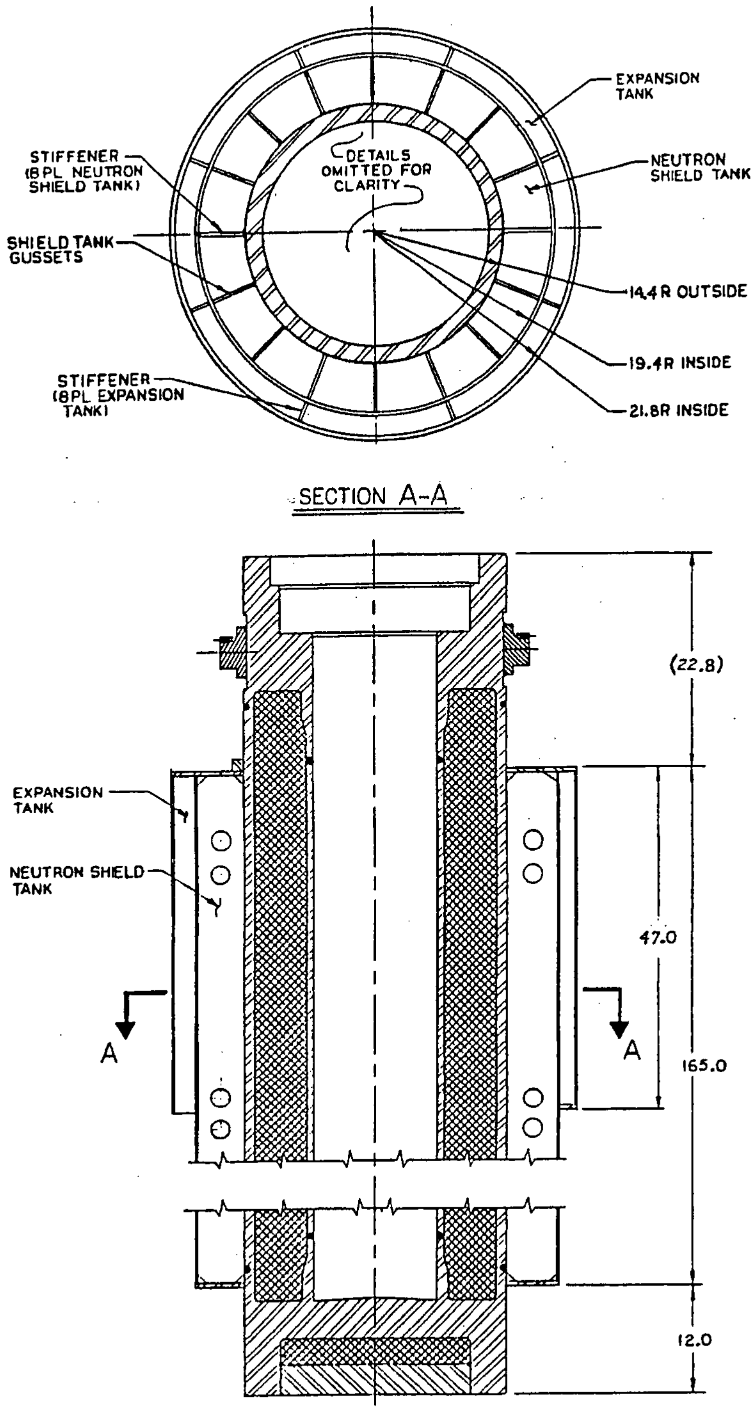

Figure 2.6.7-23 Component Parts of Shield Tank Structure

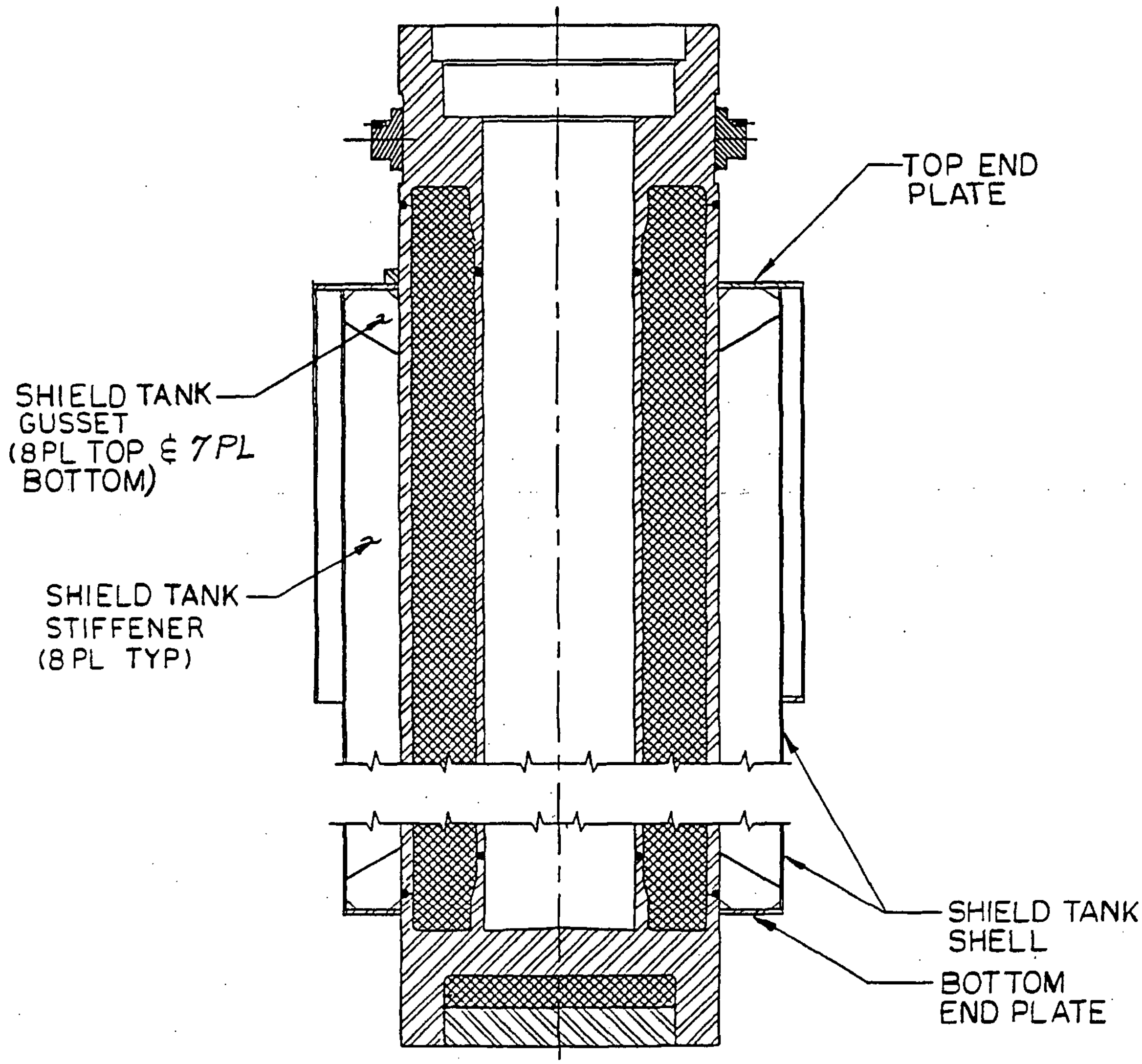

Figure 2.6.7-24 Shield Tank Cross-Section

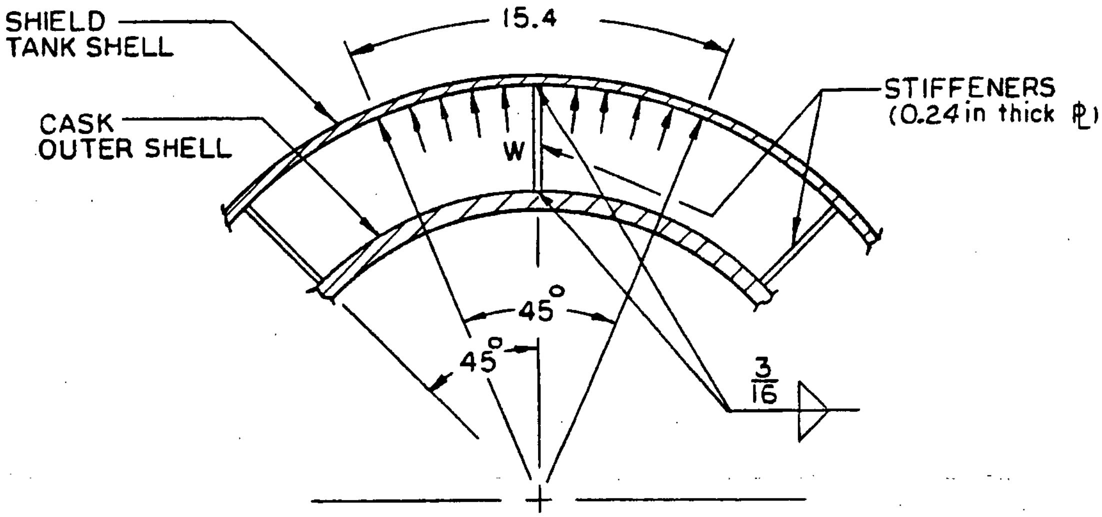

Figure 2.6.7-25 Shield Tank Quarter-Section Geometry

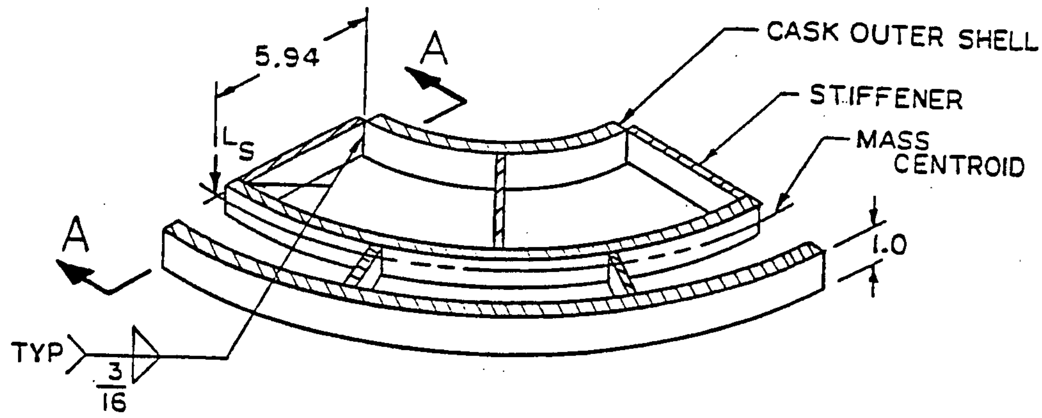

One Quarter of Tank Unit Section

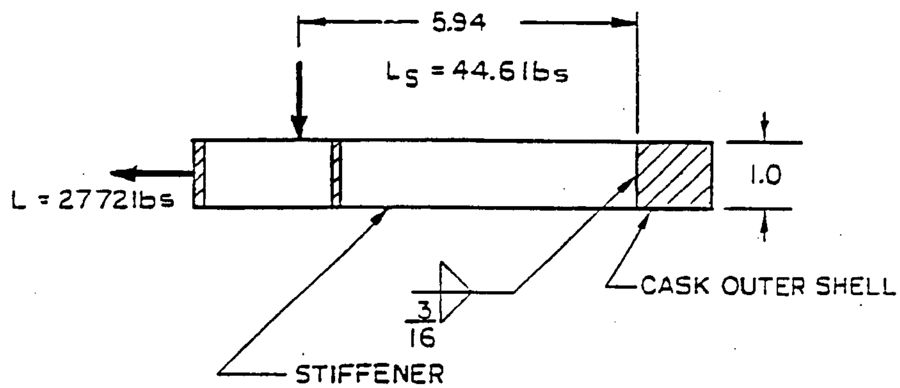

Section A-A

Figure 2.6.7-26 Partial Bottom/Top End Plate Plan and Cross-Section

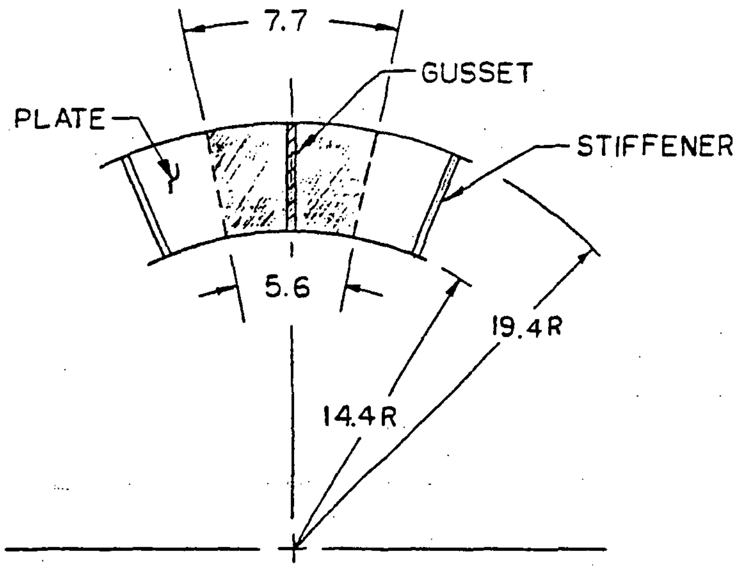

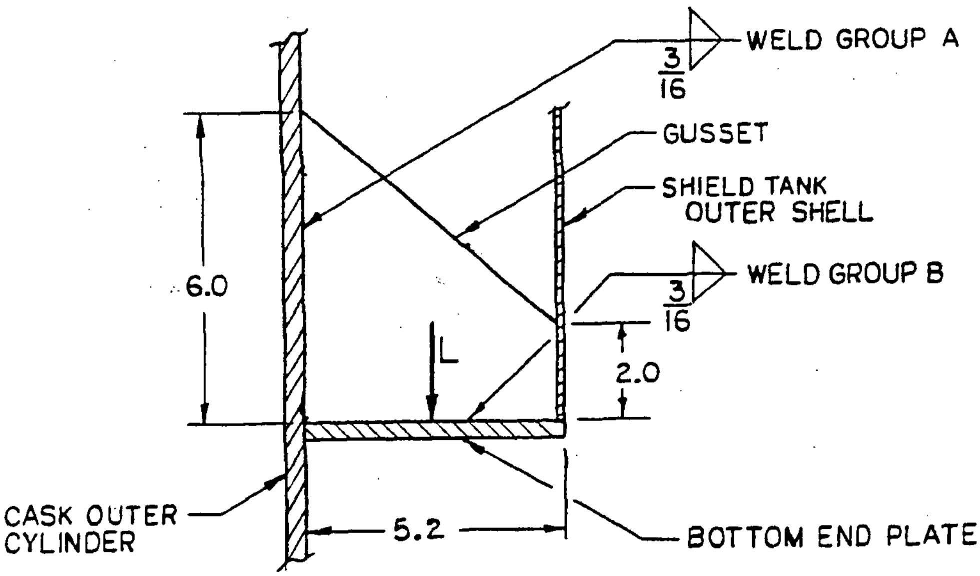

Figure 2.6.7-27 Shield Tank End Plate

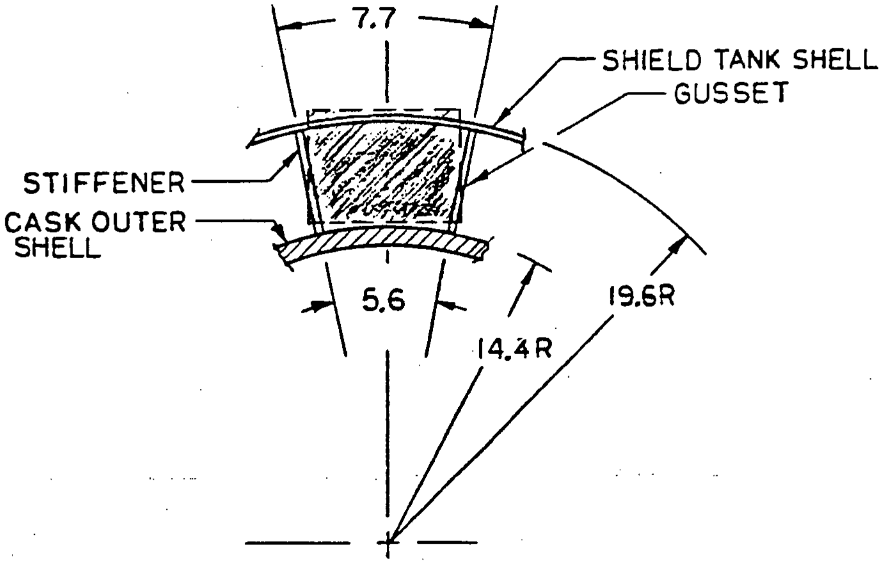

Figure 2.6.7-28 Gusset Profile

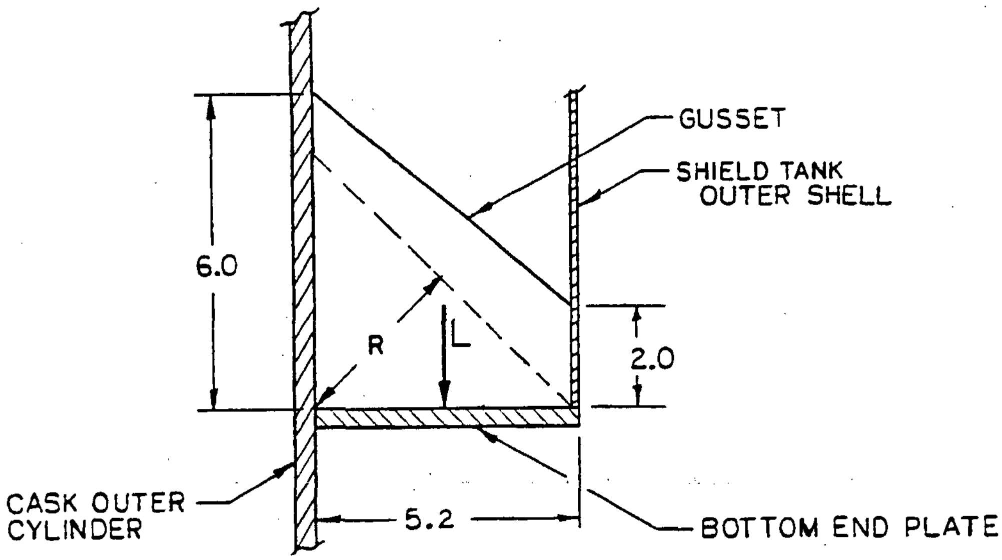

Figure 2.6.7-29 End Plate Welds

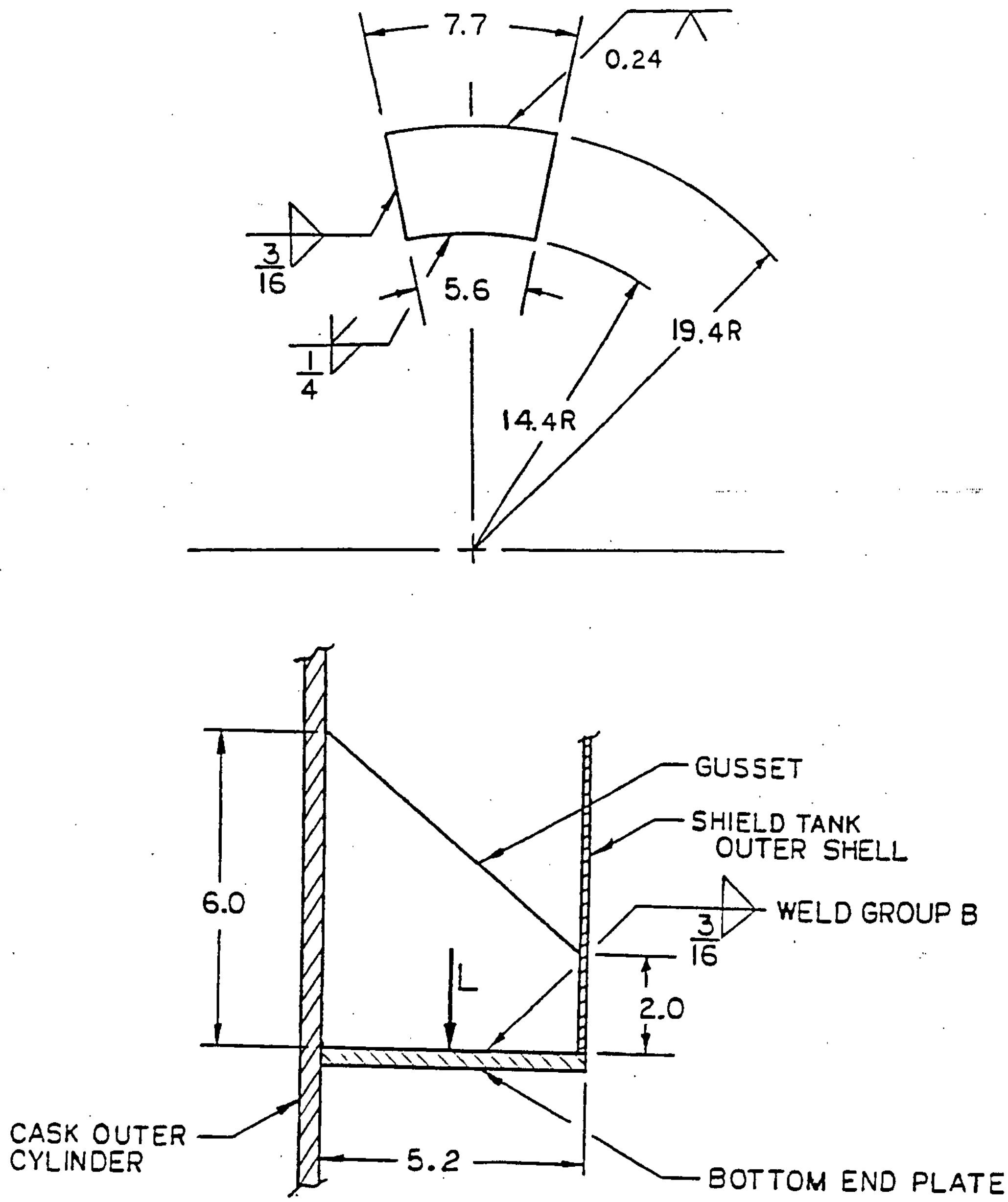

Figure 2.6.7-30 Component Parts of the Expansion Tank Structure

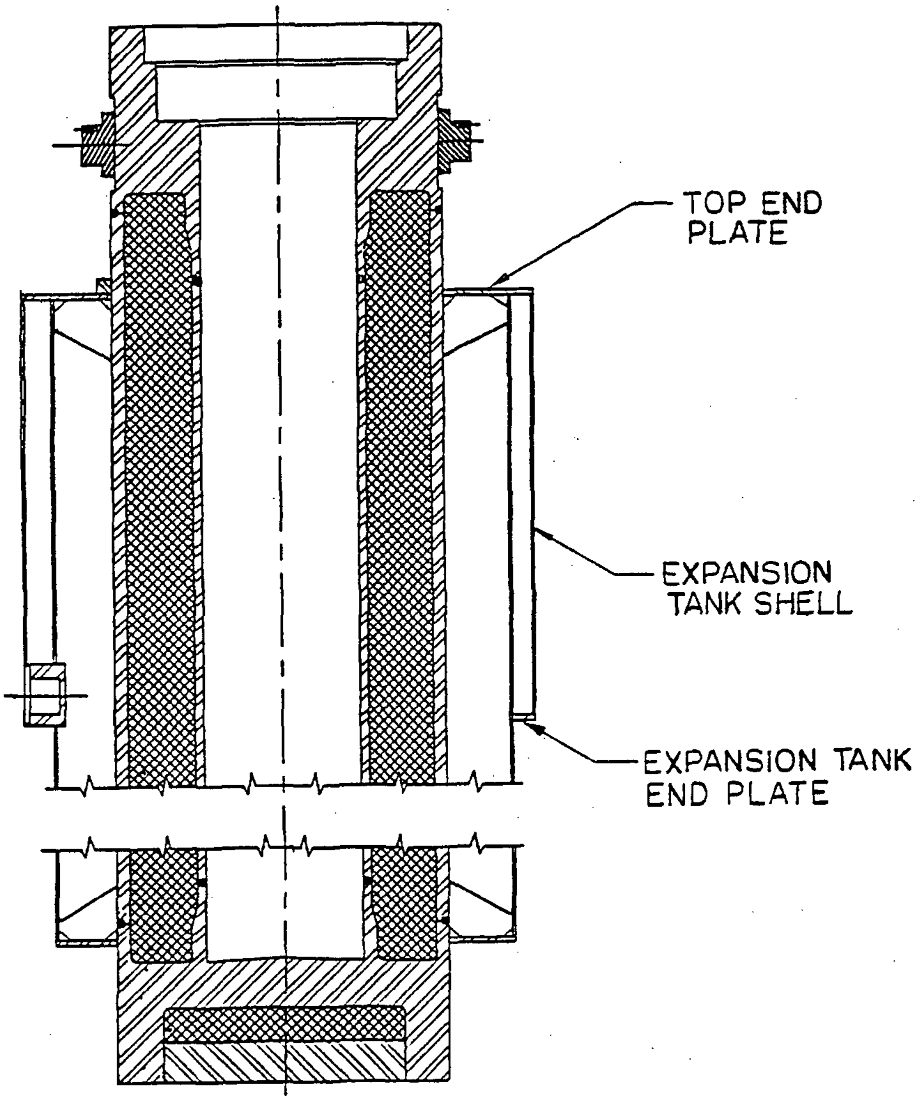

Figure 2.6.7-31 Expansion Tank Top and Bottom End Plate

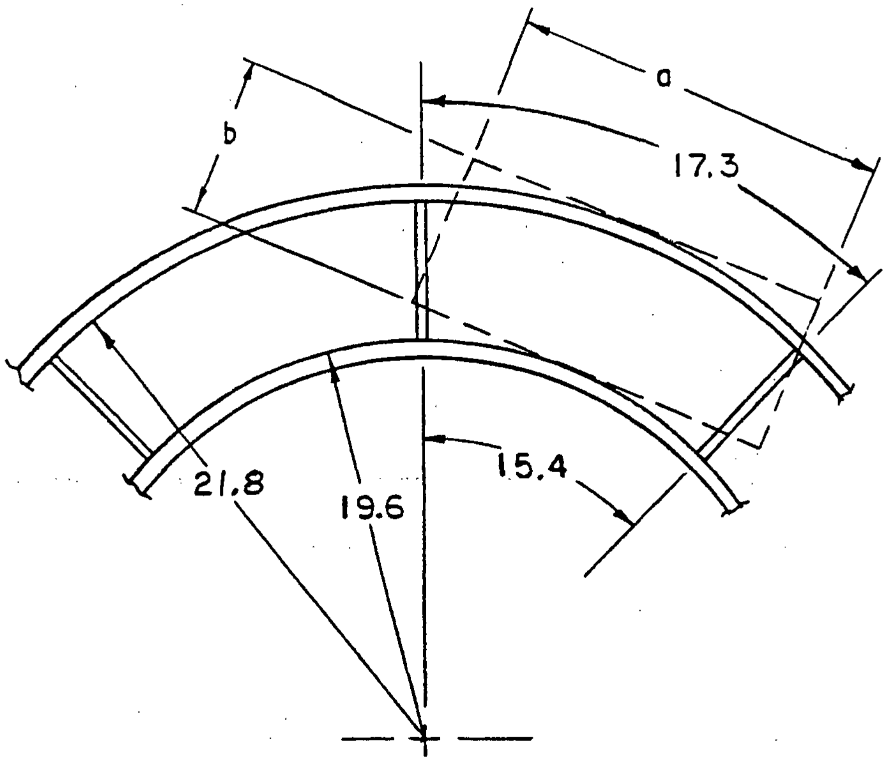

Figure 2.6.7-32 Expansion Tank Stiffener Load Geometry

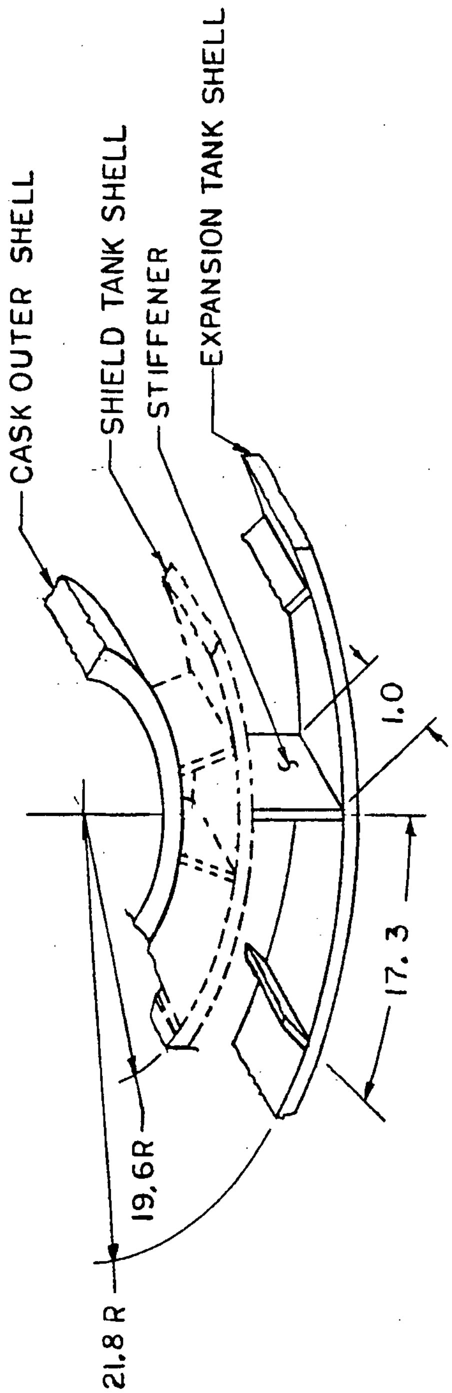

Figure 2.6.7-33 Cask Upper Ring at Trunnion - ANSYS Model

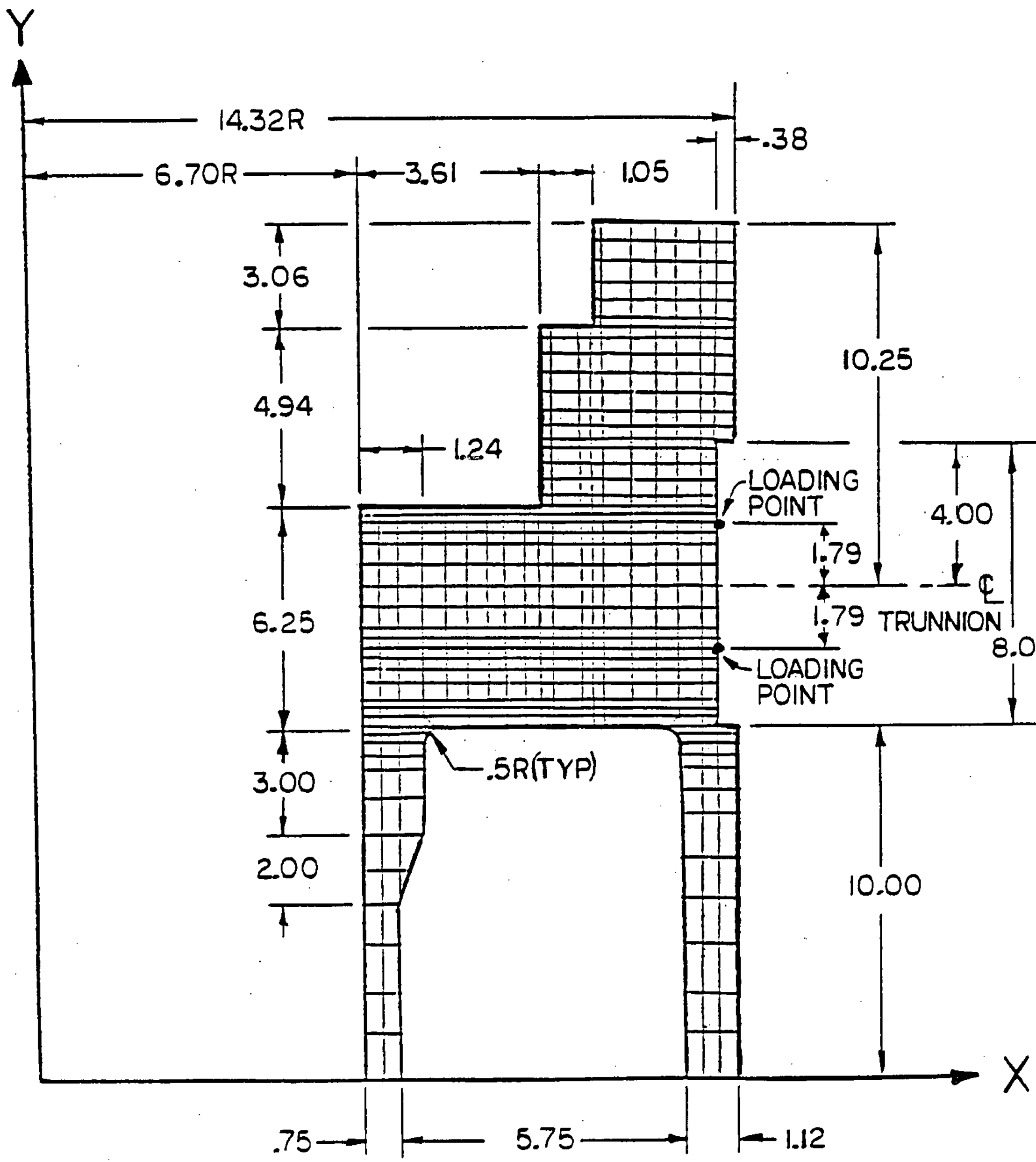

Figure 2.6.7-34 Cask Upper Ring at Trunnion - Model Loads and Boundary Conditions

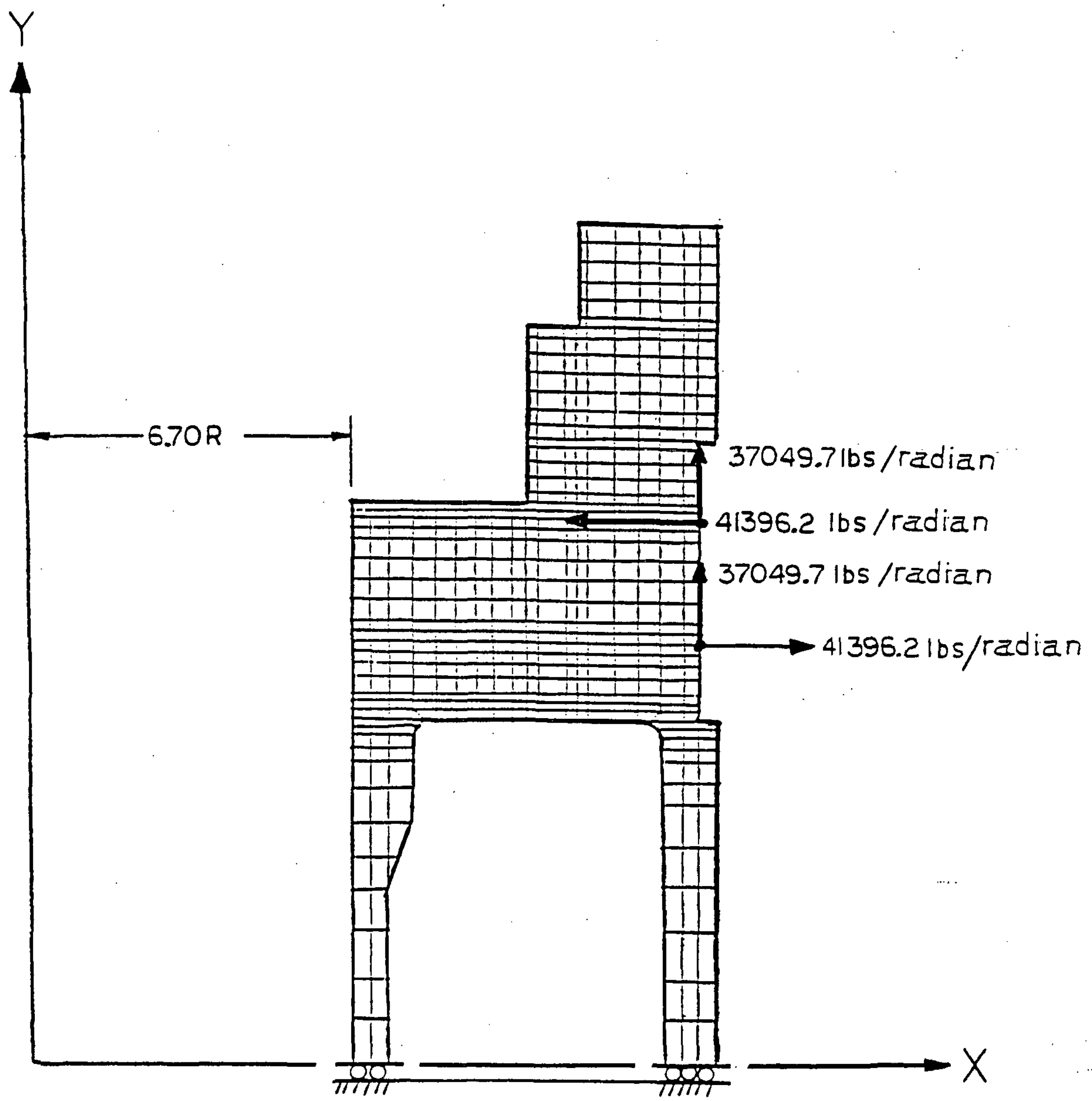

Figure 2.6.7-35 NAC-LWT Cask Upper Ring at Trunnion - Critical Sections

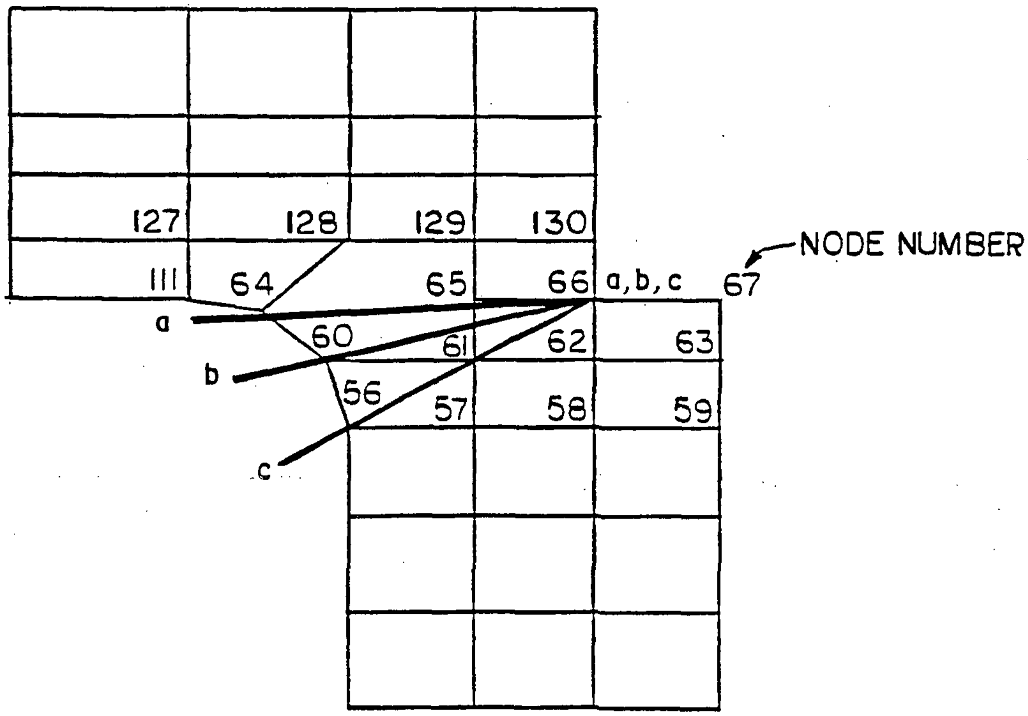

Table 2.6.7-1 Critical Stress Summary (1-Foot Bottom End Drop) – Loading Condition 1 – P_m

Loading Condition 1: 130°F Ambient Temperature and Maximum Decay Heat Load

		P_m Stresses[1] (ksi)				Principal Stresses					
Comp. No.[2]	Section Cut Node to Node	S_x	S_y	S_z	S_{xy}	S_1	S_2	S_3	S.I.	Allow. Stress 1.0 S_m	Margin of Safety
	2-2										
1	2375 to 2575	-0.17	-0.23	0.62	0.40	0.62	0.2	-0.6	1.22	20.0	Large
	4-4										
3	1581 to 1584	-0.1	-4.54	-0.16	-0.14	-0.1	-0.16	-4.55	4.45	20.0	+3.49
	7-7										
4	701 to 704	-0.03	-8.44	0.51	-0.02	0.51	-0.03	-8.44	8.94	31.4	+2.51
	6-6										
6	1515 to 1518	0.00	1.98	-0.16	-0.04	1.98	0.00	-0.16	2.14	31.4	Large
	11-11										
7	192 to 342	-6.50	1.18	1.28	1.69	1.54	1.28	-6.85	8.39	20.0	+1.38
	10-10										
8	361 to 365	0.77	-5.40	3.89	-0.99	3.89	0.92	-5.55	9.44	20.0	+1.19

[1] Conservatively based on a 1.12-inch thick outer shell and on a 3850-psi crush strength aluminum honeycomb impact limiter (Section 2.6.7.1.1).

[2] Refer to Figure 2.10.2-9 for component identification.

Table 2.6.7-2 Critical Stress Summary (1-Foot Bottom End Drop) – Loading Condition 1 - $P_m + P_b$

Loading Condition 1: 130°F Ambient Temperature and Maximum Decay Heat Load

		$P_m + P_b$ Stresses[1] (ksi)				Principal Stresses					
Comp. No.[2]	Section Cut Node to Node	S_x	S_y	S_z	S_{xy}	S_1	S_2	S_3	S.I.	Allow. Stress 1.5 S_m	Margin of Safety
	1-1										
1	2371 to 2571	-3.91	-0.35	0.11	0.00	0.11	-0.35	-3.91	4.01	30.0	+6.48
	3-3										
3	1835 to 1838	-0.1	4.66	2.25	0.29	4.68	2.25	-0.1	4.76	30.0	+5.30
	8-8										
4	621 to 624	0.15	-10.37	-1.16	0.28	0.16	-1.16	-10.38	10.54	47.1	+3.47
	5-5										
6	1595 to 1598	-0.01	3.03	0.57	0.00	3.03	0.57	-0.01	3.04	47.1	Large
	12-12										
7	150 to 193	9.25	-5.21	2.76	0.63	9.27	2.76	-5.24	14.51	30.0	+1.06
	9-9										
8	381 to 385	-0.21	-13.14	2.03	-1.07	2.03	-0.12	-13.23	15.26	30.0	+0.97

[1] Conservatively based on a 1.12-inch thick outer shell and on a 3850-psi crush strength aluminum honeycomb impact limiter (Section 2.6.7.1.1).

[2] Refer to Figure 2.10.2-9 for component identification.

Table 2.6.7-3 Critical Stress Summary (1-Foot Bottom End Drop) – Loading Condition 1 - Total Range

Loading Condition 1: 130°F Ambient Temperature and Maximum Decay Heat Load

		Total Stress Range[1] (ksi)				Principal Stresses			Stress Differences		
Comp. No.[2]	Node	S_x	S_y	S_z	S_{xy}	S_1	S_2	S_3	S_1-S_2	S_2-S_3	S_3-S_1
1	2376	0.80	-4.48	-0.22	-0.31	0.82	-0.22	-4.50	1.04	4.28	-5.32
3	1805	-0.19	-5.27	-2.19	-0.78	-0.07	-2.19	-5.39	2.12	3.20	-5.32
4	604	-0.69	-12.07	-1.65	0.61	-0.66	-1.65	-12.10	0.99	10.45	-11.44
6	1595	-0.02	2.93	0.48	0.00	2.93	0.48	-0.02	2.45	0.50	-2.95
7	192	12.54	-7.35	3.46	-3.90	13.28	3.46	-8.09	9.82	11.55	-21.37
8	361	-0.03	-16.44	0.82	-1.40	0.82	0.09	-16.57	0.73	16.65	-17.38

1 Conservatively based on a 1.12-inch thick outer shell and on a 3850-psi crush strength aluminum honeycomb impact limiter (Section 2.6.7.1.1).

2 Refer to Figure 2.10.2-9 for component identification.

Table 2.6.7-4 Critical Stress Summary (1-Foot Bottom End Drop) – Loading Condition 2 – P_m

Loading Condition 2: -40°F Ambient Temperature and Maximum Decay Heat Load

Comp. No.[2]	Section Cut Node to Node	P_m Stresses[1] (ksi)				Principal Stresses				Allow. Stress 1.0 S_m	Margin of Safety
		S_x	S_y	S_z	S_{xy}	S_1	S_2	S_3	S.I.		
	2-2										
1	2478 to 2578	0.03	-0.11	1.28	0.02	1.28	0.03	-0.11	1.39	20.0	Large
	4-4										
3	1581 to 1584	-0.15	-7.90	-0.93	-0.26	-0.14	-0.93	-7.91	7.77	20.0	+1.57
	6-6										
4	701 to 704	-0.02	-12.08	0.20	-0.03	0.20	-0.02	-12.08	12.28	31.4	+1.56
	8-8										
6	615 to 618	0.00	-2.85	0.80	0.00	0.80	0.00	-2.85	3.65	31.4	+7.60
	11-11										
7	100 to 143	-3.18	-4.19	2.15	2.18	2.15	-1.45	-5.93	8.07	20.0	+1.50
	7-7										
8	601 to 604	-0.23	-11.12	-1.21	0.46	-0.21	-1.21	-11.13	10.93	20.0	+0.83

1 Conservatively based on a 1.12-inch thick outer shell and on a 3850-psi crush strength aluminum honeycomb impact limiter (Section 2.6.7.1.1).

2 Refer to Figure 2.10.2-9 for component identification.

Table 2.6.7-5 Critical Stress Summary (1-Foot Bottom End Drop) – Loading Condition 2 - $P_m + P_b$

Loading Condition 2: -40°F Ambient Temperature and Maximum Decay Heat Load

		$P_m + P_b$ Stresses[1] (ksi)				Principal Stresses					
Comp. No.[2]	Section Cut Node to Node	S_x	S_y	S_z	S_{xy}	S_1	S_2	S_3	S.I.	Allow. Stress 1.5 S_m	Margin of Safety
	1-1										
1	2371 to 2571	-4.10	-0.43	0.14	0.00	0.14	-0.43	-4.10	4.24	30.0	+6.08
	3-3										
3	1701 to 1705	0.04	-8.08	-1.59	-0.34	0.05	-1.59	-8.10	8.15	30.0	+2.68
	5-5										
4	621 to 624	0.18	-13.91	-1.67	0.32	0.19	-1.67	-13.91	14.10	47.1	+2.34
	8-8										
6	615 to 618	0.03	-4.12	0.63	0.00	0.63	0.03	-4.12	4.75	47.1	+8.92
	10-10										
7	193 to 200	3.76	-9.04	1.83	-0.76	3.81	1.83	-9.09	12.89	30.0	+1.32
	9-9										
8	185 to 335	-12.66	-0.38	-0.11	1.93	-0.09	-0.11	-12.96	12.87	30.0	+1.33

1 Conservatively based on a 1.12-inch thick outer shell and on a 3850-psi crush strength aluminum honeycomb impact limiter (Section 2.6.7.1.1).

2 Refer to Figure 2.10.2-9 for component identification.

Table 2.6.7-6 Critical Stress Summary (1-Foot Bottom End Drop) – Loading Condition 2 - Total Range

Loading Condition 2: -40°F Ambient Temperature and Maximum Decay Heat Load

		Total Stress Range[1] (ksi)				Principal Stresses			Stress Differences		
Comp. No.[2]	Node	S_x	S_y	S_z	S_{xy}	S_1	S_2	S_3	S_1-S_2	S_2-S_3	S_3-S_1
1	2376	0.67	-4.03	0.05	-0.35	0.70	0.05	-4.06	0.65	4.11	-4.75
3	1805	-0.32	-9.36	-3.82	-1.34	-0.12	-3.82	-9.56	3.70	5.74	-9.44
4	604	-0.90	-15.99	-2.51	0.80	-0.86	-2.51	-16.03	1.65	13.52	-15.17
6	618	0.03	-4.20	0.57	0.00	0.57	0.03	-4.20	0.54	4.23	-4.77
7	143	-5.58	-14.56	-1.04	0.55	-1.04	-5.55	-14.59	4.51	9.05	-13.55
8	361	0.01	-14.97	-0.81	-1.62	0.18	-0.81	-15.14	0.99	14.33	-15.33

1 Conservatively based on a 1.12-inch thick outer shell and on a 3850-psi crush strength aluminum honeycomb impact limiter (Section 2.6.7.1.1).
2 Refer to Figure 2.10.2-9 for component identification.

Table 2.6.7-7 Critical Stress Summary (1-Foot Bottom End Drop) – Loading Condition 3 – P_m

Loading Condition 3: -40°F Ambient Temperature and No Decay Heat Load

		P_m Stresses[1] (ksi)				Principal Stresses					
Comp. No.[2]	Section Cut Node to Node	S_x	S_y	S_z	S_{xy}	S_1	S_2	S_3	S.I.	Allow. Stress 1.0 S_m	Margin of Safety
	1-1										
1	2375 to 2575	-0.21	0.00	-0.03	0.18	0.1	-0.03	-0.31	0.41	20.0	Large
	2-2										
3	1581 to 1584	-0.22	-3.78	-5.48	-0.28	-0.19	-3.80	-5.48	5.29	20.0	+2.78
	3-3										
4	621 to 624	0.04	-7.76	-1.05	0.24	0.04	-1.05	-7.77	7.81	31.4	+3.02
	5-5										
6	615 to 618	0.00	-6.85	-0.13	0.00	0.00	-0.13	-6.85	6.85	31.4	+3.58
	8-8										
7	18 to 118	-10.02	-0.60	-2.86	2.62	0.08	-2.86	-10.70	10.78	20.0	+0.86
	4-4										
8	601 to 604	-0.16	-7.07	-0.78	0.34	-0.14	-0.78	-7.09	6.95	20.0	+1.88

1 Conservatively based on a 1.12-inch thick outer shell and on a 3850-psi crush strength aluminum honeycomb impact limiter (Section 2.6.7.1.1).

2 Refer to Figure 2.10.2-9 for component identification.

Table 2.6.7-8 Critical Stress Summary (1-Foot Bottom End Drop) – Loading Condition 3 - $P_m + P_b$

Loading Condition 3: -40°F Ambient Temperature and No Decay Heat Load

		$P_m + P_b$ Stresses[1] (ksi)				Principal Stresses					
Comp. No.[2]	Section Cut Node to Node	S_x	S_y	S_z	S_{xy}	S_1	S_2	S_3	S.I.	Allow. Stress 1.5 S_m	Margin of Safety
	1-1										
1	2375 to 2575	-1.99	0.00	-0.03	0.18	0.01	-0.03	-2.01	2.02	30.0	Large
	2-2										
3	1581 to 1584	0.01	-3.30	-5.65	-0.28	0.03	-3.33	-5.65	5.68	30.0	+4.28
	3-3										
4	621 to 624	0.12	-8.99	-1.30	0.24	0.13	-1.30	-9.00	9.13	47.1	+4.16
	5-5										
6	615 to 618	0.00	-7.06	-0.19	0.00	0.00	-0.19	-7.06	7.06	47.1	+5.67
	8-8										
7	18 to 118	-20.14	-0.6	-2.86	2.62	-0.25	-2.86	-20.49	20.23	30.0	+0.48
	6-6										
8	185 to 335	-8.83	1.55	1.16	2.22	2.0	1.16	-9.29	11.29	30.0	+1.66

1 Conservatively based on a 1.12-inch thick outer shell and on a 3850-psi crush strength aluminum honeycomb impact limiter (Section 2.6.7.1.1).

2 Refer to Figure 2.10.2-9 for component identification.

Table 2.6.7-9 Critical Stress Summary (1-Foot Bottom End Drop) – Loading Condition 3 - Total Range

Loading Condition 3: -40°F Ambient Temperature and No Decay Heat Load

		Total Stress Range[1] (ksi)				Principal Stresses			Stress Differences		
Comp. No.[2]	Node	S_x	S_y	S_z	S_{xy}	S_1	S_2	S_3	S_1-S_2	S_2-S_3	S_3-S_1
1	2376	0.96	-3.75	-0.64	-0.11	0.96	-0.64	-3.75	1.60	3.11	-4.71
3	2176	3.74	-17.36	-1.84	-2.41	4.01	-1.84	-17.90	5.85	16.06	-21.91
4	604	-0.58	-10.47	-1.81	0.56	-0.55	-1.81	-10.50	1.26	8.69	-9.95
6	615	0.01	-7.05	-0.19	0.00	0.01	-0.19	-7.05	0.20	6.86	-7.06
7	143	0.08	-23.96	-3.03	-2.73	0.39	-3.03	-24.27	3.42	21.24	-24.66
8	361	-0.02	-10.55	0.26	-1.38	0.26	-0.16	-10.73	0.10	10.89	-10.99

1 Conservatively based on a 1.12-inch thick outer shell and on a 3850-psi crush strength aluminum honeycomb impact limiter (Section 2.6.7.1.1).
2 Refer to Figure 2.10.2-9 for component identification.

Table 2.6.7-10 Critical Stress Summary (1-Foot Top End Drop) – Loading Condition 1 – P_m

Loading Condition 1: 130°F Ambient Temperature and Maximum Decay Heat Load

		P_m Stresses[1] (ksi)				Principal Stresses					
Comp. No.[2]	Section Cut Node to Node	S_x	S_y	S_z	S_{xy}	S_1	S_2	S_3	S.I.	Allow. Stress 1.0 S_m	Margin of Safety
	2-2										
1	2377 to 2577	-7.46	-0.06	0.09	0.15	0.09	-0.05	-7.46	7.55	20.0	+1.65
	4-4										
3	1581 to 1584	-0.20	-7.58	-0.57	-0.33	-0.18	-0.57	-7.60	7.42	20.0	+1.70
	5-5										
4	1481 to 1484	-0.03	-8.19	0.52	0.02	0.52	-0.03	-8.19	8.71	31.4	+2.60
	12-12										
6	695 to 698	0.00	2.39	-0.10	0.04	2.40	0.00	-0.10	2.50	31.4	Large
	10-10										
7	17 to 117	-1.04	1.54	2.36	-2.84	3.37	2.36	-2.87	6.23	20.0	+2.21
	7-7										
8	401 to 405	-0.03	-2.63	1.89	-0.39	1.89	0.03	-2.69	4.58	20.0	+3.37

1 Conservatively based on a 1.12-inch thick outer shell and on a 3850-psi crush strength aluminum honeycomb impact limiter (Section 2.6.7.1.1).

2 Refer to Figure 2.10.2-9 for component identification.

Table 2.6.7-11 Critical Stress Summary (1-Foot Top End Drop) – Loading Condition 1 - $P_m + P_b$

Loading Condition 1: 130°F Ambient Temperature and Maximum Decay Heat Load

		$P_m + P_b$ Stresses[1] (ksi)				Principal Stresses					
Comp. No.[2]	Section Cut Node to Node	S_x	S_y	S_z	S_{xy}	S_1	S_2	S_3	S.I.	Allow. Stress 1.5 S_m	Margin of Safety
	1-1										
1	2371 to 2571	-12.69	-0.13	-0.22	-1.01	-0.05	-0.22	-12.77	12.72	30.0	+1.36
	3-3										
3	1941 to 1956	0.84	-10.28	-3.31	0.03	0.84	-3.31	-10.28	11.12	30.0	+1.70
	11-11										
4	1561 to 1564	0.12	-9.50	-0.89	-0.22	0.13	-0.89	-9.51	9.64	47.1	+3.89
	6-6										
6	615 to 618	-0.02	3.50	0.78	0.00	3.50	0.78	-0.02	3.52	47.1	Large
	9-9										
7	143 to 150	-7.68	6.60	1.37	1.33	6.72	1.37	-7.80	14.52	30.0	+1.07
	8-8										
8	381 to 385	-0.15	-6.77	0.67	-0.49	0.67	-0.12	-6.81	7.47	30.0	+3.02

1 Conservatively based on a 1.12-inch thick outer shell and on a 3850-psi crush strength aluminum honeycomb impact limiter (Section 2.6.7.1.1).

2 Refer to Figure 2.10.2-9 for component identification.

Table 2.6.7-12 Critical Stress Summary (1-Foot Top End Drop) – Loading Condition 1 - Total Range

Loading Condition 1: 130°F Ambient Temperature and Maximum Decay Heat Load

		Total Stress Range[1] (ksi)				Principal Stresses			Stress Differences		
Comp. No.[2]	Node	S_x	S_y	S_z	S_{xy}	S_1	S_2	S_3	S_1-S_2	S_2-S_3	S_3-S_1
1	2371	2.76	-10.30	0.04	3.56	3.67	0.04	-11.21	3.63	11.25	-14.88
3	1962	-1.54	-12.69	-5.46	-1.00	-1.45	-5.46	-12.78	4.01	7.32	-11.33
4	1584	-0.62	-10.96	-1.54	-0.54	-0.59	-1.54	-10.98	0.95	9.44	-10.39
6	615	-0.01	3.43	0.72	-0.01	3.43	0.72	-0.01	2.71	0.73	-3.44
7	143	-7.68	6.79	1.34	2.96	7.37	1.34	-8.26	6.03	9.60	-15.63
8	361	-0.07	-8.76	-0.09	-0.78	0.00	-0.09	-8.83	0.09	8.74	-8.83

1 Conservatively based on a 1.12-inch thick outer shell and on a 3850-psi crush strength aluminum honeycomb impact limiter (Section 2.6.7.1.1).

2 Refer to Figure 2.10.2-9 for component identification.

Table 2.6.7-13 Critical Stress Summary (1-Foot Top End Drop) – Loading Condition 2 – P_m

Loading Condition 2: -40°F Ambient Temperature and Maximum Decay Heat Load

		P_m Stresses[1] (ksi)				Principal Stresses					
Comp. No.[2]	Section Cut Node to Node	S_x	S_y	S_z	S_{xy}	S_1	S_2	S_3	S.I.	Allow. Stress 1.0 S_m	Margin of Safety
	2-2										
1	2377 to 2577	-7.42	-0.08	0.30	0.18	0.30	-0.08	-7.42	7.72	20.0	+1.59
	4-4										
3	1581 to 1584	-0.24	-10.89	-1.33	-0.44	-0.22	-1.33	-10.91	10.69	20.0	+0.87
	6-6										
4	1481 to 1484	-0.02	-11.77	0.24	0.04	0.24	-0.02	-11.77	12.01	31.4	+1.61
	5-5										
6	1595 to 1598	0.01	-2.37	1.0	0.02	1.0	0.01	-2.37	3.37	31.4	+8.32
	10-10										
7	375 to 378	-1.35	1.92	2.97	-0.61	2.97	2.03	-1.45	4.42	20.0	+3.52
	8-8										
8	601 to 604	-0.13	-7.55	-0.80	0.27	-0.12	-0.80	-7.56	7.44	20.0	+1.69

[1] Conservatively based on a 1.12-inch thick outer shell and on a 3850-psi crush strength aluminum honeycomb impact limiter (Section 2.6.7.1.1).
[2] Refer to Figure 2.10.2-9 for component identification.

Table 2.6.7-14 Critical Stress Summary (1-Foot Top End Drop) – Loading Condition 2 - $P_m + P_b$

Loading Condition 2: -40°F Ambient Temperature and Maximum Decay Heat Load

		$P_m + P_b$ Stresses[1] (ksi)				Principal Stresses					
Comp. No.[2]	Section Cut Node to Node	S_x	S_y	S_z	S_{xy}	S_1	S_2	S_3	S.I.	Allow. Stress 1.5 S_m	Margin of Safety
	1-1										
1	2371 to 2571	-12.88	-0.21	-0.19	-1.02	-0.13	-0.19	-12.96	12.84	30.0	+1.34
	4-4										
3	1581 to 1584	-0.52	-12.05	-1.44	-0.45	-0.51	-1.44	-12.07	11.56	30.0	+1.60
	3-3										
4	1561 to 1564	0.17	-13.22	-1.52	-0.30	0.17	-1.52	-13.23	13.40	47.1	+2.51
	5-5										
6	1595 to 1598	0.04	-3.78	0.86	0.02	0.86	0.04	-3.78	4.64	47.1	+9.15
	9-9										
7	395 to 398	-0.18	7.35	4.97	-0.78	7.42	4.97	-0.26	7.69	30.0	+2.90
	8-8										
8	601 to 604	-0.18	-7.94	-0.67	0.27	-0.18	-0.67	-7.95	7.78	30.0	+2.86

1 Conservatively based on a 1.12-inch thick outer shell and on a 3850-psi crush strength aluminum honeycomb impact limiter (Section 2.6.7.1.1).

2 Refer to Figure 2.10.2-9 for component identification.

Table 2.6.7-15 Critical Stress Summary (1-Foot Top End Drop) – Loading Condition 2 - Total Range

Loading Condition 2: -40°F Ambient Temperature and Maximum Decay Heat Load

		Total Stress Range[1] (ksi)				Principal Stresses			Stress Differences		
Comp. No.[2]	Node	S_x	S_y	S_z	S_{xy}	S_1	S_2	S_3	S_1-S_2	S_2-S_3	S_3-S_1
1	2371	2.56	-10.43	0.01	3.61	3.50	0.01	-11.37	3.49	11.38	-14.87
3	1962	-1.54	-12.88	-5.92	-1.05	-1.44	-5.92	-12.98	4.48	7.06	-11.54
4	1584	-0.85	-15.19	-2.48	-0.76	-0.81	-2.48	-15.23	1.67	12.75	-14.42
6	1598	0.02	-3.94	0.76	0.02	0.76	0.02	-3.94	0.74	3.96	-4.70
7	378	-0.19	7.42	4.95	-0.07	7.42	4.95	-0.19	2.47	5.14	-7.61
8	361	-0.02	-7.21	-1.70	-1.00	0.16	-1.70	-7.38	1.86	5.68	-7.54

1 Conservatively based on a 1.12-inch thick outer shell and on a 3850-psi crush strength aluminum honeycomb impact limiter (Section 2.6.7.1.1).

2 Refer to Figure 2.10.2-9 for component identification.

Table 2.6.7-16 Critical Stress Summary (1-Foot Side Drop) – Loading Condition 1 – P_m

Loading Condition 1: 100°F Ambient Temperature and Maximum Decay Heat Load

		P_m Stresses (ksi)				Principal Stresses					
Comp. No.[1]	Section Cut Node to Node	S_x	S_y	S_z	S_{xy}	S_1	S_2	S_3	S.I.	Allow. Stress 1.0 S_m	Margin of Safety
	1-1										
1	2361 to 2370	-3.39	-0.30	0.06	-0.26	0.06	-0.28	-3.42	3.48	20.0	+4.74
	2-2										
3	1969 to 1976	-10.14	1.89	-4.53	-1.65	2.11	-4.53	-10.37	12.47	20.0	+0.60
	3-3										
4	1141 to 1144	-0.11	15.43	0.25	0.00	15.43	0.25	-0.11	15.54	31.4	+1.02
	4-4										
6	1115 to 1118	-0.05	31.36	1.31	0.00	31.36	1.31	-0.05	31.4	31.4	+0.00
	5-5										
7	395 to 398	-2.17	4.06	-5.51	0.78	4.15	-2.27	-5.51	9.66	20.0	+1.07
	6-6										
8	192 to 342	-5.47	-0.35	-3.06	0.18	-0.35	-3.06	-5.48	5.13	20.0	+2.89

[1] Refer to Figure 2.10.2-9 for component identification.

Table 2.6.7-17 Critical Stress Summary (1-Foot Side Drop) – Loading Condition 1 - $P_m + P_b$

Loading Condition 1: 100°F Ambient Temperature and Maximum Decay Heat Load

		$P_m + P_b$ Stresses (ksi)				Principal Stresses					
Comp. No.[1]	Section Cut Node to Node	S_x	S_y	S_z	S_{xy}	S_1	S_2	S_3	S.I.	Allow. Stress 1.5 S_m	Margin of Safety
	7-7										
1	2301 to 2561	-0.78	0.06	0.82	3.96	3.62	0.82	-4.34	7.96	30.0	+2.77
	8-8										
3	2150 to 2156	-4.40	-0.08	-20.16	0.01	-0.08	-4.40	-20.16	20.08	30.0	+0.49
	3-3										
4	1141 to 1144	-0.07	16.41	0.86	0.00	16.41	0.86	-0.07	16.48	47.1	+1.86
	4-4										
6	1115 to 1118	0.01	33.37	1.50	0.00	33.37	1.50	0.01	33.36	47.1	+0.41
	5-5										
7	395 to 398	-1.11	16.09	-0.89	0.78	16.12	-0.89	-1.14	17.26	30.0	+0.74
	9-9										
8	177 to 327	-8.25	-1.80	0.27	-1.47	0.27	-1.48	-8.58	8.85	30.0	+2.39

[1] Refer to Figure 2.10.2-9 for component identification.

Table 2.6.7-18 Critical Stress Summary (1-Foot Side Drop) – Loading Condition 1 - S_n

Loading Condition 1: 100°F Ambient Temperature and Maximum Decay Heat Load

		S_n Stresses (ksi)				Principal Stresses					
Comp. No.[1]	Section Cut Node to Node	S_x	S_y	S_z	S_{xy}	S_1	S_2	S_3	S.I.	Allow. Stress 3.0 S_m	Margin of Safety
	1-1										
1	2361 to 2370	-9.54	-1.04	-1.24	-0.19	-1.04	-1.24	-9.55	8.51	60.0	+6.05
	10-10										
3	1815 to 1818	-0.09	22.64	2.62	-1.58	22.75	2.62	-0.20	22.95	60.0	+1.61
	3-3										
4	1141 to 1144	-0.07	17.55	0.98	0.00	17.55	0.98	-0.07	17.62	94.2	+4.34
	4-4										
6	1115 to 1118	0.01	38.01	1.65	0.00	38.01	1.65	0.01	38.00	94.2	+1.48
	11-11										
7	395 to 398	-1.10	19.46	0.52	0.51	19.47	0.52	-1.12	20.59	60.0	+1.91
	6-6										
8	177 to 327	-12.34	-1.86	-3.80	-1.48	-1.66	-3.80	-12.55	10.89	60.0	+4.51

[1] Refer to Figure 2.10.2-9 for component identification.

Table 2.6.7-19 Critical Stress Summary (1-Foot Side Drop) – Loading Condition 1 - Total Range

Loading Condition 1: 100°F Ambient Temperature and Maximum Decay Heat Load

		Total Stress Range (ksi)				Principal Stresses			Stress Differences		
Comp. No.[1]	Node	S_x	S_y	S_z	S_{xy}	S_1	S_2	S_3	S_1-S_2	S_2-S_3	S_3-S_1
1	2561	0.06	0.02	1.33	15.24	15.28	1.33	-15.19	13.95	16.52	-30.47
3	1815	1.72	24.87	3.61	7.38	27.05	3.61	-0.46	23.44	4.07	-27.51
4	1144	-0.07	17.55	0.96	0.00	17.55	0.96	-0.07	16.59	1.03	-17.62
6	1118	0.01	37.98	1.61	0.00	37.98	1.61	0.01	36.37	1.60	-37.97
7	395	-1.10	22.68	1.30	1.50	22.78	1.30	-1.20	21.48	2.50	-23.98
8	192	-22.96	-1.15	-9.18	-0.81	-1.10	-9.18	-23.00	8.08	13.82	-21.90

[1] Refer to Figure 2.10.2-9 for component identification.

Table 2.6.7-20 Critical Stress Summary (1-Foot Top Corner Drop) – Loading Condition 1 – P_m – Drop Orientation = 15.74 Degrees

Loading Condition 1: 130°F Ambient Temperature and Maximum Decay Heat Load

		P_m Stresses[1] (ksi)				Principal Stresses					
Comp. No.[2]	Section Cut Node to Node	S_x	S_y	S_z	S_{xy}	S_1	S_2	S_3	S.I.	Allow. Stress 1.0 S_m	Margin of Safety
	1-1										
1	2377 to 2577	-5.07	-0.37	-0.71	-0.29	-0.35	-0.71	-5.09	4.74	20.0	+3.22
	2-2										
3	1775 to 1778	-0.05	-4.39	0.55	0.01	0.55	-0.05	-4.39	4.95	20.0	+3.04
	3-3										
4	1501 to 1504	-0.03	-3.11	0.36	0.01	0.36	-0.03	-3.11	3.47	31.4	+8.05
	4-4										
6	1595 to 1598	-0.01	-3.94	0.52	0.03	0.52	-0.01	-3.94	4.46	31.4	+6.04
	5-5										
7	18 to 118	-1.72	2.83	0.47	-2.50	3.94	0.47	-2.83	6.76	20.0	+1.96
	6-6										
8	381 to 385	-1.83	-2.67	0.82	-0.32	0.82	-1.73	-2.77	3.60	20.0	+4.56

1 Conservatively based on a 1.12-inch thick outer shell and on a 3850-psi crush strength aluminum honeycomb impact limiter (Section 2.6.7.3.1).

2 Refer to Figure 2.10.2-9 for component identification.

Table 2.6.7-21 Critical Stress Summary (1-Foot Top Corner Drop) – Loading Condition 1 - $P_m + P_b$ – Drop Orientation = 15.74 Degrees

Loading Condition 1: 130°F Ambient Temperature and Maximum Decay Heat Load

		$P_m + P_b$ Stresses[1] (ksi)				Principal Stresses					
Comp. No.[2]	Section Cut Node to Node	S_x	S_y	S_z	S_{xy}	S_1	S_2	S_3	S.I.	Allow. Stress 1.5 S_m	Margin of Safety
	1-1										
1	2377 to 2577	-6.69	-0.37	-0.71	-0.29	-0.35	-0.71	-6.70	6.34	30.0	+3.73
	7-7										
3	1821 to 1825	-0.02	-4.40	1.73	0.32	1.73	0.00	-4.43	6.16	30.0	+3.87
	8-8										
4	1561 to 1564	0.06	-4.51	-0.67	-0.13	0.06	-0.67	-4.52	4.58	47.1	+9.28
	4-4										
6	1595 to 1598	0.01	-4.03	0.45	0.03	0.45	0.01	-4.03	4.47	47.1	+9.54
	9-9										
7	143 to 150	-7.82	11.71	1.04	1.55	11.83	1.04	-7.94	19.77	30.0	+0.52
	10-10										
8	176 to 326	-2.87	7.16	0.74	-0.96	0.74	-2.66	-7.37	8.10	30.0	+2.70

1 Conservatively based on a 1.12-inch thick outer shell and on a 3850-psi crush strength aluminum honeycomb impact limiter (Section 2.6.7.3.1).

2 Refer to Figure 2.10.2-9 for component identification.

Table 2.6.7-22 Critical Stress Summary (1-Foot Top Corner Drop) – Loading Condition 1 - S_n – Drop Orientation = 15.74 Degrees

Loading Condition 1: 130°F Ambient Temperature and Maximum Decay Heat Load

		S_n Stresses[1] (ksi)				Principal Stresses					
Comp. No.[2]	Section Cut Node to Node	S_x	S_y	S_z	S_{xy}	S_1	S_2	S_3	S.I.	Allow. Stress 3.0 S_m	Margin of Safety
	1-1										
1	2377 to 2577	-6.82	-0.40	0.32	-0.13	0.32	-0.40	-6.82	7.14	60.0	+7.40
	11-11										
3	1852 to 1856	-0.19	7.89	4.10	-0.42	7.91	4.10	-0.21	8.12	60.0	+6.39
	12-12										
4	601 to 604	0.09	-3.42	-0.54	-0.21	0.11	-0.54	-3.44	3.54	94.2	Large
	13-13										
6	615 to 618	-0.02	15.94	1.30	0.00	15.94	1.30	-0.02	15.95	94.2	+4.90
	14-14										
7	193 to 343	-7.81	12.82	1.50	1.46	12.93	1.50	-7.92	20.84	60.0	+1.88
	6-6										
8	381 to 385	-4.22	-7.18	-0.60	-0.96	-0.60	-3.93	-7.47	6.86	60.0	+7.74

1 Conservatively based on a 1.12-inch thick outer shell and on a 3850-psi crush strength aluminum honeycomb impact limiter (Section 2.6.7.3.1).
2 Refer to Figure 2.10.2-9 for component identification.

Table 2.6.7-23 Critical Stress Summary (1-Foot Top Corner Drop) – Loading Condition 1 - Total Range – Drop Orientation = 15.74 Degrees

Loading Condition 1: 130°F Ambient Temperature and Maximum Decay Heat Load

		Total Stress Range[1] (ksi)				Principal Stresses			Stress Differences		
Comp. No.[2]	Node	S_x	S_y	S_z	S_{xy}	S_1	S_2	S_3	S_1-S_2	S_2-S_3	S_3-S_1
1	2561	1.48	-1.26	0.20	43.95	44.08	0.20	-43.86	43.88	44.06	-87.94
3	1856	-0.19	7.24	3.70	0.08	7.24	3.70	-0.19	3.54	3.89	-7.43
4	1584	-0.13	-2.05	0.02	-0.11	0.02	0.12	-2.06	0.14	1.93	-2.08
6	1595	-0.05	7.09	0.97	0.01	7.09	0.97	-0.05	6.12	1.02	-7.14
7	192	-7.81	14.07	1.73	3.37	14.58	1.73	-8.32	12.85	10.05	-22.90
8	385	-7.64	-8.88	-3.12	-1.02	-3.12	-7.07	-9.46	3.95	2.39	-6.34

1 Conservatively based on a 1.12-inch thick outer shell and on a 3850-psi crush strength aluminum honeycomb impact limiter (Section 2.6.7.3.1).
2 Refer to Figure 2.10.2-9 for component identification.

Table 2.6.7-24 Critical Stress Summary (1-Foot Bottom Corner Drop) – Loading Condition 1 – P_m – Drop Orientation = 15.74 Degrees

Loading Condition 1: 130°F Ambient Temperature and Maximum Decay Heat Load

		P_m Stresses[1] (ksi)				Principal Stresses					
Comp. No.[2]	Section Cut Node to Node	S_x	S_y	S_z	S_{xy}	S_1	S_2	S_3	S.I.	Allow. Stress 1.0 S_m	Margin of Safety
	1-1										
1	2301 to 2561	-1.28	-0.32	0.62	0.30	0.62	-0.24	-1.37	1.99	20.0	Large
	2-2										
3	1595 to 1598	-3.44	-3.78	-1.65	-0.68	-1.65	-2.91	-4.31	2.66	20.0	+6.51
	3-3										
4	661 to 664	-0.04	-2.98	0.28	0.02	0.28	-0.04	-2.98	3.26	31.4	+8.63
	4-4										
6	615 to 618	-0.01	-4.93	0.28	-0.03	0.28	-0.01	-4.93	5.21	31.4	+5.03
	5-5										
7	2 to 102	-5.98	-3.63	-0.03	2.73	-0.03	-1.83	-7.78	7.76	20.0	+1.58
	6-6										
8	601 to 604	-0.10	-2.94	0.09	0.13	0.09	-0.09	-2.95	3.04	20.0	+5.58

1 Conservatively based on a 1.12-inch thick outer shell and on a 3850-psi crush strength aluminum honeycomb impact limiter (Section 2.6.7.3.1).

2 Refer to Figure 2.10.2-9 for component identification.

Table 2.6.7-25 Critical Stress Summary (1-Foot Bottom Corner Drop) – Loading Condition 1 - $P_m + P_b$ – Drop Orientation = 15.74 Degrees

Loading Condition 1: 130°F Ambient Temperature and Maximum Decay Heat Load

		$P_m + P_b$ Stresses[1] (ksi)				Principal Stresses					
Comp. No.[2]	Section Cut Node to Node	S_x	S_y	S_z	S_{xy}	S_1	S_2	S_3	S.I.	Allow. Stress 1.5 S_m	Margin of Safety
	1-1										
1	2301 to 2561	-4.05	-0.32	0.38	1.31	0.38	0.09	-4.46	4.84	30.0	+5.20
	7-7										
3	1815 to 1818	-1.55	4.49	-4.47	0.28	4.51	-1.56	-4.47	8.98	30.0	+2.34
	8-8										
4	621 to 624	0.04	-4.09	-0.52	0.09	0.04	-0.52	-4.10	4.14	47.1	Large
	4-4										
6	615 to 618	-0.02	-5.20	0.30	-0.03	0.30	-0.02	-5.20	5.49	47.1	+7.58
	9-9										
7	168 to 175	9.21	-3.47	-0.15	-0.29	9.22	-0.15	-3.48	12.70	30.0	+1.36
	10-10										
8	176 to 326	-6.65	0.00	-0.82	0.00	0.00	-0.82	-6.65	6.65	30.0	+3.51

1 Conservatively based on a 1.12-inch thick outer shell and on a 3850-psi crush strength aluminum honeycomb impact limiter (Section 2.6.7.3.1).

2 Refer to Figure 2.10.2-9 for component identification.

Table 2.6.7-26 Critical Stress Summary (1-Foot Bottom Corner Drop) – Loading Condition 1 - S_n – Drop Orientation = 15.74 Degrees

Loading Condition 1: 130°F Ambient Temperature and Maximum Decay Heat Load

		S_n Stresses[1] (ksi)				Principal Stresses					
Comp. No.[2]	Section Cut Node to Node	S_x	S_y	S_z	S_{xy}	S_1	S_2	S_3	S.I.	Allow. Stress 3.0 S_m	Margin of Safety
	1-1										
1	2301 to 2561	-6.94	-0.68	-0.30	-0.06	-0.30	-0.68	-6.94	6.64	60.0	+8.04
	11-11										
3	1852 to 1856	-0.13	11.99	3.05	-0.24	12.00	3.05	-0.13	12.13	60.0	+3.95
	12-12										
4	1301 to 1304	0.00	4.74	0.69	0.00	4.74	0.69	0.00	4.74	94.2	Large
	13-13										
6	1275 to 1278	-0.01	12.83	0.30	0.00	12.83	0.30	-0.01	12.84	94.2	+6.34
	14-14										
7	193 to 343	17.94	-0.43	1.20	2.27	18.22	1.20	-0.71	18.93	60.0	+2.17
	15-15										
8	192 to 342	-16.86	-0.12	-1.41	3.03	0.41	-1.41	-17.40	17.81	60.0	+2.37

1 Conservatively based on a 1.12-inch thick outer shell and on a 3850-psi crush strength aluminum honeycomb impact limiter (Section 2.6.7.3.1).

2 Refer to Figure 2.10.2-9 for component identification.

Table 2.6.7-27 Critical Stress Summary (1-Foot Bottom Corner Drop) – Loading Condition 1 - Total Range – Drop Orientation = 15.74 Degrees

Loading Condition 1: 130°F Ambient Temperature and Maximum Decay Heat Load

		Total Stress Range[1] (ksi)				Principal Stresses			Stress Differences		
Comp. No.[2]	Node	S_x	S_y	S_z	S_{xy}	S_1	S_2	S_3	S_1-S_2	S_2-S_3	S_3-S_1
1	2561	0.80	-4.34	0.23	4.73	3.61	0.23	-7.15	3.38	7.38	-10.76
3	1815	0.38	3.10	-0.93	1.68	3.90	-0.42	-0.93	4.32	0.51	-4.83
4	604	-0.19	-2.77	0.11	0.15	0.11	-0.18	-2.78	0.29	2.60	-2.89
6	615	-0.03	5.78	0.94	-0.03	5.78	0.94	-0.03	4.84	0.97	-5.81
7	1	3.73	-1.26	1.97	-43.45	44.76	1.97	-42.29	42.79	44.26	-87.04
8	192	0.11	-18.73	-9.11	2.58	0.46	-9.11	-19.08	9.57	9.97	-19.53

1 Conservatively based on a 1.12-inch thick outer shell and on a 3850-psi crush strength aluminum honeycomb impact limiter (Section 2.6.7.3.1).
2 Refer to Figure 2.10.2-9 for component identification.

Table 2.6.7-28 Critical Stress Summary (1-Foot Top Corner Drop) – Loading Condition 3 – P_m – Drop Orientation = 15.74 Degrees

Loading Condition 3: -40°F Ambient Temperature and No Decay Heat Load

		P_m Stresses[1] (ksi)				Principal Stresses					
Comp. No.[2]	Section Cut Node to Node	S_x	S_y	S_z	S_{xy}	S_1	S_2	S_3	S.I.	Allow. Stress 1.0 S_m	Margin of Safety
	1-1										
1	2377 to 2577	-4.89	-0.34	-0.78	-0.34	-0.32	-0.78	-4.91	4.59	20.0	+3.36
	2-2										
3	1775 to 1778	-0.06	-4.13	0.62	0.01	0.62	-0.06	-4.13	4.75	20.0	+3.21
	3-3										
4	1561 to 1564	0.02	-2.72	-0.33	-0.11	0.03	-0.33	-2.73	2.75	31.4	Large
	4-4										
6	1595 to 1598	-0.01	-3.71	0.53	0.03	0.53	-0.01	-3.71	4.23	31.4	+6.42
	5-5										
7	168 to 175	-2.03	3.20	1.06	-0.33	3.22	1.06	-2.05	5.27	20.0	+2.79
	6-6										
8	381 to 385	-1.93	-7.44	-1.79	0.32	-1.79	-1.91	-7.46	5.67	20.0	+2.53

[1] Conservatively based on a 1.12-inch thick outer shell and on a 3850-psi crush strength aluminum honeycomb impact limiter (Section 2.6.7.3.1).
[2] Refer to Figure 2.10.2-9 for component identification.

Table 2.6.7-29 Critical Stress Summary (1-Foot Top Corner Drop) – Loading Condition 3 - $P_m + P_b$ – Drop Orientation = 15.74 Degrees

Loading Condition 3: -40°F Ambient Temperature and No Decay Heat Load

		$P_m + P_b$ Stresses[1] (ksi)				Principal Stresses					
Comp. No.[2]	Section Cut Node to Node	S_x	S_y	S_z	S_{xy}	S_1	S_2	S_3	S.I.	Allow. Stress 1.5 S_m	Margin of Safety
	1-1										
1	2377 to 2577	-6.71	-0.34	-0.78	-0.34	-0.33	-0.78	-6.72	6.40	30.0	+3.69
	7-7										
3	1821 to 1825	0.03	-4.61	1.68	0.43	1.68	0.07	-4.65	6.33	30.0	+3.74
	3-3										
4	1561 to 1564	0.06	-3.75	-0.84	-0.11	0.06	-0.84	-3.75	3.81	94.2	Large
	4-4										
6	1595 to 1598	0.01	-3.81	0.45	0.03	0.45	0.01	-3.81	4.26	94.2	Large
	8-8										
7	143 to 150	-0.54	12.44	4.53	-0.50	12.46	4.53	-0.56	13.02	30.0	+1.30
	9-9										
8	176 to 326	-2.90	-8.30	-0.56	-0.22	-0.56	-2.89	-8.31	7.74	30.0	+2.87

1 Conservatively based on a 1.12-inch thick outer shell and on a 3850-psi crush strength aluminum honeycomb impact limiter (Section 2.6.7.3.1).
2 Refer to Figure 2.10.2-9 for component identification.

Table 2.6.7-30 Critical Stress Summary (1-Foot Top Corner Drop) – Loading Condition 3 - S_n – Drop Orientation = 15.74 Degrees

Loading Condition 3: -40°F Ambient Temperature and No Decay Heat Load

		S_n Stresses[1] (ksi)				Principal Stresses					
Comp. No.[2]	Section Cut Node to Node	S_x	S_y	S_z	S_{xy}	S_1	S_2	S_3	S.I.	Allow. Stress 3.0 S_m	Margin of Safety
	1-1										
1	2377 to 2577	-6.95	-0.47	-1.07	-0.53	-0.43	-1.07	-6.99	6.56	60.0	+8.15
	10-10										
3	1801 to 1805	0.47	14.21	7.54	1.89	14.46	7.54	0.22	14.25	60.0	+3.21
	11-11										
4	661 to 664	0.14	-7.03	-1.15	-0.29	0.15	-1.15	-7.04	7.20	94.2	Large
	4-4										
6	1595 to 1598	0.02	-7.43	0.70	0.05	0.70	0.02	-7.43	8.13	94.2	Large
	8-8										
7	143 to 150	-0.54	13.55	4.99	-0.59	13.58	4.99	-0.56	14.14	60.0	+3.24
	6-6										
8	381 to 385	-4.25	-8.32	-1.90	-0.23	-1.90	-4.23	-8.33	6.42	60.0	+8.34

1 Conservatively based on a 1.12-inch thick outer shell and on a 3850-psi crush strength aluminum honeycomb impact limiter (Section 2.6.7.3.1).

2 Refer to Figure 2.10.2-9 for component identification.

Table 2.6.7-31 Critical Stress Summary (1-Foot Top Corner Drop) – Loading Condition 3 - Total Range – Drop Orientation = 15.74 Degrees

Loading Condition 3: -40°F Ambient Temperature and Maximum Decay Heat Load

		Total Stress Range[1] (ksi)				Principal Stresses			Stress Differences		
Comp. No.[2]	Node	S_x	S_y	S_z	S_{xy}	S_1	S_2	S_3	S_1-S_2	S_2-S_3	S_3-S_1
1	2561	0.05	-1.17	-1.15	40.01	39.49	-1.15	-40.61	40.64	39.46	-80.10
3	1805	0.47	16.81	8.08	2.75	17.26	8.08	0.02	9.18	8.06	-17.24
4	1584	-0.04	4.04	-3.61	-0.44	4.09	-0.09	-3.61	4.17	3.52	-7.70
6	1598	-0.02	-7.58	0.65	0.03	0.65	-0.02	-7.58	0.67	7.56	-8.23
7	2	-0.55	14.68	5.23	0.43	14.69	5.23	-0.56	9.46	5.79	-15.25
8	385	-7.60	-7.37	-4.68	-1.24	-4.68	-6.24	-8.73	1.56	2.48	-4.05

1 Conservatively based on a 1.12-inch thick outer shell and on a 3850-psi crush strength aluminum honeycomb impact limiter (Section 2.6.7.3.1).
2 Refer to Figure 2.10.2-9 for component identification.

Table 2.6.7-32 Summary of Results - Impact Limiter Analysis for 1-Foot Free Drop

Analysis Description	Displacement (in)	Force (lb)	Equivalent[1] G Load Factor
Flat End Impact			
Bottom Limiter with Max Crush Strength	0.76	8.22×10^5	15.8
Bottom Limiter with Min Crush Strength	0.94	6.60×10^5	12.7
Top Limiter with Max Crush Strength	0.82	8.22×10^5	15.8
Top Limiter with Min Crush Strength	0.96	6.71×10^5	12.9
Corner Impact			
Bottom Limiter with Max Crush Strength	3.16	6.29×10^5	12.1
Bottom Limiter with Min Crush Strength	3.40	6.29×10^5	12.1
Top Limiter with Max Crush Strength	3.18	6.40×10^5	12.3
Top Limiter with Min Crush Strength	3.42	5.98×10^5	11.5

[1] Equivalent g load factor = Force/52,000.

Table 2.6.7-32 Summary of Results - Impact Limiter Analysis for 1-Foot Free Drop (continued)

Analysis Description	Displacement (in)	Force (lb)	Equivalent[1] G Load Factor
Flat Side Impact			
Bottom Limiter with Max Crush Strength	0.83	1.21×10^6	23.3
Bottom Limiter with Min Crush Strength	0.95	1.03×10^6	19.8
Top Limiter with Max Crush Strength	0.83	1.26×10^6	24.3
Top Limiter with Min Crush Strength	0.94	1.07×10^6	20.6

[1] Equivalent g load factor = Force/52,000.

Table 2.6.7-33 Summary of Results - Impact Limiter Analysis for 30-Foot Free Drop Subsequent to a 1-Foot Fall

Analysis Description	Displacement (in)	Force (lb)	Equivalent[1] G Load Factor
Flat End Impact			
Bottom Limiter with Max Crush Strength	8.50	2.50×10^6	48.1
Bottom Limiter with Min Crush Strength	10.30	2.03×10^6	39.0
Top Limiter with Max Crush Strength	8.47	2.51×10^6	48.3
Top Limiter with Min Crush Strength	10.24	2.04×10^6	39.2
Corner Impact			
Bottom Limiter with Max Crush Strength	11.30	3.08×10^6	59.2
Bottom Limiter with Min Crush Strength	12.70	2.58×10^6	49.6
Top Limiter with Max Crush Strength	11.38	3.14×10^6	60.4
Top Limiter with Min Crush Strength	12.72	2.98×10^6	57.3

[1] Equivalent g load factor = Force/52,000.

Table 2.6.7-33 Summary of Results - Impact Limiter Analysis for 30-Foot Free Drop Subsequent to a 1-Foot Fall (continued)

Analysis Description	Displacement (in)	Force (lb)	Equivalent[1] G Load Factor
Flat Side Impact			
Bottom Limiter with Max Crush Strength	8.60	2.65×10^6	48.7
Bottom Limiter with Min Crush Strength	10.30	2.17×10^6	41.8
Top Limiter with Max Crush Strength	8.42	2.71×10^6	49.7
Top Limiter with Min Crush Strength	10.00	2.22×10^6	42.7

[1] Equivalent g load factor = Force/52,000.

Table 2.6.7-34 Summary of Cask Drop Equivalent G Load Factors

	Equivalent G Load Factor[1]			
Direction	1-Foot Drop	31-Foot Drop		
		Total	Axial[2] Comp.	Lateral[3] Comp.
Lateral (Side)	24.3	49.7	—	49.7
Longitudinal	15.8	60.0	60.0	—
Corner (15.74°)	12.3	60.4	58.2	16.4
Oblique (30°)	—	54.4	47.1	27.2
Oblique (45°)	—	43.8	31.0	31.0
Oblique (60°)	—	44.4	22.2	38.5

[1] Equivalent g load factor = Force/52,000.
[2] Axial Component = total x cosθ where θ = 15.74°, 30°, 45°, or 60°
[3] Lateral Component = total x sinθ where θ = 15.74°, 30°, 45°, or 60°

Table 2.6.7-35 NAC-LWT Cask Hot Bolt Analysis – Normal Conditions

Nominal Diameter (in):	1.00	
Number of Bolts:	12	
Service Stress, Sy (ksi):	81.9	at a 300 degree-F Service Temperature
Bolt Expansion (in/in):	9E-06	at a 300 degree-F Service Temperature
Bolt Modulus (ksi):	26700	at a 300 degree-F Service Temperature
Lid Expansion (in/in):	9E-06	at a 300 degree-F Service Temperature
Lid Modulus (ksi):	27000	at a 300 degree-F Service Temperature
Stress Area (in2):	0.6051	
Grip Length (in):	7.99	
Maximum Pressure (psi):	50	
Seal Diameter (in):	15.750	
Preload Torque (ft-lbs):	260	at RT
Nominal Room Temp, RT:	70	deg-F
Bolt Circle Diameter (in):	17.88	
Lid Diameter (in):	22.50	

(a) Longitudinal Weight (lbs):	4941
(b) Lateral Weight (lbs):	941
Service DT (degrees):	157
[default value =]	230
CALCULATED LOADS & STIFFNESS	
(c) Bolt Thermal Load (lbs):	1423
(d) Bolt Preload (lbs):	34770
(e) Bolt Pressure Load (lbs):	812
(f) Bolt Stiffness (lbs/in):	1.9E+06
(g) Lid Stiffness (lbs/in):	2.1E+07

Angle wrt Vert. (Deg)	Impact Accel. (g)	<***** LOADS (lbs.) Impact Tension	Impact Shear	Bolt Tension Applied	Net *****>	<***** STRESSES (psi) Direct Tension	Direct Shear	Principal Sig-1	Principal Sig-2	Stress Intens. *****>	Margin of Safety
	(h)		(k)	(l)	(m)	(n)	(o)		(p)	(q)	(r)
0 End	60.00	24705 (i)	0	25517	38292	63282	0	0	63282	63282	0.29
5 (+)	60.13	33641 (j)	411	34453	39027	64497	679	-7	64504	64511	0.27
10 (+)	60.25	33327	820	34138	39001	64454	1356	-29	64483	64511	0.27
15.7 Corner	60.40	32657	1282	33469	38946	64363	2118	-70	64433	64503	0.27
20 (+)	58.60	30924	1572	31736	38804	64128	2597	-105	64233	64338	0.27
25 (+)	56.50	28758	1872	29570	38626	63833	3094	-150	63983	64133	0.28
30 (calc)	54.40	26459	2133	27271	38436	63521	3525	-195	63716	63911	0.28
35 (+)	50.87	23402	2288	24213	38185	63105	3781	-226	63331	63557	0.29
40 (+)	47.33	20364	2386	21176	37935	62692	3943	-247	62939	63186	0.30
45 (calc)	43.80	17394	2429	18206	37691	62289	4014	-258	62546	62804	0.30
50 (+)	44.00	15884	2643	16696	37567	62083	4368	-306	62389	62695	0.31
55 (+)	44.20	14238	2839	15050	37431	61860	4692	-354	62213	62567	0.31
60 (calc)	44.40	12468	3015	13280	37286	61619	4983	-400	62019	62420	0.31
65 (+)	45.68	10843	3247	11655	37152	61398	5366	-465	61863	62329	0.31
70 (+)	46.97	9022	3461	9834	37002	61150	5719	-530	61681	62211	0.32
75 (+)	48.25	7014	3655	7825	36837	60877	6040	-593	61471	62064	0.32
80 (+)	49.53	4831	3825	5643	36657	60581	6322	-653	61233	61886	0.32
85 (+)	50.82	2487	3970	3299	36465	60262	6560	-706	60968	61674	0.33
90 Side	52.10	0	4086	812	36260	59924	6752	-751	60675	61427	0.33

Minimum Margin of Safety: 0.27

Table 2.6.7-36 NAC-LWT Cask Cold Bolt Analysis – Normal Conditions

Nominal Diameter (in):	1.00	
Number of Bolts:	12	
Service Stress, Sy (ksi):	85	at a 70 degree-F Service Temperature
Bolt Expansion (in/in):	8E-06	
Bolt Modulus (ksi):	27800	
Lid Expansion (in/in):	8E-06	
Lid Modulus (ksi):	28300	
Stress Area (in2):	0.6051	
Grip Length (in):	7.99	
Maximum Pressure (psi):	50	
Seal Diameter (in):	15.750	
Preload Torque (ft-lbs):	260	at RT
Nominal Room Temp, RT:	70	deg-F
Bolt Circle Diameter (in):	17.88	
Lid Diameter (in):	22.50	

Longitudinal Weight (lbs):	4941
Lateral Weight (lbs):	941
Service DT (degrees):	-90
[default value =]	0

CALCULATED LOADS & STIFFNESS

Bolt Thermal Load (lbs):	-594
Bolt Preload (lbs):	34770
Bolt Pressure Load (lbs):	812
Bolt Stiffness (lbs/in):	2.0E+06
Lid Stiffness (lbs/in):	2.2E+07

Angle wrt Vert. (Deg)	Impact Accel. (g)	<***** LOADS (lbs.) Impact Tension	Impact Shear	Bolt Tension Applied	*****> Bolt Tension Net	<***** STRESSES (psi) Direct Tension	Direct Shear	Principal Sig-1	Principal Sig-2	*****> Stress Intens.	Margin of Safety
0 End	60.00	24705	0	25517	36262	59928	0	0	59928	59928	0.42
5 (+)	60.13	33641	411	34453	36993	61135	679	-8	61143	61150	0.39
10 (+)	60.25	33327	820	34138	36967	61093	1356	-30	61123	61153	0.39
15.7 Corner	60.40	32657	1282	33469	36912	61002	2118	-73	61076	61149	0.39
20 (+)	58.60	30924	1572	31736	36771	60768	2597	-111	60879	60990	0.39
25 (+)	56.50	28758	1872	29570	36594	60475	3094	-158	60633	60791	0.40
30 (calc)	54.40	26459	2133	27271	36406	60165	3525	-206	60371	60577	0.40
35 (+)	50.87	23402	2288	24213	36156	59752	3781	-238	59990	60228	0.41
40 (+)	47.33	20364	2386	21176	35908	59341	3943	-261	59602	59863	0.42
45 (calc)	43.80	17394	2429	18206	35665	58940	4014	-272	59212	59484	0.43
50 (+)	44.00	15884	2643	16696	35541	58736	4368	-323	59059	59382	0.43
55 (+)	44.20	14238	2839	15050	35407	58514	4692	-374	58888	59262	0.43
60 (calc)	44.40	12468	3015	13280	35262	58275	4983	-423	58698	59121	0.44
65 (+)	45.68	10843	3247	11655	35129	58055	5366	-492	58547	59039	0.44
70 (+)	46.97	9022	3461	9834	34980	57809	5719	-560	58369	58930	0.44
75 (+)	48.25	7014	3655	7825	34816	57538	6040	-627	58165	58792	0.45
80 (+)	49.53	4831	3825	5643	34638	57243	6322	-690	57933	58622	0.45
85 (+)	50.82	2487	3970	3299	34446	56926	6560	-746	57672	58419	0.46
90 Side	52.10	0	4086	812	34243	56590	6752	-794	57384	58179	0.46

Minimum Margin of Safety: 0.39

Table 2.6.7-37 Summary of Neutron Shield Tank Analysis

Load Condition: 1-Foot End Drop and 1-Foot Side Drop

Description	Stress Magnitude (psi)	Margin of Safety[1]
Tank Shell	12,841	+0.07
Stiffener	11,746	+0.17
Stiffener Weld	2,424 lb/in	+0.23
Gusset Weld	1,418 lb/in	+1.10
Bottom End Plate	8,525	+1.79
Gusset Plate Cross Section	7,180	+LARGE
End Plate Welds	1,593	+LARGE
Top End Plate	11,172	+0.23

This table summarizes the stresses and margins for a design condition of 180 psig (Section 2.6.7.7.4), which envelops both the end drop and side drop conditions.

[1] Based on an allowable stress equal to the yield strength of Type 304 stainless steel at 250°F.

Table 2.6.7-38 Normal Transport Shield Tank Temperatures

Transport Condition	Average Fluid Temperature
100°F/Full Heat Load	227°F
68°F/No Heat Load	68°F
-20°F/Full Heat Load	99°F
-20°F/No Heat Load	-20°F

Table 2.6.7-39 Normal Transport Shield Tank Pressures

Transport Condition	Calculated Tank Pressure
PRVR	165 psig
100°F/Full Heat Load	25.6 psig
68°F/No Heat Load	0 psig

Table 2.6.7-40 Summary of Expansion Tank Analysis

Load Condition: 1-Foot End Drop and 1-Foot Side Drop

Description	Stress Magnitude (psi)	Margin of Safety[1]
Bottom/Top End Plate	3,375	+LARGE
Tank Shell	10,857	+0.26
Tank Stiffener	9,997	+0.37
Shell Weld	11,750	+0.17

This table summarizes the stresses and margins for a design condition of 180 psig (Sections 2.6.7.8 and 2.6.7.7.4), which envelops both the end drop and side drop conditions.

[1] Based on an allowable stress equal to the yield strength of Type 304 stainless steel at 250°F.

Table 2.6.7-41 Upper Ring – Cross-Section Principal Stresses

Section	P_m Stresses							$P_m + P_b$ Stresses						
	Component (ksi)				Principal (ksi)			Component (ksi)				Principal (ksi)		
	S_x	S_y	S_z	S_{xy}	S_1	S_2	S_3	S_x	S_y	S_z	S_{xy}	S_1	S_2	S_3
a-a	-0.8	4.7	1.9	-0.1	4.7	-0.8	1.9	-2.6	9.0	4.0	-1.0	9.1	-2.7	4.0
b-b	0.1	4.9	1.9	-0.2	4.9	0.1	1.9	1.2	8.0	2.9	-1.0	8.1	1.1	2.9
c-c	-0.1	5.5	2.0	0.5	5.5	-0.3	2.0	-0.2	6.5	2.6	1.0	6.6	-0.3	2.6

October 2009

Revision LWT-09E

NAC-LWT

Legal Weight Truck Cask System

SAFETY ANALYSIS REPORT

Volume 2 of 2

Docket No. 71-9225

NAC INTERNATIONAL

Atlanta Corporate Headquarters: 3930 East Jones Bridge Road, Norcross, Georgia 30092 USA
Phone 770-447-1144, Fax 770-447-1797, www.nacintl.com

List of Effective Pages

LIST OF EFFECTIVE PAGES

LIST OF EFFECTIVE PAGES

LIST OF EFFECTIVE PAGES (Continued)

Chapter 8

Table of Contents

List of Figures

List of Tables

8.2 Maintenance Program

Each NAC-LWT cask is subjected to a series of tests and inspections prior to each loaded shipment and annually, as shown in the Maintenance Program Schedule (Table 8.2-1).

Prior to each loaded transport, the metallic O-rings of the closure lid and Alternate B port covers, if used, are replaced. The O-ring seals of the alternate port covers are inspected and replaced as necessary. The cask cavity, trunnions, and all removable components (i.e., closure lid, port covers, attachment bolts, impact limiters, etc.) are visually inspected for damage. Following loading, the closure lid and port covers are installed and the bolting torqued. Leakage rate tests are performed on the closure lid and port covers as detailed in the cask loading procedures of Chapter 7.1.

The completion of the annual maintenance and test program is required for each NAC-LWT cask while it is in service. The completion of the annual maintenance is documented on an annual inspection certification document. Each NAC-LWT cask must have a current annual certification before it can be used. The required annual cask maintenance test program is performed during or before the calendar month in which the annual program is due, but it is required to be performed no later than 30 days following the due date. During periods when the cask is not in use, the annual maintenance program may be deferred provided that the annual maintenance is completed and documented prior to the cask's next use.

For NAC-LWT casks to be used to transport TPBAR contents, a one-time post-fabrication hydrostatic test of the cask containment boundary, including Alternate B port covers, shall be performed to a pressure of 450 + 15/-0 psig. The annual maintenance program certification documentation shall specifically identify that a NAC-LWT packaging has been qualified by testing for TPBAR contents.

Helium leakage rate testing to the leaktight criteria of ANSI N14.5-1997 is performed on the closure lid, and alternate and Alternate B port cover containment seals.

Engineering approval is required prior to making any repairs of damaged areas or areas that need refurbishing as a result of normal wear and tear. All such repairs shall be fully documented in accordance with NAC's approved Quality Assurance program. The replacement of valves, fittings, seals, thread fasteners, or use of calibrated pressure gauges are considered normal maintenance and do not require engineering approval.

Testing of the cask shielding and heat rejection capabilities is conducted during original packaging acceptance testing. The structures that provide shielding and heat rejection are passive and do not require verification during routine use of the package. Consequently, the efficiency of these systems is not tested during the annual maintenance program. Radiation surveys conducted at the time of cask loading provide verification of continued shielding effectiveness.

Testing of the neutron absorber material utilized in TRIGA poisoned basket modules are conducted prior to fabrication of the basket modules. The neutron absorber material is in the form of borated stainless steel sheets that are visually inspected for wear or damage prior to each use, and do not require routine maintenance.

8.2.1 Authorized Repairs

Repairs are authorized to correct cracks and blemishes resulting from normal wear and tear of the components of the NAC-LWT packaging. Performance of authorized repairs will result in an as-licensed configuration. The specific weld repair procedure for the impact limiter attachment lugs is described in Section 8.2.1.1.

8.2.1.1 Impact Limiter Attachment Lug Repairs

Impact limiter lugs shall be visually examined prior to each transport to ensure that the impact limiters can be attached to the NAC-LWT cask body in accordance with the Transport Cask Assembly drawings presented in Chapter 1. During annual NAC-LWT packaging maintenance, the impact limiter attachment lugs and the welds sealing the impact limiter shell to the lugs are visually examined with acceptance criteria in accordance with ANSI/AWS Code D1.2, Paragraph 8.8.1. If defects in the impact limiter shell-to-lug welds or in the lug base material are identified, the weld is repaired in accordance with the applicable License Drawing requirements.

Defects in the shell-to-lug weld are removed by grinding, and the shell is rewelded to the lug. If the lug base material has a defect or is broken in two pieces, the lug base material is prepared to allow completion of a full-penetration weld. The weld repairs shall be performed by qualified welders utilizing approved welding procedures prepared, approved and qualified in accordance with ASME Code, Section IX, or ANSI/AWS D1.2. Approved lug repair welding procedures will validate that the axial load path minimum yield strength and ultimate strength of the completed repair will be 10.0 ksi and 20.0 ksi, respectively, or greater, and that the maximum temperature in the base lug material local (within 0.5 inch) to the weld repaired is maintained less than 350°F during the welding process. Following shell-to-lug weld repairs or completion of the full-penetration welding of the lug base material, the weld shall be examined by liquid penetrant examination in accordance with ASME Code, Section V, Article 6, or ANSI/AWS D1.2. Weld acceptance criteria for the liquid penetrant examination shall be in accordance with the ASME Code, Section VIII, Division 1, Appendix 8, or ANSI/AWS D1.2, Paragraph 6.17, as applicable.

Inspection and weld repair documentation shall be maintained as part of the maintenance records for the specific NAC-LWT packaging.

Table 8.2-1 Maintenance Program Schedule

Cask Cavity (Including Port Cover and Lid Seals)	
Annually	Visual Inspection Lid and Port Cover Seal Replacement Periodic Helium Leak Tests (per Section 8.1.3)
Valve Port Covers	
Each Loaded Shipment	Visual Inspection Air Pressure Drop Test at 15 +1/-0 psig (Alternate port covers) Maintenance Helium Leakage Testing (Alternate B port covers) Seal Replacement as Necessary[1]
Drain Line Gasket	
Each Shipment	Seal Replacement as Necessary
Annually	Seal Replacement
Water Jacket and Expansion Tank	
Annually	Visual Inspection Check Fluid Level, Specific Gravity, and Boron Concentration[2]
Each Shipment	Visually Inspect Fill, Drain and Inspection Port Plugs for Leakage
Cask Lid Bolts	
Each Shipment	Visually Inspect for Damage and Replace, as required.
Long Term Maintenance	Bolt replacement upon reaching 20-year life or 550 operational cycles.

[1] Helium leak testing (per Section 8.1.3.2.2) is required following replacement of alternate port cover containment (i.e., face) O-ring seals. For Alternate B port covers, seal replacement and leak testing are required for each shipment per the requirements specified in the Operating Procedures in Chapter 7 and Section 8.1.3.2.2.

[2] The neutron shield fluid must be verified to contain greater than 1.0 wt % boron and the specific gravity must be such that the solution does not freeze at temperatures above -40°F.

Table 8.2-1 Maintenance Program Schedule (continued)

Water Jacket Relief Valve	
Annually	Replace With New Pre-set Valve, or Verify Opening and Reseating Pressure (Allowable variation is ± 10 psig of Nominal Valve Opening Pressure, 165 psig)
Fasteners, Valved Nipples, Washers, Reusable O-rings, and Helicoils	
Each Shipment	Inspect and Replace as necessary
Lid and Alternate B Port Cover Metallic O-rings	
Each Loaded Shipment	Replace and perform helium leakage rate testing to the criteria specified in Section 8.1.3.

Chapter 9

Table of Contents

9 REFERENCES

"AISC Manual of Steel Construction," 8th Edition, The American Institute of Steel Construction, Inc., 1990.

Alcoa Aluminum Handbook, Pittsburgh, PA, Aluminum Company of America, 1959.

"Aluminum Construction Manual," 2nd Edition, Section 3, The Aluminum Association, Washington, D.C., 1972.

"Annual Book of ASTM Standards," Section 3, Volume 03.01, American Society for Testing and Materials, 1986.

"ANSYS' Computer Code for Large-Scale General Purpose Engineering Analysis," Swanson Analysis Systems, Inc., Houston, PA.

"ASME Boiler and Pressure Vessel Code," Section III, Subsection NG – Core Support Structures and Subsection NH – Class 1 – Components in Elevated Temperature Service, The American Society of Mechanical Engineers, 1995 with Addenda through 1997.

Baker, E.H., L. Kovalevsky, and F.L. Rish, Structural Analysis of Shells, New York, McGraw-Hill Book Co., December 1966.

Bates, O.K., "Thermal Conductivities of Aqueous Ethylene Glycol Solutions," St. Lawrence University, Canton, NY.

Baumeister, T. and L.S. Marks, Standard Handbook for Mechanical Engineers, 7th Edition, New York, McGraw-Hill Book Co., December 1966.

BAW-246, "NULIF – A Neutron Spectrum Generator, Few-Group Constant Calculator, and Depletion Code," Babcock & Wilcox, August 1976.

Bevington, P.R., Data Reduction and Error Analysis for the Physical Sciences, New York, McGraw-Hill Book Company.

Biggs, J.M., Introduction to Structural Dynamics, New York, McGraw-Hill Book Co., 1964.

Blake, A., "Charts Simplify Calculations for Moments and Deflections of Circular Arches," Machine Design, Cleveland, Penton Publishing Co., December 25, 1958.

Blodgett, O.W., Design of Welded Structures, Cleveland, James F. Lincoln Arc Welding Foundation, 1972.

Book of Standards, Part 7, American Society for Testing and Materials, 1970.

Bruhn, E.F., Analysis and Design of Flight Vehicle Structures, 1st Edition, Cincinnati, Tri-State Offset, Co., 1965.

Bucholz, J.A., "Scoping Design Analyses for Optimized Shipping Casks Containing 1-, 2-, 3-, 5-, 7-, or 10-year old PWR Spent Fuel," Oak Ridge National Laboratory, ORNL/CSD/TM-149, January 1983.

Bucholz, J.A., "XSDOSE: A Module for Calculating Fluxes and Dose Rates at Points Outside A Shield," Vol. 2, Sect. F4 of SCALE-4, August 1981.

Bucholz, J.A., et. Al., "SAS1: A One-Dimensional Shielding Analysis Module."

Cain, V.R. and R.E. Malenfant, "QAD-CG, The Combinatorial Geometry Version of the QAD-P5A Point Kernam Shielding Code," Bechtel Power Corporation, July 1977.

CCC-545, "SCALE-4, A Modular Code System for Performing Standardized Computer Analysis of Licensing Evaluation," ORNL, June 1990.

Chun, R., M. Witte, and M. Schwartz, "Dynamic Impact Effects on Spent Fuel Assemblies," UCID-21246, Lawrence Livermore National Laboratory, October 1987.

"Coefficient of Cubical Expansion for Glycol, Water, and Glycol-Water Solutions," E.I. du Pont de Nemours & Co., Inc., Wilmington, DE, 1963.

Cook, I. And R.S. Peckover, "Effective Thermal Conductivity of Debris Beds," Post Accident Debris Cooling, Proceedings of the Fifth Post Accident Heat Removal Information Exchange Meeting, 40-45, 1982.

Cragoe, C.S., "Properties of Ethylene Glycol and Its Aqueous Solutions," National Bureau of Standards.

DOE/ET/34014-10, "Extended Fuel Burnup Demonstration Program," U.S. Department of Energy, September 1983.

Ebner, M. A., "Stability of Uranium-Zirconium Hydride Spent Fuel in Wet Storage," INEL Report MAE-03-94, July, 1994.

Gallagher, C., "NL Industries Internal Test Report on Tensile Properties of Chemical Lead at Elevated Temperatures," Central Research Laboratory, Highstown, NJ, February 1976.

General Atomics Report UZR-28, "Uranium-Zirconium Hydride Fuels for TRIGA Reactors," 1997.

Gerard, G. and H. Becker, "Handbook of Structural Stability," Part III, TN3783, National Advisory Committee for Aeronautics, 1957.

Greene, N.M., J.L. Lucius, L.M. Petrie, W.E. Ford III, J.E. White, and R.Q. Wright, "AMPX – A Modular Code System for Generating Multigroup Neutron-Gamma Libraries from ENDF/B," ORNL/TM-3706, Oak Ridge National Laboratory, March 1976.

Greene, N.M. and L.M. Petrie, "XSDRNPM-S: A One-Dimensional Discrete Ordinates Code for Transport Analysis," Vol. 2, Sect. F3 of SCALE-4, January 1983.

Handbook of Chemistry and Physics, 49th Edition, Cleveland, OH, The Chemical Rubber Company, 1968.

Hermann, O.W. and R.M. Westfall, "ORIGEN-S: SCALE System Module to Calculate Fuel Depletion, Actinide Transmutation, Fission Product Buildup and Decay and Associated Radiation Source Terms," Vol. 2, Sect. F7 of SCALE-4, February 1989.

Hermann, O.W., "SAS2(H): A Coupled One-Dimensional Depletion and Shielding Analysis Code," Vol. 1, Sect. S2 of SCALE-4, June 1990.

IAEA Transportation Safety Standards (TS-R-1), "Regulations for the Safe Transport of Radioactive Material," June 2000.

Johnson, E.B. and R.K. Reedy, "Critical Experiments with SPERT-D Fuel Elements," ORNL-TM-1207, July 14, 1965.

Jordan, W.C., N.F. Landers, and L.M. Petrie, "Validation of KENO-Va Comparison with Critical Experiments," ORNL/CSD/TM-238, December 1986.

Juvinall, R.C., Stress, Strain, and Strength, New York, McGraw-Hill Book Co., 1967.

Kinsey, R., "Data Formats and Procedures for the Evaluated Nuclear Data File, ENDF," ENDF-102, Second Edition, Brookhaven National Laboratory, 1979.

Kreith, F., Principles of Heat Transfer, 2nd Edition, Scranton, PA, International Textbook Company, 1965.

Manual of Steel Construction, 8th Edition, New York, American Institute of Steel Construction, Inc., 1990.

Mark's Standard Handbook for Mechanical Engineers, 9th Edition, McGraw-Hill Book Company, New York.

Merritt, F.S., Standard Handbook for Civil Engineers, McGraw-Hill Book Company, New York, 1968.

Metals Handbook, 9th Edition, American Society of Metals.

MIL-HDBK-5A, "Metallic Materials and Elements for Aerospace Vehicle Structures," Department of Defense, February 1966.

MIL-HDBK-5C, "Metallic Materials and Elements for Aerospace Vehicle Structures," Department of Defense, December 1978.

MIL-HDBK-5E, "Metallic Materials and Elements for Aerospace Vehicle Structures," Department of Defense, May 1989.

Nelms, H.A., "Effects of Jacket Physical Properties and Curvature on Puncture Resistance," Structural Analysis of Shipping Casks, Volume 3, ORNL/TM-1312, Oak Ridge National Laboratory, June 1968.

"Nuclear Systems Materials Handbook," Volume 1, Revision 1, Hanford Engineering Development Laboratories, Richland, WA, March 10, 1976.

NUREG-0612, "Control of Heavy Loads at Nuclear Power Plants," U.S. Nuclear Regulatory Commission, July 1980.

NUREG-1617, Supplement 1, "Standard Review Plan for Transportation Packages for MOX Spent Nuclear Fuel," U.S. Nuclear Regulatory Commission, September 2005.

NUREG/CR-0733, "Critical Separation Between Sub-Critical Clusters of 4.29 w/o U^{235} Enriched UO_2 Rods in Water with Fixed Neutron Poisons," S.R. Bierman, B.M. Durst, E.D. Clayton, Battelle Pacific Northwest Laboratories, May 1978.

NUREG/CR-0200, Volume 2, Section F2, "SCALE-2 NITAWL-S, Resonance Self-Shielding by the Nordheim Method," N. M. Green and L. M. Petrie, Oak Ridge National Laboratory, October 1981.

NUREG/CR-6361, "Criticality Benchmark Guide for Light-Water-Reactor Fuel in Transportation and Storage Packages," U.S. Nuclear Regulatory Commission, March 1997.

NUREG/CR-6487, Anderson, B.L., Carlson, R.W., and Fisher, L.E., "Containment Analysis for Type B Packages Used to Transport Various Contents," Lawrence Livermore Laboratory, 1996.

NUREG/CR-0200, Volume 2, Section F3, "SCALE-2 XSDRNMP-S, A One Dimensional Discrete Ordinates Program for Transport Analysis," R.M. Westfall, L.M. Petrie, N.M. Greene, J.L. Lucius, Oak Ridge National Laboratory, June 1983.

NUREG/CR-0481, "An Assessment of Stress-Strain Data Suitable for Finite-Element Elastic-Plastic Analysis of Shipping Containers," H.J. Rack and G.A. Knorovsky, Sandia Laboratories, SAND77-1872, September 1978.

NUREG/CR-0796 PNL-2827, "Criticality Experiments with Sub-Critical Clusters of 2.35 and 4.29 w/o U^{235} Enriched $U0_2$ Rods in Water with Uranium or Lead Reflecting Walls," S.R. Bierman, B.M. Durst, E.D. Clayton, Battelle Pacific Northwest Laboratories, April 1979.

Paxton, H.C., Critical Dimensions of Systems Containing U^{235}, Pu^{239}, and U^{233}," TID-7028, June 1964.

Peery, D.J., Aircraft Structures, New York, McGraw-Hill Book Company, 1950.

Petrie, L.M. and N.F. Cross, "KENO-IV: An Improved Monte Carlo Criticality Program," ORNL-4938, Oak Ridge National Laboratory, November 1975.

PNL-2438, "Critical Separation Between Sub-Critical Clusters of 2.35 w/o U^{235} Enriched UO_2, Rods in Water with Fixed Neutron Poisons," S.R. Bierman, E.D. Clayton, B.M. Durst, Battelle Pacific Northwest Laboratories, October 1977.

Radiological Health Handbook, U.S. Department of Health, Education and Welfare, Rockville, MD, January 1970.

"Regulations for the Safe Transport of Radioactive Materials," Safety Series No. 6, Revised Edition, International Atomic Energy Agency, 1973.

"Research and Advanced Development Applied Mechanics," Volume 1, Engineering Data Sheets, Avco Corporation, 1962.

Resnick, R. and D. Halliday, Physics, 3rd Edition, Part 1, New York, John Wiley & Sons, 1977.

Roark, R.J., Formulas for Stress and Strain, 4th Edition, New York, McGraw-Hill, Inc., 1965.

Roark, R.J., and W.C. Young, Formulas for Stress and Strain, 5th Edition, New York, McGraw-Hill, Inc., 1975; 6th Edition, 1989.

Roddy, J.W., H.C. Claiborne, R.C. Ashline, P.J. Johnson, B.T. Rhyne, "Physical and Decay Characteristics of Commercial LWR Spent Fuel," ORNL/TM-9591/Vl-Rl, Oak Ridge National Laboratory, January 1986.

"Safety Analysis Report for the NLI-1/2 Spent Fuel Shipping Cask," Nuclear Assurance Corporation, USA/9010/B()F, December 12, 1985.

Schaeffer, N.M., Reactor Engineering for Nuclear Engineers, Springfield, VA, 1984.

"Screw-Thread Standards for Federal Services," U.S. Department of Commerce, 1957.

Shamban TFE O-Ring Seals, Spec. 22-53, Part No. S11214-460, W.S. Shamban & Co., Fort Wayne, IN, 1966.

Shappert, L.B., "Cask Designer's Guide: A Guide for the Design, Fabrication, and Operation of Shipping Casks for Nuclear Applications," ORNL-NSIC-68, Oak Ridge National Laboratories, February 1970.

Shappert, L.B., and W.D. Box, "The Drop Test Facility at the Oak Ridge National Laboratory: A Facility Available to Private Industry," Oak Ridge National Laboratory, Oak Ridge, TN.

Shigley, J.E., Mechanical Engineering Design, 3rd Edition, New York, McGraw-Hill, Inc., 1977.

Shigley, J.E., and C.R. Mischke, Standard Handbook of Machine Design, New York, 1986.

Singer, F.L., Strength of Materials, New York, Harper & Brothers, 1951.

"Table Speeds Calculation of Strength of Threads," Product Engineering, November 27, 1961.

Tang, J.S. "SAS4: A Monte Carlo Cask Shielding Analysis Module Using An Automated Biasing Procedure," March 1989.

"Test Plan: LWT Quarter-Scale Model Drop Tests," Document No. 315-P-01. Nuclear Assurance Corporation, May 31, 1988.

Tietz, T.E., "Determination of the Mechanical Properties of High Purity Lead and a 0.058% Copper-Lead Alloy," Stanford Research Institute, Menlo Park, CA, WADC Technical Report 57-695, ASTIA Document No. 151165, April 1958.

Timoshenko, S., Strength of Materials, 3rd Edition, New York, R. E. Krieger Publishing Co., 1976.

Timoshenko, S., Theory of Plates and Shells, 1st Edition, New York, McGraw-Hill Book Co., 1940.

Timoshenko and Gere, Theory of Elastic Stability, 2nd Edition, New York, McGraw-Hill, Inc., 1961.

Timoshenko, S. and Young, Theory of Structures, New York, McGraw-Hill Book Co., 1965.

Turner, W.D., D.C. Elrod, and I.I. Simon-Tov, "HEATING 5 - An IBM 360 Heat Conduction Program," Oak Ridge National Laboratory, ORNL/CSD/TM-15, March 1977.

Williamson, R.A. and R.R. Alvy, "Impact Effect of Fragments Striking Structural Elements," Holmes and Harver, Inc., 1973.

Childs, K.W., HEATING 7.2 User's Manual, Oak Ridge National Laboratory, ORNL/NUREG/CSD-2/V2/R5, September 1995.

Avallone, E. and T. Baumeister, Marks' Standard Handbook for Mechanical Engineers, 9th Edition, New York, McGraw-Hill Book Company, 1987.

"SCALE 4.3 Modular Code System for Performing Standardized Computer Analyses for Licensing Evaluation for Workstations and Personal Computers," CCC-545, September 1995.

Herman, O.W., "SAS2H: A Coupled One-Dimensional Depletion and Shielding Analysis Module," and C.V. Parks, ORNL/NUREG/CSD-2/V1/R5, Volume 1, Section S2, September. 1995.

Tang, S., "SAS4: A Monte Carlo Cask Shielding Analysis Module Using an Automated Biasing Procedure," ORNL/NUREG/CSD-2/V1/R5, Volume 1, Section S4, September, 1995.

Bucholz, J.A., Landers, N.F., and Petrie, L.M., ORNL/NUREG/CSD-2/V3/R5, Section M7, "The Material Information Processor For Scale," September 1995.

Greene, M., Westfall, R.M., and L.M. Petrie, ORNL/NUREG/CSD-2/V2/R5, "NITAWL-II: Scale System Module For Performing Resonance Shielding And Working Library Production" September 1995.

Jordan, W.C., ORNL/NUREG/CSD-2/V3/R5, Section M4, "Scale Cross-Section Libraries," September 1995.

Landers, N. F., and Petrie L.M, ORNL/NUREG/CSD-2/V1/R5, Section C4, "CSAS: Control Module For Enhanced Criticality Safety Analysis Sequences," September 1995.

Mele, Ravink and Trkov, "TRIGA Mark II Benchmark Experiment, Part I Steady State Operation," Jozef Stefan Institute, Nuclear Technology, Vol. 105, January 1994.

Petrie L.M., and Landers, N.F., ORNL/NUREG/CSD-2/V2/R5, Section F11, "KENO-Va: An Improved Monte Carlo Criticality Program with Supergrouping," September 1995.

Tomsio, M., "Characterization of Triga Fuel," ORNL/Sub/86-22047/3, GA-C18542, Oak Ridge National Laboratory, Oak Ridge, Tennessee, October 1986.

Krieth, F., and Bohn, M.S., "Principals of Heat Transfer," 5th Edition, West Publishing Company, 1993.

Incropera, F.P., and DeWitt, D.P., "Fundamentals of Heat and Mass Transfer," 4th Edition, John Wiley and Sons, 1996.

Owen, D.B., "Factors for One-Sided Tolerance Limits and for Variables Sampling Plans," SCR-607, 1963.

ANSI N14.5-1987, "American National Standard for Radioactive Materials - Leakage Tests on Packages for Shipment," American National Standards Institute, 1987.

ANSI/ANS - 8.1-1983, "Nuclear Criticality Safety in Operations with Fissionable Materials Outside Reactors."

ANSI/ANS - 8.17-1984, "Criticality Safety Criteria for the Handling, Storage, and Transportation of LWR Fuel Outside Reactors."

Bierman, S.R., Clayton, E.D., "Criticality Experiments with Subcritical Clusters of 2.35 w/o and 4.31 w/o ^{235}U Enriched UO_2 Rods in Water at a Water-to-Fuel Volume Ratio of 1.6," NUREG/CR-1547, July 1980.

Baldwin, N.M., Hoovler, G.S., Eng, R.L., and Welfare, F.G., "Critical Experiments Supporting Close Proximity Water Storage of Power Reactor Fuel," B&W-1484-7, July 1979.

Bierman, S.R., and E.D. Clayton, "Criticality Experiments with Subcritical Clusters of 2.35 w/o and 4.31 w/o ^{235}U Enriched UO_2 Rods in Water with Steel Reflecting Walls," Nuclear Technology, Volume 54, pp. 131-144, August 1981.

Bierman, S.R., Durst, B.M., and Clayton, E.D., "Criticality Experiments with Subcritical Clusters of 2.35 and 4.31 w/o ^{235}U Enriched UO_2 Rods in Water with Uranium or Lead Reflecting Walls," NUREG/CR-0796, April 1979.

Bierman, S.R., "Criticality Experiments to Provide Benchmark Data on Neutron Flux Traps," PNL-6205/UC-714, June 1988.

Manaranche, J.C. et al, "Dissolution and Storage Experiment with 4.75 w/o ^{235}U Enriched UO_2 Rods," Nuclear Technology, Volume 50, September 1980.

Machinery's Handbook, 25th Edition, Industrial Press, Inc., New York, NY, 1996.

BISCO Products Data, "FPC Fireblock Silicone Foam," BISCO Products, Inc., Park Ridge, IL, February 1988.

Letter from Rogers Corporation, Bisco Materials Unit, dated February 2, 1999, from Daniel J. Kubrick.

Interim Staff Guidance-11 (ISG-11), Revision 3, "Cladding Considerations for the Transportation and Storage of Spent Fuel," U.S. Nuclear Regulatory Commission, November 2003.

Holometrix Micromet test report NCN-2, dated May 2000.

Ugural, A.C. and Fenster, S.K., "Advanced Strength and Applied Elasticity," Second Edition, Elsevier Science Publishing Company, New York, New York, 1987.

NAC Specification 315-S-09, "O-Ring Temperature Testing for the LWT Alternate Port Cover," Revision 0, February 2000.

"HTGR/RERTR Fuel Materials Characterization and Packaging Report," PC-00384/1, General Atomics, San Diego, CA, April 2002.

UNIFRAX Product Specifications, Fiberfrax® Ceramic Fiber Paper, C-1423, Unifrax Corporation, Niagara Falls, NY, June 1996.

LLNL Report UCRL-53441, "Review of Hydrogen Isotope Permeability Through Materials"

RSIC Computer Code Collection, *ORIGEN2.1; Isotope Generation and Depletion Code – Matrix Exponential Method,* CCC-371, Oak Ridge National Laboratory, Oak Ridge TN, 1996.

Y.K. Sakamoto and M. Sugisaki, "Fusion Science and Technology," Vol. 41, pp 912-914, May 2002.

"Aluminum Standards and Data," Table 2.2, The Aluminum Association, Washington, DC, 1997.

Blake, Alexander, "Practical Stress Analysis in Engineering Design," 2nd Edition, Marcel Dekker Inc., New York, 1990.

ORNL/TM-12667, "Validation of the SCALE System for PWR Spent Fuel Isotopic Composition Analyses," Oak Ridge National Laboratory, March 1995.

ORNL/TM-13317, "An Extension of the Validation of SCALE (SAS2H) Isotopic Prediction for PWR Spent Fuel," Oak Ridge National Laboratory, September 1996.

NUREG/CR-6798, "Isotopic Analysis of High Burnup PWR Spent Fuel Samples from the Takahama-3 Reactor," US Nuclear Regulatory Commission, January 2003.

ORNL/TM-13315, "Validation of SCALE (SAS2H) Isotopic Predictions for BWR Spent Fuel," Oak Ridge National Laboratory, September 1998.

ORNL/TM-13687, "Prediction of the Isotopic Composition of UO_2 Fuel from a BWR: Analysis of the DU1 Sample from the Dodewaard Reactor," Oak Ridge National Laboratory, October 1998.

ASME Boiler and Pressure Vessel Code, Section V, "Nondestructive Examination," American Society of Mechanical Engineers, New York, NY, 2001 Edition with 2003 Addenda.

ASME Boiler and Pressure Vessel Code, Section VIII, "Rules for Construction of Pressure Vessels," American Society of Mechanical Engineers, New York, NY, 2001 Edition with 2003 Addenda.

ASME Boiler and Pressure Vessel Code, Section IX, "Qualification Standard for Welding and Brazing Procedures, Welders, Brazers, and Welding and Brazing Operators," American Society of Mechanical Engineers, New York, NY, 2001 Edition with 2003 Addenda.

AWS D1.2, "Structural Welding Code–Aluminum," The American Welding Society, Miami, FL, 2003.